ROMANIAN ACADEMY

ROMANIAN ASTRONOMICAL JOURNAL

Vol. 10, No. 2
2000

EDITURA ACADEMIEI ROMÂNE

ROMANIAN ACADEMY

ROMANIAN ASTRONOMICAL JOURNAL

The ROMANIAN ASTRONOMICAL JOURNAL appears twice a year. Orders from abroad (issues or subscriptions) should be sent to:
EDITURA ACADEMIEI ROMÂNE, Calea 13 Septembrie 13, P.O. Box 5-42, RO-76117, Bucharest, Romania, Phone +(401) 411 90 08, +(401) 410 32 00, Fax: +(401) 410 39 83.
RODIPET S.A., Piaţa Presei Libere 1, P.O. Box 33-57, Bucharest, Romania, Phone: +(401) 618 51 03, Fax: +(401) 222 64 07.
ORION PRESS IMPEX 2000, P.O. Box 17-19, Bucharest 3, Romania, Phone: +(401) 653 79 85, Fax: +(401) 324 06 38.

The manuscripts, the books and journals proposed in exchange and the mail should be sent to the Editorial Board.

Editorial Board's Address:

ROMANIAN ASTRONOMICAL JOURNAL
Astronomical Institute of the Romanian Academy
Str. Cuţitul de Argint 5
RO-75212, Bucharest 28
Phone: +(401) 335 68 92, +(401) 335 80 10
Phone/Fax: +(401) 337 33 89
E-mail: roaj@roastro.astro.ro
http://roastro.astro.ro/~ roaj/
Romania

ROMANIAN ASTRONOMICAL JOURNAL

Vol. 10, No. 2, 2000

CONTENTS

Rom. Astron. J., Vol. 10, No. 2, p. 109–204, Bucharest, 2000

FIRST GROUND-BASED BV PHOTOMETRY OF THE ECLIPSING BINARY VW LEO MINORIS

ALEXANDRU DUMITRESCU

Astronomical Institute of the Romanian Academy
Str. Cuțitul de Argint 5, RO-75212, Bucharest, Romania
E-mail: alex@roastro.astro.ro

Abstract. The paper presents the first ground-based photoelectric observations of the newly discovered eclipsing binary VW Leo Minoris. The observations were carried out with an EMI 9502 B type photomultiplier attached to the 50 cm Cassegrain reflector of the Bucharest Observatory.The light curves in B and V colors are presented.

Key words: photoelectric photometry – eclipsing variable stars.

1. INTRODUCTION

VW Leo Minoris (HIP 54003, HD 95660) was found to be a variable star by the HIPPARCOS/TYCHO space mission. The Variability Annex of the Hipparcos Catalogue (ESA, 1997) reports VW LMi to have a period of 0.477547 days, with H_p magnitude ranging between 8.031 to 8.446. The star was classified as a W UMa eclipsing binary-type. The spectral type is listed as F3V. Up to present, our observations are the first ones performed from the ground. Our preliminary photometric data were already published (Dumitrescu, 2000).

2. OBSERVATIONS

Nine nights of data were obtained along about one year, between 15 April 1999 and 9 May 2000. The differential observations were carried out by means of an EMI 9502 B type photomultiplier attached to the 50 cm Cassegrain reflector of the Astronomical Institute. The filters used (B and V) are in close accordance with the standard UBV system, and reduction of observations was made in the usual way. As comparison and check stars, HD 95977 and HD 95880 have been used, respectively.

From the light curves, four times of light minima, one primary and three secondaries, have been determined using the method described by Kwee and van

Rom. Astron. J., Vol. 10, No. 2, p. 111–116, Bucharest, 2000

Woerden. In the determination of the minimum times, we used only the data collected in pass-band V, because these ones are the best ones. The results are presented in Table 1.

Table 1

New minimum times of VW LMi

HJD 2400000.0 +	Minimum Type	E
51288.3670	II	– 726.5
51617.3998	II	– 37.5
51635.3084	I	0
51671.3594	II	75.5

During the observational campaign, 314 differential measurements in V and 307 differential measurements in B were secured. The standard deviations of the individual determinations are less than 0.007 magnitude. The phased light curves were obtained according to the ephemeris:

$$HJD(I) = 2451635.3084 + 0.477547 \times E\,. \qquad (1)$$

In Figs. 1 and 2 are shown the observed light curves in the colors V and B, respectively. After the transformation to the standard UBV system, one obtained the normal light curves. The orbital phases and the relative fluxes are given in Tables 2 and 3.

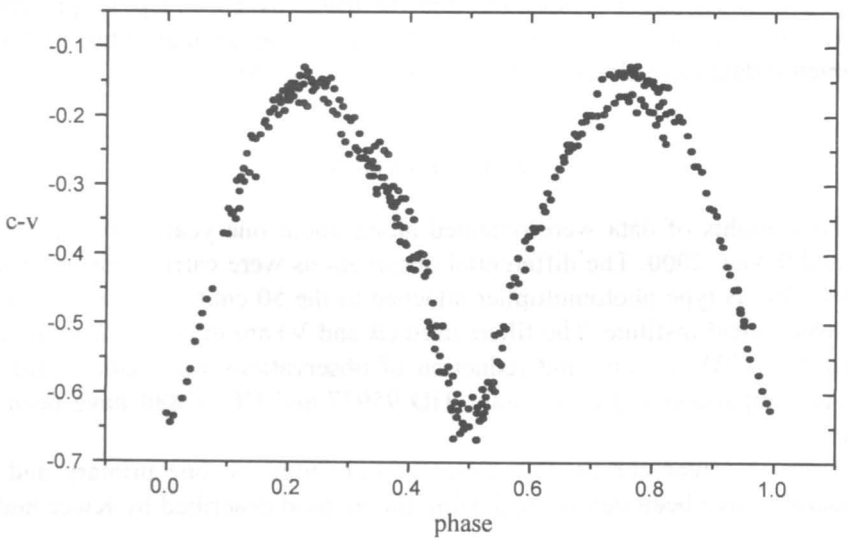

Fig. 1 – VW LMi: light curve observed in V.

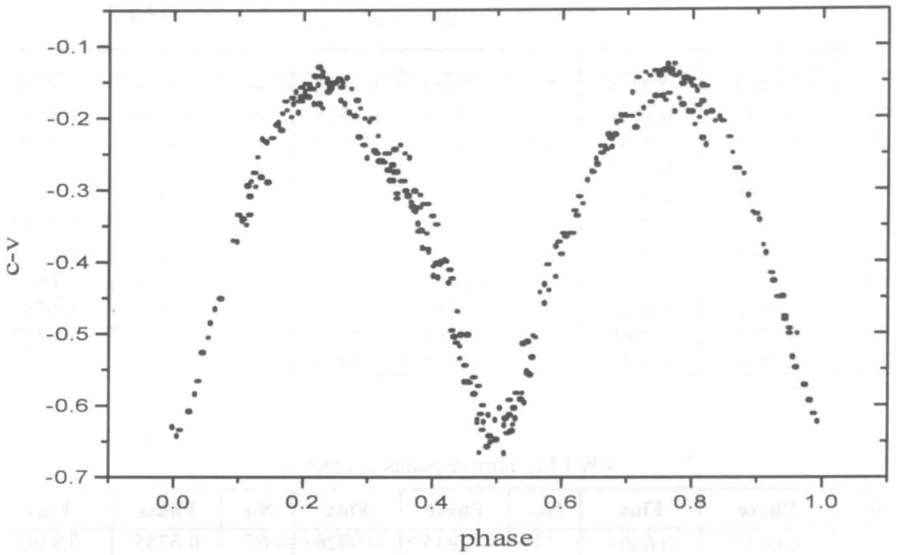

Fig. 2 – VW LMi: light curve observed in B.

Table 2

VW LMi: normal points in color V

No.	Phase	Flux	No.	Phase	Flux	No.	Phase	Flux
1	2	3	1	2	3	1	2	3
1	0.0032	0.6482	23	0.2345	1.0019	45	0.4662	0.6970
2	0.0148	0.6554	24	0.2452	0.9946	46	0.4738	0.6783
3	0.0264	0.6667	25	0.2547	0.9938	47	0.4842	0.6678
4	0.0366	0.6936	26	0.2646	0.9850	48	0.4955	0.6638
5	0.0468	0.7085	27	0.2751	0.9800	49	0.5040	0.6622
6	0.0579	0.7396	28	0.2851	0.9755	50	0.5137	0.6716
7	0.0730	0.7704	29	0.3050	0.9595	51	0.5233	0.6808
8	0.0831	0.7949	30	0.3156	0.9500	52	0.5346	0.6913
9	0.0955	0.8164	31	0.3241	0.9440	53	0.5448	0.7126
10	0.1054	0.8429	32	0.3351	0.9279	54	0.5539	0.7380
11	0.1160	0.8666	33	0.3442	0.9169	55	0.5638	0.7588
12	0.1235	0.8805	34	0.3555	0.9018	56	0.5733	0.7797
13	0.1339	0.9178	35	0.3649	0.8863	57	0.5842	0.8063
14	0.1434	0.9220	36	0.3753	0.8730	58	0.5946	0.8328
15	0.1552	0.9363	37	0.3848	0.8502	59	0.6033	0.8311
16	0.1651	0.9678	38	0.3935	0.8389	60	0.6158	0.8567
17	0.1750	0.9739	39	0.4047	0.8167	61	0.6240	0.8740
18	0.1850	0.9724	40	0.4152	0.8045	62	0.6320	0.8716
19	0.1953	0.9848	41	0.4255	0.7896	63	0.6453	0.8944
20	0.2057	0.9998	42	0.4342	0.7644	64	0.6556	0.9116
21	0.2149	0.9909	43	0.4443	0.7374	65	0.6656	0.9342
22	0.2256	1.0005	44	0.4550	0.7201	66	0.6755	0.9337

Table 2 (continued)

1	2	3	1	2	3	1	2	3
67	0.6862	0.9464	78	0.7945	0.9943	89	0.9050	0.8612
68	0.6942	0.9619	79	0.8046	0.9818	90	0.9159	0.8347
69	0.7056	0.9631	80	0.8137	0.9669	91	0.9261	0.8008
70	0.7162	0.9801	81	0.8228	0.9686	92	0.9348	0.7804
71	0.7268	0.9925	82	0.8352	0.9526	93	0.9453	0.7577
72	0.7370	0.9893	83	0.8461	0.9401	94	0.9551	0.7382
73	0.7461	1.0020	84	0.8577	0.9278	95	0.9624	0.7203
74	0.7573	1.0040	85	0.8664	0.9200	96	0.9755	0.6917
75	0.7652	1.0060	86	0.8766	0.9052	97	0.9850	0.6781
76	0.7758	1.0060	87	0.8860	0.8923	98	0.9944	0.6527
77	0.7836	1.0015	88	0.8955	0.8805			

Table 3

VW LMi: normal points in color B

No.	Phase	Flux	No.	Phase	Flux	No.	Phase	Flux
1	0.0032	0.6403	34	0.3445	0.9026	67	0.6755	0.9303
2	0.0119	0.6418	35	0.3571	0.8880	68	0.6857	0.9464
3	0.04	0.6567	36	0.3661	0.8712	69	0.6952	0.9596
4	0.0366	0.6773	37	0.3756	0.8514	70	0.7065	0.9684
5	0.0468	0.7083	38	0.3848	0.8406	71	0.7167	0.9805
6	0.0562	0.7288	39	0.3938	0.8245	72	0.7275	0.9909
7	0.0657	0.7492	40	0.4052	0.8039	73	0.7370	0.9922
8	0.0744	0.7596	41	0.4160	0.7957	74	0.7449	0.9996
9	0.0840	0.7876	42	0.4265	0.7664	75	0.7541	1.0020
10	0.0933	0.8185	43	0.4345	0.7367	76	0.7648	1.0015
11	0.1042	0.8362	44	0.4433	0.7221	77	0.7748	0.9986
12	0.1167	0.8559	45	0.4549	0.6932	78	0.7836	0.9909
13	0.1245	0.8840	46	0.4661	0.6709	79	0.7961	0.9904
14	0.1348	0.9102	47	0.4735	0.6507	80	0.8058	0.9877
15	0.1441	0.9130	48	0.4846	0.6453	81	0.8146	0.9764
16	0.1552	0.9386	49	0.4970	0.6385	82	0.8228	0.9599
17	0.1656	0.9525	50	0.5034	0.6468	83	0.8330	0.9581
18	0.1750	0.9723	51	0.5145	0.6394	84	0.8461	0.9450
19	0.1854	0.9764	52	0.5251	0.6530	85	0.8577	0.9337
20	0.2046	0.9902	53	0.5351	0.6699	86	0.8664	0.9057
21	0.2156	0.9931	54	0.5452	0.6919	87	0.8737	0.8966
22	0.2256	1.0012	55	0.5549	0.7055	88	0.8864	0.8778
23	0.2350	0.9962	56	0.5638	0.7434	89	0.8970	0.8468
24	0.2452	0.9974	57	0.5740	0.7635	90	0.9057	0.8391
25	0.2569	0.9968	58	0.5806	0.7802	91	0.9137	0.8087
26	0.2652	0.9944	59	0.5935	0.8028	92	0.9260	0.7792
27	0.2755	0.9823	60	0.6040	0.8170	93	0.9348	0.7603
28	0.2866	0.9707	61	0.6148	0.8257	94	0.9435	0.7469
29	0.3054	0.9541	62	0.6245	0.8528	95	0.9527	0.7201
30	0.3152	0.9336	63	0.6334	0.8670	96	0.9624	0.7099
31	0.3246	0.9230	64	0.6457	0.8898	97	0.9755	0.6795
32	0.3246	0.9230	65	0.6548	0.9045	98	0.9850	0.6604
33	0.3348	0.0150	66	0.6646	0.9198	99	0.9944	0.6483

The normal light curves are presented in Figs. 3 and 4.

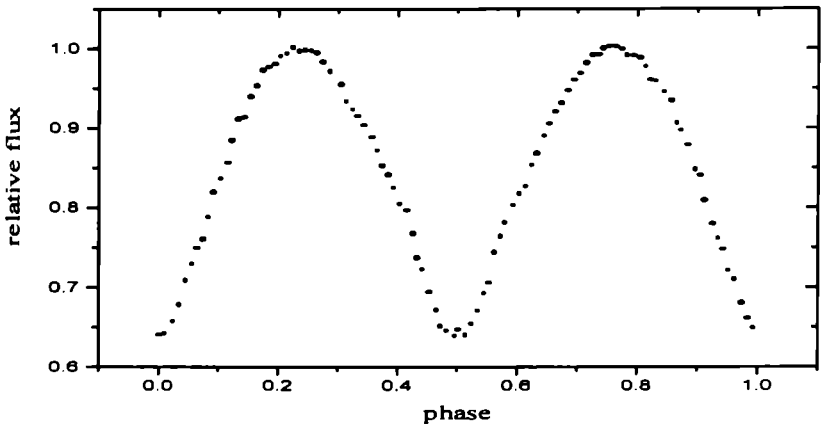

Fig. 3 – VW LMi: normal light curve in V.

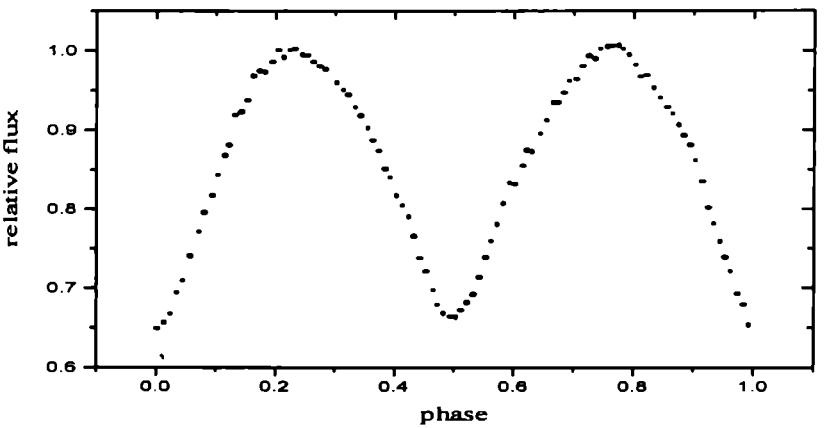

Fig. 4 – VW LMi: normal light curve in B.

3. CONCLUSIONS

A summary analysis of the observed light curves points out that these ones are relatively stable during our observation campaign. Around the light maxima, one can remark small variations of about 0.05 magnitude, probably due to the scattering of observations or to the intrinsic fluctuations of the star. No significant asymmetry of curves is observed. In the pass-band V, the secondary minimum is very well defined and is less deep than the primary one. On the other hand, both minima in the pass-band B have practically the same depths and the secondary one

shows a nonnegligible scattering. The normal light curves are good enough to allow the synthesis of the binary system elements.

REFERENCES

Dumitrescu, A.: 2000, *Inf. Bull. Variable Stars*, No. 4952.
ESA: 1997, *HIPPARCOS Catalogue*, SP-1200.

Received on 15 December 2000

HIGH-SPEED PLASMA STREAMS IN SOLAR WIND DURING THE ELEVEN YEARS SOLAR CYCLE (I)

GEORGETA MARIŞ[1], OVIDIU MARIŞ[2]

[1] *Astronomical Institute of the Romanian Academy*
Str. Cuţitul de Argint 5, RO-75212 Bucharest, Romania
E-mail: gmaris@roastro.astro.ro

[2] *Space Science Institute*
Str. Atomiştilor 1, P.O. Box MG-6, RO-76900 Bucharest – Măgurele, Romania
E-mail: maris@venus.nipne.ro

Abstract. The characteristics of the high-speed plasma streams (HSPS) in the solar wind during the eleven years solar cycle are investigated taking into account only their importance. The analysis is performed on solar cycles 20–22 (more precisely, 1964–1982), separately on the different types of HSPS according to their solar origin. The HSPS solar sources cannot be only solar flares and coronal holes but every energetic event able to produce particle acceleration. The differences between the solar cycle 20 and 21, found in the present study, could be due to the structure of the 22-years solar magnetic cycle.

Key words: solar wind – high-speed plasma streams – 11-years solar cycle.

1. INTRODUCTION

The High-Speed Plasma Streams (HSPS) in the solar wind were put into evidence by many registerings of the Earth-orbiting or solar-orbiting spacecrafts. They are travelling in the heliosphere up to the Earth's orbit and beyond, determining some interplanetary disturbances. They are produced in the solar corona; the identification of their sources is an important task for the understanding of their origin.

The best established sources of the HSPSs are *the coronal holes* – the regions with open magnetic fields in the corona. From the '70s a lot of authors have studied the coronal holes and the recurrent high-speed streams. It has become clear there are also some non-recurrent HSPS that are produced by other solar energetic phenomena.

Four definitions for HSPS, at least, were given, all of them using different limits of *the increase in the wind velocity, the duration of this increase, combined*

or not, with some increase in the density or the temperature of the wind. The corresponding catalogues of the HSPS were established, for different periods of time. Unfortunately, in the last 15 years, the authors have not found such a new catalogue. This is the period when a lot of space missions were, and/or still are, in operation, very important and special missions, such as: Helios I and Helios II, Ulysses, Wind, SOHO, ACE.

The authors intend to study the HSPS distributions during the 11-years solar cycle for a period as long as possible, taking into account their solar origin. It is hard to believe, at present, that all the HSPS could be divided, according to their origin, only in two groups: *co-rotating* – produced by the coronal hole – and *produced by solar flares*. It is well known that other energetic coronal phenomena, such as: sudden disappearing filaments, eruptive prominences, some coronal streamers and coronal mass ejections, are also producing travelling interplanetary disturbances and, consequently, the Earth's magnetosphere disturbances. All these heliospheric "disturbances" have to be registered as *some specific currents in the solar wind.*

2. DATA AND METHOD

We begin with the data having the classic form of the HSPS catalogue. The longest catalogues of this kind for the 1964–1982 period were made by Lindblad et al. (1981, 1983, 1989). We adopted their *selection criteria for the HSPS that emphasized the leading edge of a stream (the velocity gradient* $\Delta V_0 \geq 100$ km/s*) and not the maximum velocity.* The catalogues give the duration (d) of the streams, in days, and the maximum velocity (V_{max}), in km/s. We used these last two parameters to characterize the HSPS and introduce a new parameter, *the importance* of the stream, defined by:

$$I = \Delta V_{max} \times d,$$

where:

$$\Delta V_{max} = V_{max} - V_0.$$

The importance for all the streams registered during each Bartels rotation, $I_B = \sum I$, was calculated. This index gives information about the summed importance of all the streams that appeared during the respective rotation. In the same manner we calculated, $I_Y = \sum I$, the sum of the importance for all the streams registered during a year. Using Lindblad's catalogues, the two indices, I_B and I_Y, were calculated for:

– all the HSPS of Lindblad's Catalogues during each Bartels rotation (Fig. 1a) and during each year (Fig. 1b);

– the co-rotational HSPS during each Bartels rotation (Fig. 2a) and during each year (Fig. 2b);

– the HSPS produced by flares during each Bartels rotation (Fig. 3a) and during each year (Fig. 3b), respectively.

In all figures, the time is marked on the horizontal axis by the number of the Bartels rotation (Figs. 1a, 2a, and 3a) or by years (Figs. 1b, 2b, and 3b). The sums I_γ or I_B for HSPS (total, co-rotational or produced by flares) are represented on the vertical axis.

During the chosen period, two minima and two maxima of solar cycles (SC) took place and twice the polarity of the solar poloidal magnetic field was changed. So, the minimum of the SC 20 was registered on July 1964 and those of the SC 21 on July 1976. Taking into account the monthly relative sunspot number, the maximum value of the SC 20 was registered on March 1969 and those of the SC 21 on September 1979. As for the yearly relative sunspot number the minima of the SCs 20 and 21 were registered during 1964 and 1976, respectively while the two maxima, on 1968 and 1979, respectively. During an eleven years solar cycle, the most stable large-scale magnetic regions are the polar fields. The polar fields reverse polarity at, or a little later than, the solar maximum epoch, and are gradually increasing in strength until the following minimum. The two solar hemispheres do not necessarily reverse magnetic polarity at the same time. Between 1964 and 1982, two magnetic reversions took place: during mid 1969 in south and mid 1971 in north (for SC 20), and during mid 1980 in north and mid 1981 in south (for SC 21).

3. RESULTS AND DISCUSSIONS

The analysis of the HSPS distribution during the solar cycle taking into account only their importance is an incomplete analysis. However, we can see some results in Figs. 1a – 3b.

– The total number of HSPS presents a greater importance in the second part of the descending branch of the solar cycle 20 (Fig. 1a, the Bartels rotations nos 1910–1946, Fig. 1b, 1973–1976). As for the solar cycle 21, it seems to be the same situation for the 1982-year (Fig. 2b). *The two periods with the maximum of the HSPS intensity are situated after the reversal of the polar solar magnetic fields in both solar hemispheres.*

– There also are some *secondary maxima of the HSPS intensity before or just during the maximum of the solar cycles*: 1967–1968 and 1978–1979 (Fig. 1b).

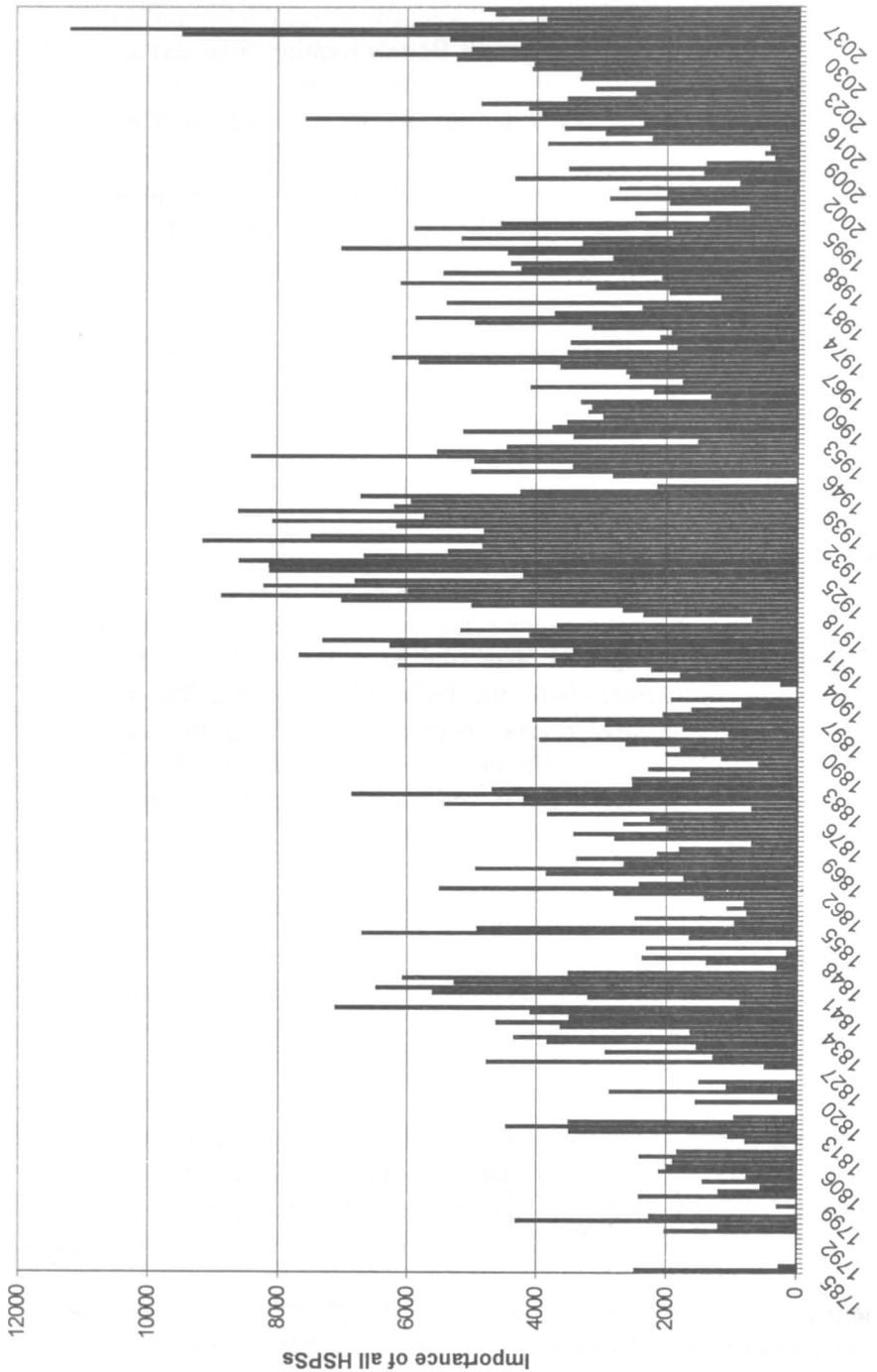

Fig. 1a – The importance of all HSPSs, summed on each Bartels rotation.

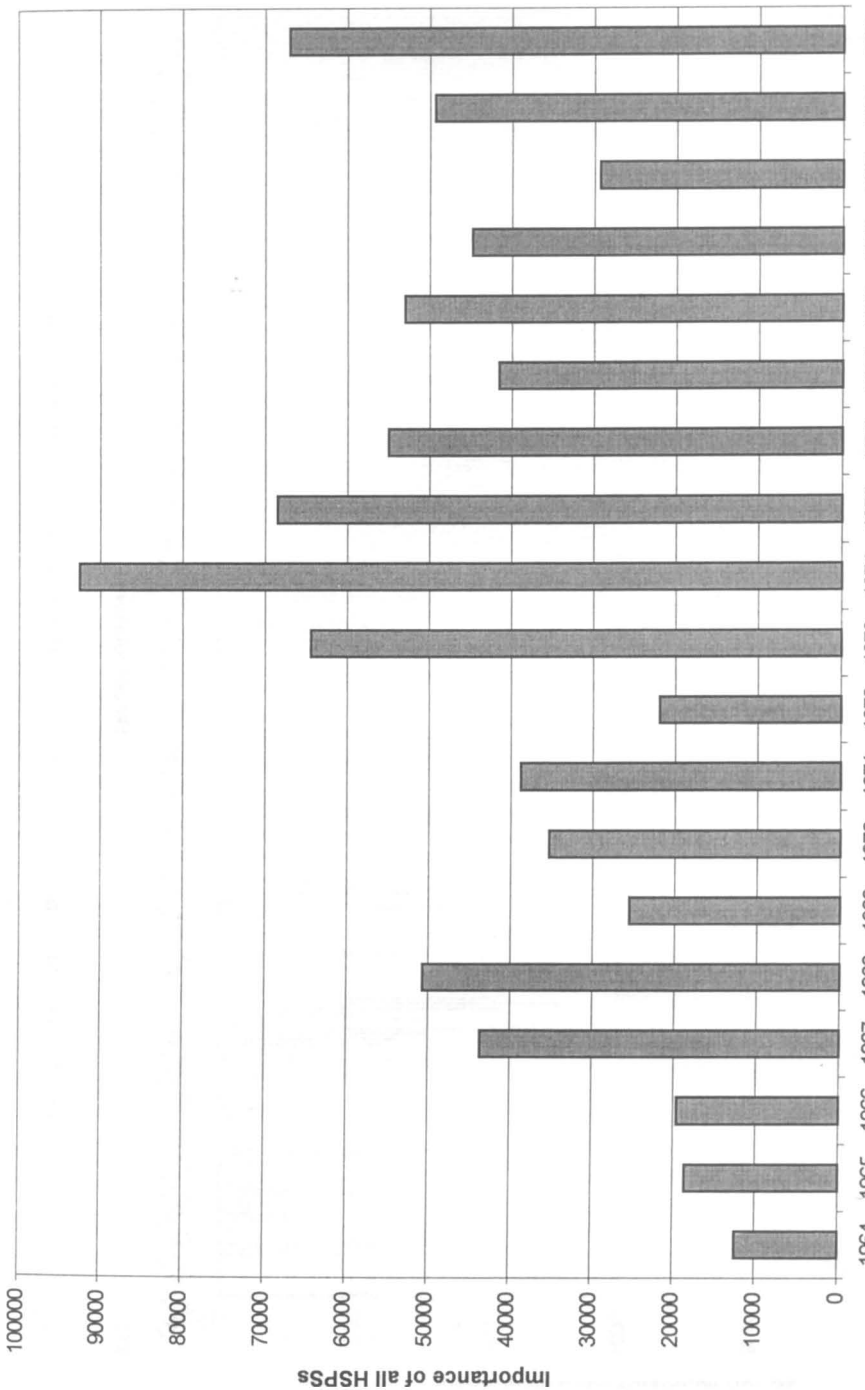

Fig. 1b – The importance of all HSPSs, summed on each year.

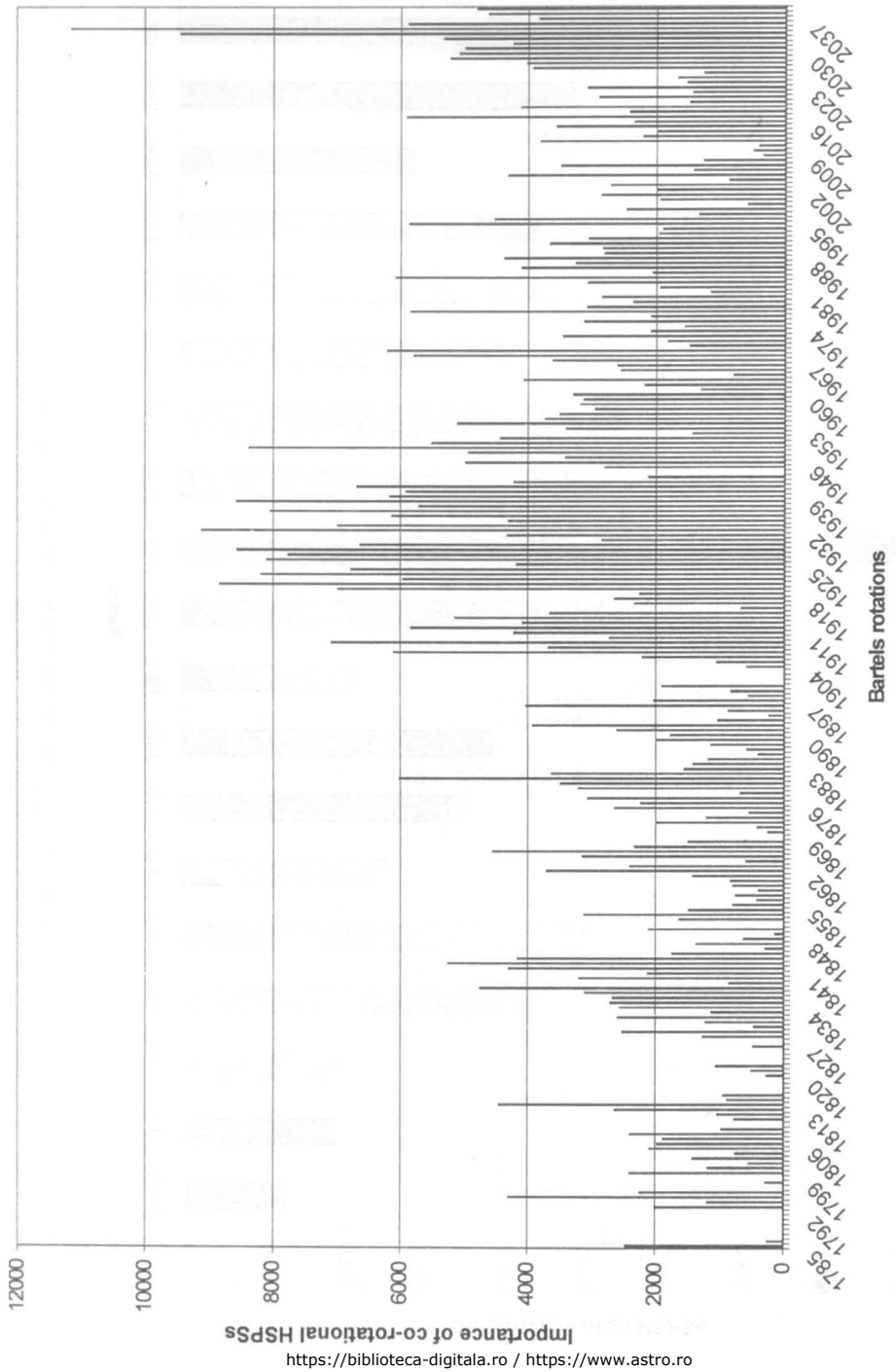

Fig. 2a – The importance of the co-rotational HSPSs, summed on each Bartels rotation.

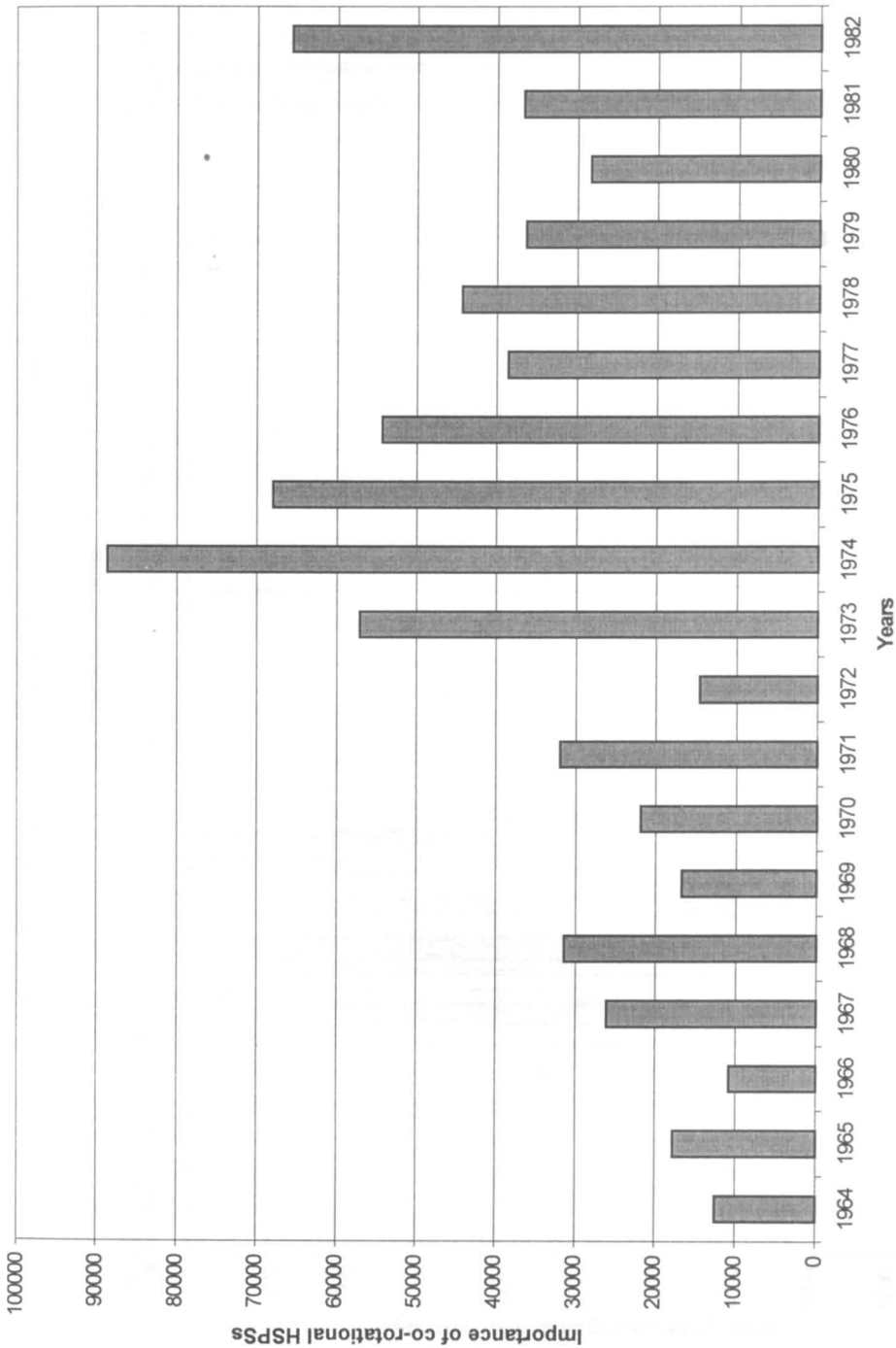

Fig. 2b – The importance of the co-rotational HSPSs, summed on each year.

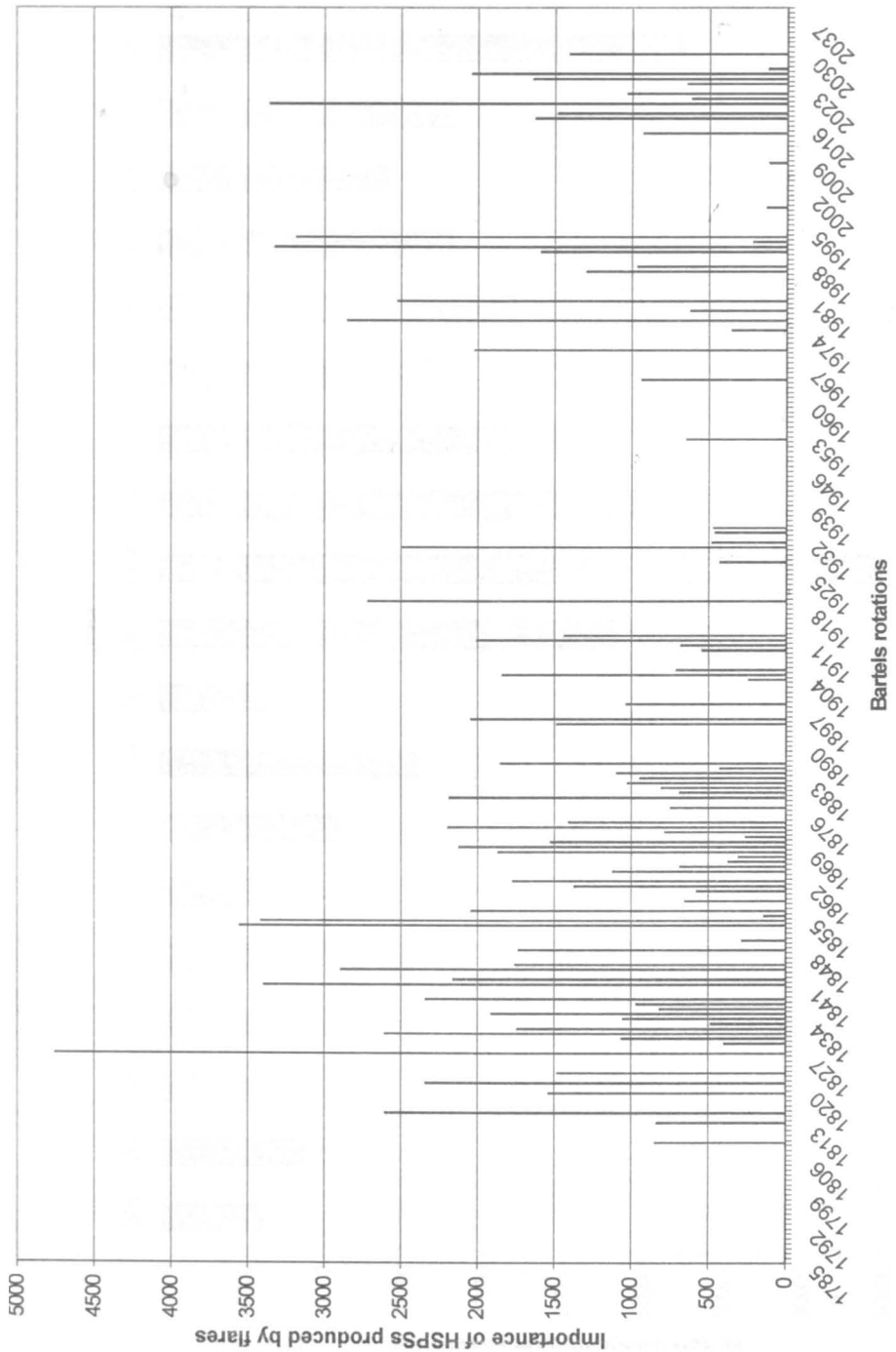

Fig. 3a – The importance of the HSPSs produced by flares, summed on each Bartels rotation.

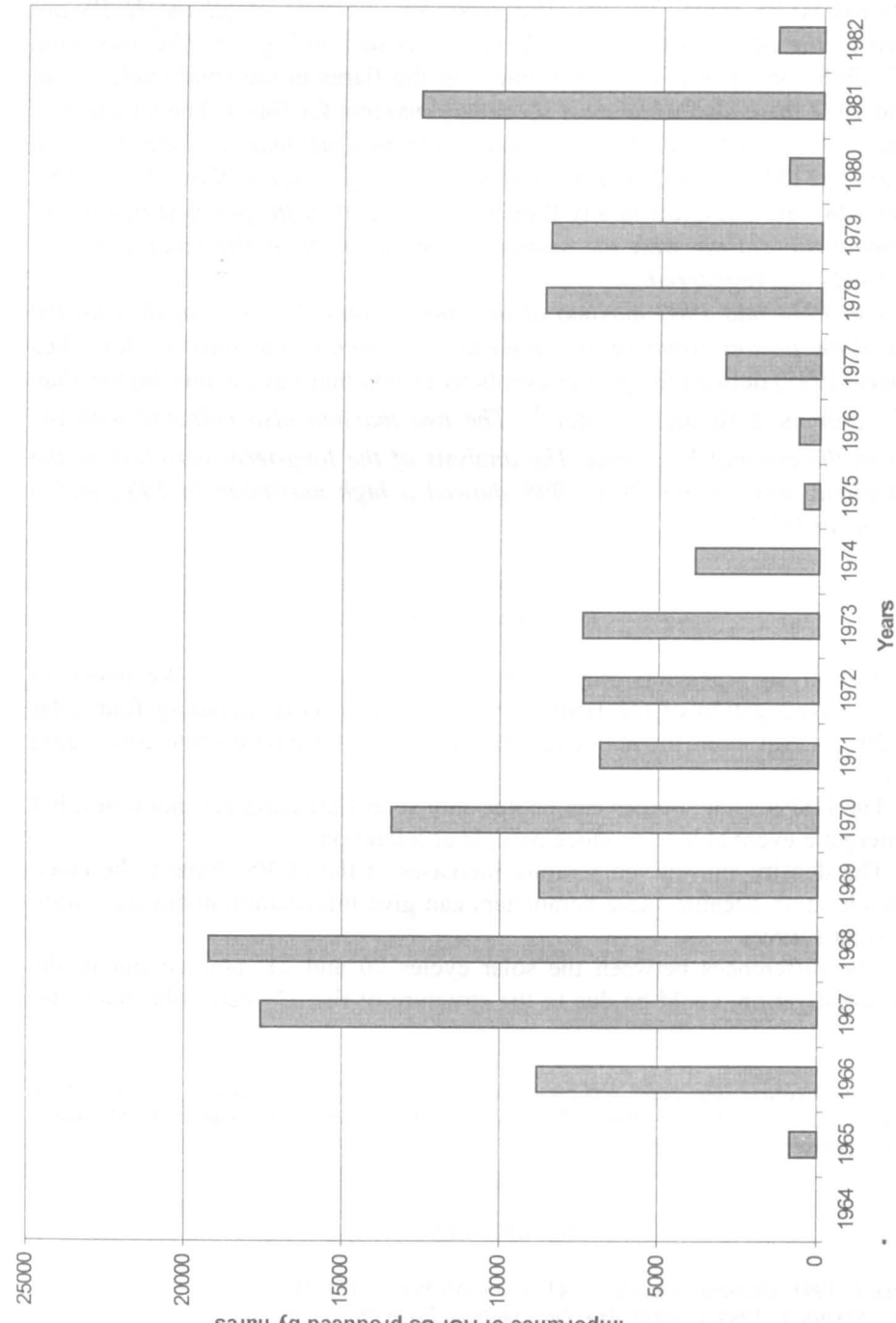

Fig. 3b – The importance of the HSPSs produced by flares, summed on each year.

– The general trend of the total number of HSPS variation is imprinted by the co-rotational HSPS (Figs. 2a, 2b). The *secondary maxima of all the HSPS are imprinted by the HSPSs produced by flare*, as it is seen in Fig. 3b. The maximum of 1967–1968 corresponds to the maximum of the flares in the solar cycle 20. In 1970 and 1972 there also were some secondary maxima for flares. The situation of the solar cycle 21 is totally different: *there were two maxima for solar flares in 1980 and 1982* (Mariş, 1992) *but these years had not productive flares for HSPSs.* The year 1981 did not excel in any flare activity, but then *the greatest number of the geomagnetic storms with the sudden commencement of the solar cycle 21* (Mariş, 1992) *was registered.*

– *The 1974 and 1982 maxima of the co-rotational HSPS coincide with the maxima of the proton events on the descending branch of the solar cycles.* Shea and Smart (1995) defined the proton events as events that have a flux higher than 10 MeV protons ≥ 10 cm^{-2} s^{-1} ster^{-1}. *The two maxima also coincide with the maxima in the coronal hole area. The analysis of the long-term variation in the open magnetic flux during 1971–1998 showed a high maximum in 1982 and a smaller one in 1974.*

4. CONCLUSIONS

This analysis represents only the first step of a longer study. We intend to extend the investigation of the HSPSs over a longer period including four solar cycles: 20–23. However, the above results allow us to formulate some concluding remarks:

– The HSPS solar sources can be not only solar flares and coronal holes, but every energetic event able to produce particle acceleration.

– The density and the temperature increases of the HSPSs have to be taken into consideration because these parameters can give information about the nature of their solar sources.

– The differences between the solar cycles 20 and 21, pointed out in the present investigation, could be due to the structure of the 22-years solar magnetic cycle.

Acknowledgement. The paper was presented at JENAM 2000, S07: *Solar Cycle: Sun at the Top of Maximum*, May 29 – June 3, 2000, Moscow, Russia. One of the authors (G. M.) thanks the organizers for travel support.

REFERENCES

Hoeksema, J.: 1991, *Geomagn. Geoelectr.*, **43**, (COSPAR Paper STPI. 25).
Kulcar, L., Sykora, J.: 1994, *Contrib. Astr. Obs. Skalnate Pleso*, 79.

Lindblad, B. A., Lundstedt, H.: 1981, *Solar Phys.*, **74**, 197.
Lindblad, B. A., Lundstedt, H.: 1983, *Solar Phys.*, **88**, 377.
Lindblad, B. A., Lundstedt, H., Larsson, B.: 1989, *Solar Phys.*, **120**, 142.
Mariş, G.: 1992, *Rom. Astron. J.*, **2**, 25.
Sanchez-Ibarra, A.: 1990, *Solar Phys.*, **122**, 125.
Shea, M. A., Smart, D. F.: 1995, *Adv. Space Res.*, **9**, 37.
Tang, F., Wang, H.: 1991, *Solar Phys.*, **132**, 247.
Wang, Y.-M., Lean, J., Sheeley, N. R., Jr.: 2000, *Geophys. Res. Lett.*, **27**, 505.

Received on 14 November 2000

PHYSICS OF THE BASE OF THE OUTFLOW JET IN ACTIVE GALACTIC NUCLEI

FĂNEL DONEA, ALINA-CĂTĂLINA DONEA

Astronomical Institute of the Romanian Academy,
Str. Cuțitul de Argint 5, RO-75212 Bucharest, Romania
E-mail: fdonea@roastro.astro.ro

Abstract. A new aspect of the physics of the base of the outflow jet at the center of an active galactic nuclei is addressed. The energy budget, including the conservation laws of mass are analysed in the context of the existence of a self-symbiotic system with a black hole, a relativistic disc and a bipolar outflow. The velocity of expansion of the jet anchored at the boundary layer is analysed. A thorough discussion is dedicated to the boundary layer and the corona of the accretion disc.

Key words: accretion disc – X-ray fluxes – active galactic nuclei – symbiosis.

1. INTRODUCTION

Every active galactic nucleus has jets and relativistic accretion discs, and the two elements are strongly related. The accretion disc systems produce outflows and the budget energy of the jet is controlled by the accretion rate onto the central engine. The physics of the jet and the accretion disc is actually dominated by the black hole. The black hole may be rotating with the maximum angular momentum equal to $a_* = 0.9981$, where a_* is its specific angular momentum divided by the mass of the black hole. The great-observed luminosities observed in AGN require supermassive black holes with masses $M \in [10^8 M_{Sun}, 10^{10} M_{Sun}]$. The black holes possess deep gravitational potential wells and work like powerful engines. The disc-like accretion is an efficient mechanism for converting the rest-mass energy into radiation.

The standard relativistic disc model has been introduced by Novikov and Thorne (1973). The presence of the jet changes the accretion disc boundary at the inner edge. Since this is the key in understanding the physics of powering the jet people have been looking deeply at the short variability in spectra, which may be connected to the inner regions of the accretion discs (F. Donea, 1998; Donea et al., 2000). The matter accreted towards a supermassive black hole is the primary source

Rom. Astron. J., Vol. 10, No. 2, p. 129–135, Bucharest, 2000

for mass outflows from the inner dense part of a disc and the fact that a large fraction of the energy from the inner disc is not radiated away but dissipated into the jet.

We assume that the jet starts between R_{ms}, the last marginally stable orbit in the absence of a jet and the radius R_{jet} with $R_{jet} > R_{ms}$, extracting mass, energy and angular momentum from the disc (Donea and Biermann, 1996). The presence of the jet will modify both the behaviour of the infalling matter across the radius R_{jet} and the structure of the relativistic disc. As we mentioned before, the gravitational potential energy released between R_{ms} and the outer radius of the jet R_{jet} goes into the jet. Therefore, the total energy carried by the jet outside is strongly dependent on the mass and angular momentum of the black hole.

It has been found that the relativistic effects and the presence of the jet modify the locally emitted spectrum. Radiation emitted locally by the accretion disc is modified by general-relativistic red shift effects. For the Kerr black hole, the emerging spectrum is harder. Due to Doppler boosting and gravitational focusing the spectrum will dominate at higher frequencies if viewed by an observer at high inclination angles. These relativistic corrections to the spectrum increase in importance as a_* increases.

In this paper we revised the mass flux of the jet, right at its origin. We introduce a new element of the accretion process, the hot corona of the accretion disc. Our calculations are based on former analysis of the soft X-ray excess from some quasars (Mannheim, 1995), which suggested the dimension of the foot of jet. The Comptonization process is a key in understanding the local geometry. The hot electrons of the jet reheat the UV photons coming upwards from the disc.

2. THE MASS FLUX RATE AT THE JET BASE

The following considerations of the mass flux along the jet relate the properties of the jet base to those of the corona above the accretion discs.

For a first estimation, one considers the classical parameters of the jet-disc symbiosis for the accretion around a Kerr black hole:

$$M = 10^8 M_{Sun}\,; \qquad \dot{M} = 10^{-1} M_{Sun} / \mathrm{yr}\,.$$

Falcke and Biermann (1997) and Bicknell et al. (1998) have estimated the jet velocity and the Lorentz factor along the outflow direction. Following their suggestion, that the jet velocities in Seyfert galaxies have relativistic origins (the radio power galaxies have already been classified as AGN with highly relativistic jets), we take an initial jet velocity $\beta = 0.3c$. A mildly relativistic jet has $\beta = 0.5c$.

Falcke and Biermann (1995) and Donea and Biermann (1996, 1997, 1998) have considered that a substantial fraction of the energy dissipated by the accretion disc goes into the total power of jet. The jet is anchored at the boundary layer of the relativistic disc (see Fig. 1).

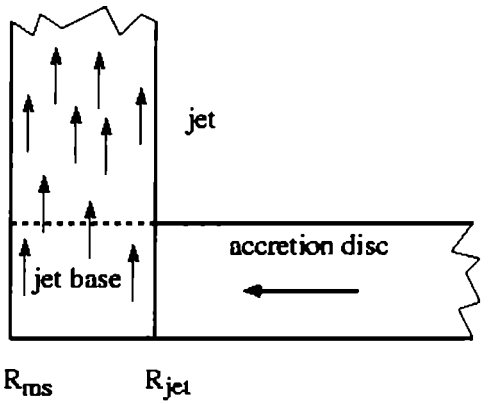

Fig. 1 – The picture of the jet base in the symbiosis model. The inner part of the disc is now part of the jet. The thickness of jet is given by R_{ms} and R_{jet}. The whole structure of the accretion disc is modified in the presence of the jet.

The subkeplerian motion of the gas, below R_{jet} drives the new properties of the jet base. The matter is no longer attracted towards the black hole, but escapes through the magnetic channels perpendicular to the plane of the disc.

The important parameter for understanding details of the physics at the base of the jet is R_{jet} (this gives the thickness of the jet at its origin, Fig. 1). A general accepted value is $R_{jet} = 10R_g$, where the gravitational radius is:

$$R_g = \frac{GM}{c^2}, \tag{1}$$

$$R_g = 1.48 \cdot 10^{13} \text{ cm},$$

where G is the gravitational constant, M is the mass of black hole, and c is the speed of light.

A redirection of the mass towards large distances from the central mass modifies the budget of energy and mass of the accretion disc. The boundary conditions of equations, at the radius R_{jet} are different (Donea and Biermann, 1996). We work with the dimensionless parameter q_m:

$$\dot{M}_{jet} = q_m \dot{M}_{accr} \tag{2}$$

($q_m = 0.1$, that is, only a small fraction of the swallowed mass is expelled outwards by the jet; Falcke and Biermann, 1995).

The relativistic mass flux at the base of the jet is:

$$\dot{M}_{jet} = \pi R_{jet}^2 n \Gamma_1 \beta_1 c m_p , \tag{3}$$

where n is the density of plasma, β_1 is the velocity of jet over the speed of light, Γ_1 is the Lorentz factor of the jet, m_p is the proton mass.

Mannheim (1995), Donea and Biermann (1996), Johnson et al. (1997), and F. Donea (1998) have calculated the UV photons of the disc which are thermally Comptonized at the base of jet. The resulting spectrum covers the soft X-ray emission of quasars. The Thompson optical depth of the base of the jet:

$$\tau = n \sigma_T R_{jet} \tag{4}$$

The density of the jet, right at its footprint, is considered to be similar with the density of the relativistic disc (Novikov and Thorne, 1973). Of course, the density of the jet can be diluted along the Z axis. One can also borrow a disc-corona model of the density of jet (Johnson et al., 1997). Soft X-ray excesses were found by ROSAT observation (Mannheim et al., 1995). Fitting the data and considering the Compton y parameter:

$$y = \frac{4KT}{m_e c^2} \max\{\tau_e, \tau_e^2\} , \tag{5}$$

where T is the disc temperature, m_e is the electron mass and τ_e is the optical depth.

Close to the accretion disc, at $R = 10R_g$: $\tau \le 3$ and $y \le 2$. Such conditions lead to a power-law spectrum attached to the UV bump from the disc, with an X-ray flux density spectral index $\alpha \le 1$.

After replacing (3) and the value of R_g in (2):

$$\dot{M}_{jet} = q_m \dot{M}_{accr} = \frac{\pi m_p c \cdot 1.5 \times 10^{13} \text{yr}}{6.67 \times 10^{-24} M_{Sun}} \cdot \tau \Gamma_1 \beta_1 m_8 \frac{r_1}{R_g} \frac{M_{Sun}}{\text{yr}} , \tag{6}$$

$$q_m = \frac{\Gamma_1 \beta_1 \cdot 5.5 \times 10^{-3} \tau m_8 \frac{r_1}{R_g}}{\dot{m}_{accr}} . \tag{7}$$

For $\tau = 3, r_1 = 10R_g, \dot{m}_{accr} = 0.1, \beta_1 = 0.3 \Rightarrow q_m = 0.5$.

For $\tau = 3, r_1 = 10R_g, \dot{m}_{accr} = 0.1, \beta_1 = 0.5 \Rightarrow q_m = 0.8$.

This result shows that the mass flux at the base of the jet is much higher than the initial assumed value $\dot{M} = 0.1\dot{M}_{accr}$. This inconsistency has suggested us a new image of the central part of an AGN. The base of the jet is indeed anchored in the inner parts of the disc. The cylindrical shape of the jet may not be a proper description of the real physics of the jet. A parabolic shape is much suitable (see Fig. 2). Since Bicknell et al. (1998) have calculated that the jet entrains the environment of the Seyfert galaxies at tens of parsecs scale, we believe that, within the smallest scale of less than one parsec, there is also an entrainment of the corona mass. The corona has a density much higher that the intergalactic medium, even larger than the NLR region. This is a clear indication of a suction mass process occurs, adding mass flux to the budget of mass.

Therefore, large values of q_m equal to 0.5, 0.8 are allowed as long as the suction process is considered:

$$\begin{aligned} &\dot{M}_{jet} = \dot{M}_{basejet} + \dot{M}_{corona}, \\ &\tilde{q}\dot{M}_{accr} + q_c\dot{M}_{accr} = q_m\dot{M}_{accr}, \\ &\tilde{q} + q_c = q_m. \end{aligned} \tag{6}$$

This result is not surprising, since the corona and the disc are also parts of the symbiosis at the inner regions of the relativistic disc. When the dimensionless parameter q_c is equal to 0, there is no contribution to the mass outflow from the corona. Parameter $\tilde{q}$ $(\tilde{q} \le 1)$ is the fraction of mass flux extracted from the accretion disk.

We emphasize here the difference between our model and Bicknell et al. (1998) model. The second model assumes that the jet originates from the coronal region of the black hole accretion disc and that the appropriate radius is of order 10 gravitational radii. We say that the jet is anchored in the disc and that the corona is an additional feeding source of the disc. Of course, there must be no coincidence in choosing the same dimension of the system $(10\,R_g)$ since this is the place where the main coronal dissipation occurs.

However, the understanding of the geometry of the jet base does not answer the question about the relativistic origin of the jet. There have been numerous observations of radio emission in Seyferts and quasars, which indicate collimated outflow. If *FR* 1 galaxies have jets, which are relativistic from their origin, the main question is whether the Seyfert jets are also relativistic. We have tried to explain in this chapter where the jet is formed and what may be the most probable image of its base.

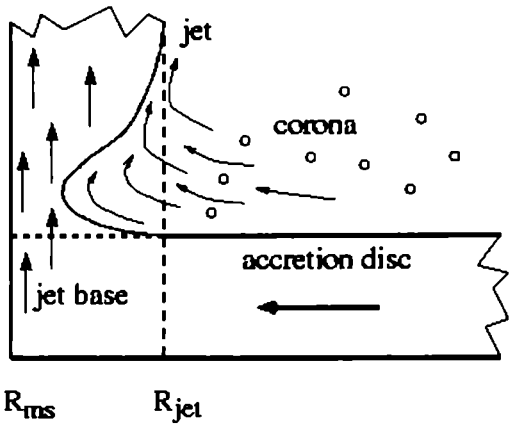

Fig. 2 – The corona of the relativistic disc is one of the important elements of the symbiotic system of an AGN. The base of the jet has a parabolic shape and the large radius of the base is $R_{jet} = 10R_g$. The corona, at the conjunction region of the disc and jet, obeys the suction process.

3. CONCLUSIONS

Active Galactic Nuclei (AGN) are among the most studied objects in current astrophysical research. Their most striking characteristic is the enormous energy output. There is enough experimental evidence that jets of matter can be thrown out of the so-called *boundary layer*, the region of the disc close to the black hole. The outflow entrains at different scales, either is subparsec or tens of parsec scale, matter surrounding the central part of an AGN. The corona of the relativistic jet provides an additional nonnegligible mass to the jet. The base of the jet should have a parabolic shape, which is much closer to a hydrodynamic description of an outflow through a very tied magnetic channel. However, a further analysis is required for understanding what is the outflow velocity of the jet. We show that corona is an important element of the symbiosis jet-disc and the final shape of the base of the jet is actually dictated by the temperature and the pressure of the corona acting on the outflow.

REFERENCES

Bicknell, G. V., Dopita, M. A., Tsvetanov, Z. I., Sutherland, R. S.: 1998, *Astrophys. J.*, **495**, 680.
Donea, A.-C., Biermann, P. L.: 1996, *Astron. Astrophys.*, **316**, 43.
Donea, A.-C., Biermann, P. L.: 1998, *Publ. Astron. Obs. Belgrade*, **60**, 34.
Donea, A.-C., Masnou, J.-L., Donea, F.: 2000, *Proc. Conf. Gamma-Ray 2000* (to appear).
Donea, F.: 1998, *Publ. Astron. Obs. Belgrade*, **60**, 30.

Falcke, H., Biermann, P. L.: 1996, *Astron. Astrophys.*, **308**, 321.
Mannheim, K.: 1995, *Astron. Astrophys.*, **297**, 321.
Mannheim, K., Schulte, M., Rachen, J.: 1995, *Astron. Astrophys.*, 303, 41.
Novikov, I. K., Thorne, K. S.: 1973, *Les astres occlus*, eds. C. DeWitt, B. DeWitt, Gordon & Breach, New York.

Received on 16 September 2000

EMISSION IN ABSORBTION LINES: RESULTS OF THE SL9 L NUCLEUS IMPACT WITH JUPITER

MIREL BÎRLAN [1,2]

[1] *Observatoire de Paris-Meudon, DESPA*
F-92195 Meudon Cedex, France
E-mail: Mirel.Birlan@obspm.fr

[2] *Astronomical Institute of the Romanian Academy*
Str. Cuțitul de Argint, RO-75212 Bucharest 28, Romania

Abstract. High-resolution spectra of the impact sites and impact of the comet Shoemaker-Levy 9 with Jupiter have been performed at the Pic-du-Midi Observatory. The excitation of several chemical elements (Fe, Ca, Ba, Na, Mn, Mg, etc.) has been identified during the analysis of the L nucleus impact spectra obtained in visible and near-IR. The article presents the atomic lines and the time evolution of nine of them.

Key words: spectroscopy – comets – atomic lines.

1. INTRODUCTION

One of the major astronomical events of 1994 was the impact of the comet Shoemaker-Levy 9 with Jupiter. The astronomical community observed this event within the framework of the coordinated program; several ground-based and space instruments have been involved. SL9/Jupiter impact was a unique event (until now); before the show "live" of the impact SL9 comes inside Jupiter's Roche limit which broken the nucleus in 22 fragments.

The first impact for each nucleus occured on an unfavourable geometry, on the hidden part of Jupiter, not far from the limb. However, relevant data concerning the impacts were collected as soon the impact effects become visible.

2. OBSERVATIONS

The paper presents the spectroscopy in the wavelength range of visible and near-IR (5460-8750 Å) performed for the L impact site. The observations were performed with the 2-meter Bernard Lyot telescope from the Pic du Midi Observatory. The spectra were recorded by a 1024 × 1024 Thomson CCD chip, and

Rom. Astron. J., Vol. 10, No. 2, p. 137–144, Bucharest, 2000

the spectral resolution was 36 000. The fibber of the spectrograph has 50 microns, which corresponds to a field of view of 2.2". This field of view is small enough to obtain high quality spectra only from the impact site (the apparent diameter of Jupiter is about 38"). The guidance software of the telescope allows both automatic/manual tracking during the exposure.

3. DATA REDUCTION

The pre-treatment of the observed data was performed using MUSICOS software. MUSICOS makes the calibration pixel-wavelength for the intensities spectra. Each spectrum was split in several wavelength intervals (named "orders") which little overlap between the adjacent orders. For the analysis in the absorption line we choose as target on Jupiter the L impact site for July 19/20 at 22:30:55 UT (referred to as S167), and July 20/21(referred to as S213), 1994. As reference, the Jupiter spectrum was taken on July 20/21 (referred to as R216). The spectrum S167 emission lines have already been analysed in several papers (Roos-Serote et al. 1995a,b; Barucci et al. 1995).

The MIDAS software procedures for spectroscopy were employed. The goal of this work was to check the atomic absorption line depth one day after the impact moment and to see the excitation of different atoms of Jupiter-SL9 L impact plume. To reach this goal, all the orders of both spectra of impact site were compared with the reference spectrum R216. Then the results S213/R216 and S167/R216 in each order were compared.

In this treatment, the major problem of the differential rotation of the atmosphere of Jupiter occured. From an order to another, in different spectra, the same atomic line presents a slight shift in wavelength, following the expression:

$$\frac{\Delta\lambda}{\lambda} = \frac{v_{diff}}{c},$$

where v_{diff} denotes the differential speed of Jupiter and c stands for the speed of light.

Thus, an automatic procedure of shift cannot be taken into account. For a good preliminary result in some orders the spectra were rebined. Then, shifting the lines in such a way made the subtraction or division between spectra, so that the minima of the lines are at the same wavelength.

The cosmic ray signatures represented another problem that occured during the treatment. This was skipped manually, each time when the spectrum of Jupiter had no lines in this region, and one given atomic line had an abnormal profile.

At least, we cannot omit the presence of the terrestrial lines, even after a major part of them where eliminated by an automatic procedure. Their presence could alter our qualitative analysis and they were carefully analysed and skipped.

4. RESULTS

The comparison of the L impact site spectra with the unperturbed Jupiter's atmosphere spectrum was made in order to minimize any ambiguity. Then the shifted spectra S167 and S213 were compared in each order. To obtain a good signature for each excited atomic line, the ratio S167/S213 has been analysed. As presented in Fig. 1, only the signatures of atomic lines with amplitude larger than three times the noise amplitude were considered (three sigma relevance).

The analysis reveals orders on which the spectral lines were not perturbed by the impact of the comet (as seen on Fig. 2). At the opposite, there are spectral intervals where almost all of the atomic lines were perturbed.

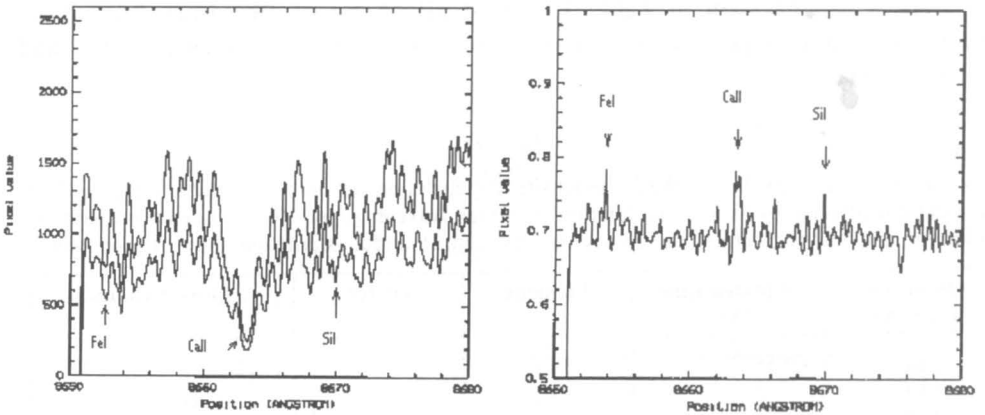

Fig. 1 – Left: Spectra of the 65-th order of R216, and S213 (upper and lower spectrum, respectively). On the center of this order the Paschen $n = 13$ absorption line of Ca II ion. Right: Signatures of Ca II, Fe I, and Si I after the S213/R216 computation.

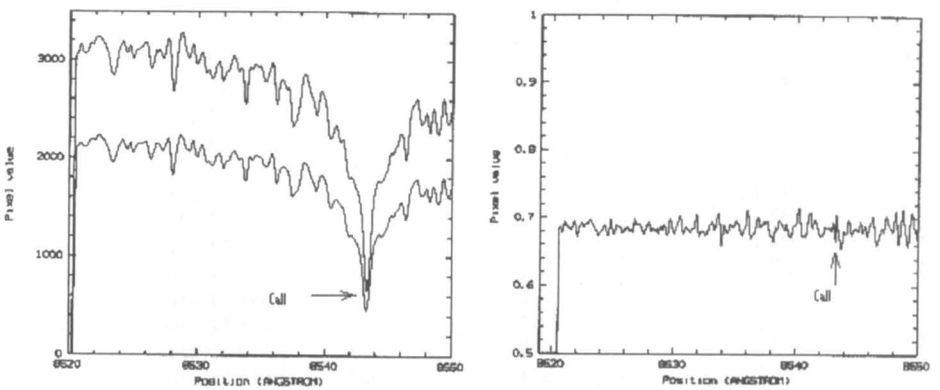

Fig. 2 – "Quiet" order. Spectra of the 66-th order of R216, and S213 (upper and lower spectrum, respectively) containing Paschen line $n = 15$ of Ca II ion (left plot). The result of the S213/R216 computation (right plot).

For the S213, almost of the orders are "quiet". At the opposite, the S167 spectrum presents high differences for several atomic lines (Fig. 3). Thus, the Fe I, II, and III lines are excited on almost all of orders as well as the representative lines of Ca I, and II ions.

Table 1 lists the excited lines. In a first time the line identification was made taking as origin the profile of spectral lines from *The High Resolution Spectral Atlas of the Solar Irradiance* by Beckers, Bridges and Gilliam (1976), and *The Solar Spectrum from λ 6000 to λ 13495* by Babcock and Moore (1947). Then our identification was refined using the articles of Morton (1991, 2000), Morton and Noreau (1994), and the VizieR database of atomic lines (http://vizier.u-strasbg.fr), Reader and Corliss, and Hirata catalogues.

As it can be seen in Table 1, almost all of the excited lines from S167 spectrum become unperturbed 24 hours after (time interval between the S167 and S213 spectra).

Table 1

Atomic lines were identified on the L impact site. For each line, the order of spectra, wavelength of spectral line affected by differential rotation of Jupiter, wavelength of spectral line from literature, element, and notes concerning these lines are presented. Doubtful assignations were marked with *

Observed Line (Å)	Tabulated Line (Å)	Element	Order	Observations
1	2	3	4	5
5498	5497.77	Fe II	103	S167/R216
5502	5502.30	Fe II	103	S167/R216
5507	5506.44	Fe II	103	S167/R216
5511	5512.98	Ca I	103	S167/R216
5511	5510.61	Cr I	103	S167/R216
5527	5526.8	Sc II	102	S167/R216
5533	5535.05	Mo I	102	S167/R216
5535	5534.83	Fe II	102	S167/R216
5536	5535.5	Ba I	102	S167/R216
5536	5535.38	Fe II	102	S167/R216
5566	5565.37	Fe II	102	S167/R216
5573	5572.62	Fe II	102	S167/R216
5582	5581.97	Ca I	101	S167/R216
5589	5588.76	Ca I	101	S167/R216
5591	5590.12	Ca I	101	S167/R216
5593	5592.28	Ni I	101	S167/R216
5595	5594.47	Ca I	101	S167/R216
5628	5627.64	V I	100	S167/R216
5631	5630.76	C I	100	S167/R216
5648	5647.22	Co II	100	S167/R216
5658	5657.88	Sc II	100	S167/R216
5676	5675.73	Si I	100	S167/R216
5710	5708.93	Fe II	99	S167/R216
5737	5736.75	Ca I	99	S167/R216
5788	5787.9	Cr I*	98	S167/R216

Table 1 (continued)

Observed Line (Å)	Tabulated Line (Å)	Element	Order	Observations
1	2	3	4	5
5853	5853.45	Fe II	97	S167/R216
5858	5857.45	Ca I	97	S167/R216
5863	5862.89	Fe I	97	S167/R216
5890	5889.95	Na I	96	S167/R216
5896	5895.92	Na I	96	S167/R216
5915	5914.97	Fe II	96	S167/R216, S213/R216
5984	5983.86	Fe II	95	S167/R216
6014	6013.5	Mn I	94	S167/R216
6017	6016.6	Mn I	94	S167/R216
6066	6065.83	Fe II	93	S167/R216
6123	6122.22	Ca I	92	S167/R216
6142	6141.72	Ba II	92	S167/R216
6163	6162.17	Ca I	92	S167/R216
6176	6176.05	N II	92	S167/R216
6210	6209.73	Fe I	91	S167/R216
6226	6225.92	Cr II*	91	S167/R216
6243	6242.87; 6242.9	Ca I*; Mn I*	91	S167/R216
6245	6244.47	Si I	91	S167/R216
6319	6318.66	Fe II	90	S167/R216
6359	6358.76	Fe II	89	S167/R216
6439	6439.07	Ca I	88	S167/R216
6451	6449.81; 6450.24	Ca I+Co I	88	S167/R216
6472	6471.66	Ca I	87	S167/R216, S213/R216
6494	6493.78	Ca I	87	S167/R216
6496	6495.78	Fe I	87	S167/R216, S213/R216
6498	6498.75	Ba I	87	S167/R216, S213/R216
6501	6499.65	Ca I	87	S167/R216, S213/R216
6563	6562.85	H I	86	S167/R216
6574	6572.78	Ca I	86	S167/R216
6679	6678.9	Fe II	85	S167/R216
6708	6707.91; 6707.76	Li I	84	S167/R216 (double)
6978	6978.48	Cr I	81	S167/R216
7289	7288.88	Fe II	78	S167/R216
7290	7290.26	Si I	78	S167/R216
7326	7326.15	Ca I	77	S167/R216, S213/R216
7327	7325.51	Mn I	77	S167/R216, S213/R216
7853	7852.86	C I*	72	S167/R216
7858	7858.09	Fe III	72	S167/R216
7938	7938.06	Fe II	71	S167/R216
8095	8094.93	Fe I	70	S167/R216
8187	8186.97; 8186.99	F III*, Mn II*	69	S167/R216
8195	8194.70	Fe I	69	S167/R216
8405	8404.77; 8404.84	Mn III*, Fe II*	66	S167/R216
8415	8414.89; 8414.95	Fe II*, F I*	66	S167/R216, S213/R216
8664	8662.14	Ca II	65	S167/R216, S213/R216
8683	8683.4	N I	65	S167/R216, S213/R216
8710	8710.03	Fe I	65	S167/R216, S213/R216
8737	8736.02; 8736.48	Mg I, Mn I	65	S167/R216
8790	8789.34	Fe I	65	S167/R216

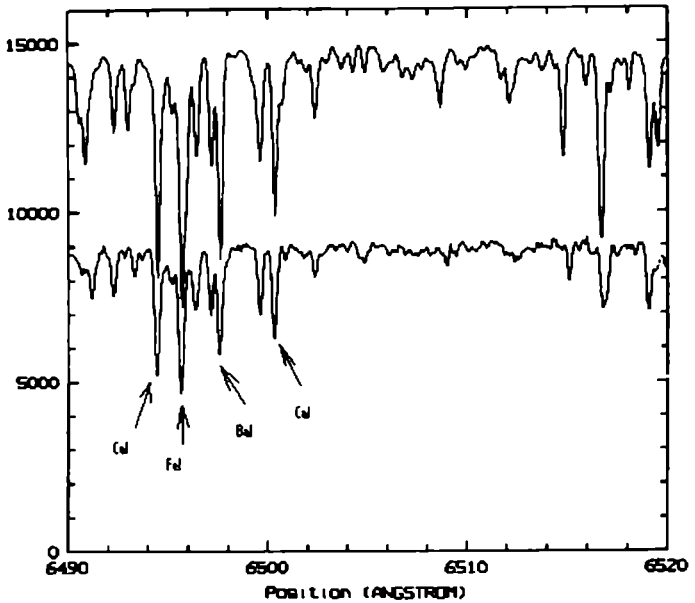

Fig. 3 – Order 87 on S167 (top), and R216 (bottom) spectra. We can distinguish the perturbed lines of Fe I, Ca I, and Ba I lines (marked by arrows).

However, some excited lines are present in both spectra (S167 and S213). In order to have their temporal evolution, casually the orders of a third spectrum were analysed. This spectrum (S166) was taken on July 19/20, 1994, just at the moment that L impact site and plume appeared on the Jupiter visible hemisphere. Table 2 presents such an evolution in the case of some important lines. The percentage values given by the last three columns of Table 2 are computed only from the geometrical consideration, taking into account the depth of the line in the R216 spectrum.

Table 2

The evolution of some spectral lines in three analysed spectra. The spectral line contains the differential rotation shift imposed by Jupiter's rotation.

Element	Wavelength (Å)	S166/R216	S167/R216	S213/R216
Ca I	6472	26%	25%	7%
Ca I	6494	13%	20%	–
Fe I	6496	26%	29%	13%
Ba I	6498	16%	20%	1%
Li I	6708	3%	24%	–
Ca II	8664	84%	70%	10%
N I	8683	15%	33%	13%
Fe I	8790	44%	35%	–
Mg I, Mn I	8737	16%	25%	–

We have paid a special attention to the hydrogen quadrupolar momentum lines. We have searched for the S(0) – S(3) H signatures (6270.24 Å, 7959.77 Å, 8150.67 Å, and 8272.67 Å, respectively), but our search has not provided positive results.

5. DISCUSSION

The greatest part of the absorption atomic lines of the solar spectrum (of our spectral interval) remained unperturbed after the reflection on Jupiter. The Jovian atmosphere does not present metallic compounds on the analysed spectral interval, the profile of Jupiter's spectrum reproduces the solar spectrum. The perturbed spectra come from the L impact site. Therefore, we can formulate the conclusion that the most significant part of this excitation was released by the cometary material.

Various mechanisms could be responsible of the presence of the atom excitation. The perturbation of atomic lines could be explained as the effect of such a mechanism (or several such mechanisms). As long as the goal of this article is to present the qualitative results of spectra analysis, these mechanisms will be only remembered. However, the author intimate conviction is that different excited lines could be explained only by individual theories.

The main known mechanisms are: the resonant fluorescence, the thermal collision (if we consider the temperature on the impact site and plume greater than 1000 K), and the electronic recombination. The resonant fluorescence mechanism is unanimously accepted as the responsible of the presence of metallic lines on the cometary's spectra as well as for the presence of molecular bands. The thermal collisions could contribute to atomic lines only if the collision rate of atoms is high enough to produce transitions between the corresponding energy levels, and the electronic recombination could be efficient for the excitation of atoms in metastable states.

6. CONCLUSIONS

The analysis of the L impact spectra reveals several excited atomic lines. Alkaline lines (Li, Na, Ba, Ca, Mg) as well as line of transition metals (Fe, Cr, Ni, Co, Mn) are listed in Table 1. Nitrogen (N) and maybe flour (F) and carbon (C) lines are presented and rest to be confirmed by further analysis and astronomical observations. The major part of the atomic lines disappear 24 hours after the impact instant, which shows the efficiency of the de-excitation mechanism and energy dissipation on Jupiter's atmosphere.

REFERENCES

Babcock, H. D., Moore, C. E.: 1947, *The Solar Spectrum from λ 6000 to λ 13495*, Carnegie Inst. Washington Publ., No. 579.

Barucci, M. A., Roos-Serote, M., Fulchignoni, M., Lecacheux, J., Crovisier, J., Drossart, P., Roques, F.: 1994, *ASP Conf. Series*, **81**, 404.

Beckers, J. M., Bridges, C. A., Gilliam, L. B.: 1976, *The High Resolution Spectral Atlas of the Solar Irradiance*, Sacramento Peak Observatory, Env. Res. Papers, No. 565.

Morton, D.: 1991, *Astrophys. J. Suppl. Ser.*, **77**, 119.

Morton, D.: 2000, *Astrophys. J. Suppl. Ser.*, **130**, 403.

Morton, D., Noreau, L.: 1994, *Astrophys. J. Suppl. Ser.*, **95**, 301.

Roos-Serote, M., Barucci, M. A., Crovisier, J., Drossart, P., Fulchignoni, M., Lecacheux, J., Roques, F.: 1995, in R. West and H. Bohnhardt (eds), *European SL-9/Jupiter Workshop*, Garching-bei-Munchen.

Roos-Serote, M., Barucci, M. A., Crovisier, J., Drossart, P., Fulchignoni, M., Lecacheux J., Roques, F.: 1995, *Geophys. Res. Lett.*, **22**, 1621.

Received on 12 December 2000

A NECESSARY CONDITION FOR COLLISION IN THE TWO-BODY PROBLEM WITH QUASIHOMOGENEOUS POTENTIALS

VASILE MIOC, MAGDA STAVINSCHI

Astronomical Institute of the Romanian Academy
Str. Cuțitul de Argint 5, RO-75212 Bucharest, Romania
E-mail: vmioc@roastro.astro.ro, magda@roastro.astro.ro

Abstract. Mioc and Stavinschi (2000) proved that in the two-body problem associated to quasihomogeneous potentials (sums of homogeneous potentials) all singularities are due to collisions. In this note we prove a necessary condition for collisions to occur: the coefficient corresponding to the maximum degree of homogeneity must be nonnegative.

Key words: celestial mechanics – two-body problem – quasihomogeneous potentials – collisions.

1. INTRODUCTION

The two-body problem associated to a quasihomogeneous potential models many concrete astronomical – and not only – situations (see Mioc and Stavinschi (2000) and the references therein). The most general case of such a potential is introduced by

Definition 1. We shall call *quasihomogeneous potential* a sum of homogeneous potentials of the form

$$U = \sum_{k=1}^{N} A_k r^{-\alpha_k} , \tag{1}$$

where $A_k \in \mathbf{R}$ are parameters, $\alpha_k \in (0, +\infty)$, $\alpha_k < \alpha_{k+1}$, $k = \overline{1, N-1}$, while r denotes the distance between two particles in the field characterized by the potential U.

Remark 1. Definition 1 is actually valid only for two-body problems. For general n-body problems, see the definition given in the above quoted paper.

In their paper, Mioc and Stavinschi (2000) completed a restant task: to probe that in the *two-body* problem associated to quasihomogeneous potentials *all singularities are due to collisions*. Such an assertion was used in a lot of papers that treated various particular cases of this topic, and many interesting and unexpected results are based on it. However, we repeat, it was rigorously substantiated only in that paper.

Rom. Astron. J., Vol. 10, No. 2, p. 145–149, Bucharest, 2000

By extrapolation, Remark 9 of the quoted paper stated the possibility of collisions only for nonnegative values of A_N. This was proved, within particular contexts, and sometimes by different methods, by Saari (1974), Delgado et al. (1996), Stoica and Mioc (1997), Mioc and Stavinschi (1998), Diacu et al. (2000), and so forth. The present paper provides the proof for the most general case: that featured by Definition 1. As in many previous (and less general) cases, we shall resort to the powerful tool of McGehee-type transformations of the second kind (McGehee 1974).

2. BASIC EQUATIONS

Without repeating the clear arguments exposed (for the Manev field) by Delgado et al. (1996), it is obvious that the general field we deal with is a central one, hence the associated two-body problem can be reduced to a central force problem. Accordingly, one particle (hereinafter *centre*) is fixed at the origin of the reference frame (a plane $\mathbf{R}^2$, since the field is central), whereas the position (configuration) of the other particle with respect to the centre is defined by the vector $\mathbf{q} = (q_1, q_2) \in \mathbf{R}^2$. Then the potential (1) reads

$$U(\mathbf{q}) = \sum_{k=1}^{N} A_k |\mathbf{q}|^{-\alpha_k} . \tag{2}$$

Introducing the momentum $\mathbf{p} = \dot{\mathbf{q}}$, $\mathbf{p} = (p_1, p_2) \in \mathbf{R}^2$, and denoting the kinetic energy by $T(\mathbf{p}) = \mathbf{p}^{\mathrm{T}}\mathbf{p}/2$, the equations that describe the particle motion with respect to the centre can be written in the canonical form

$$\begin{aligned} \dot{\mathbf{q}} &= \partial H(\mathbf{q},\mathbf{p})/\partial \mathbf{p}, \\ \dot{\mathbf{p}} &= -\partial H(\mathbf{q},\mathbf{p})/\partial \mathbf{q}, \end{aligned} \tag{3}$$

with the Hamiltonian function

$$H(\mathbf{q},\mathbf{p}) = T(\mathbf{p}) - U(\mathbf{q}) = \mathbf{p}^{\mathrm{T}}\mathbf{p}/2 - \sum_{k=1}^{N} A_k |\mathbf{q}|^{-\alpha_k} . \tag{4}$$

Of course, the Hamiltonian has the property $H(\mathbf{q},\mathbf{p}) = h/2 = \text{constant}$, i.e., it is a first integral of the motion (the energy integral, with h = constant of energy).

All above formulae easily lead to the explicit equations of motion

$$\begin{aligned} \dot{\mathbf{q}} &= \mathbf{p}, \\ \dot{\mathbf{p}} &= -\sum_{k=1}^{N} (\alpha_k A_k |\mathbf{q}|^{-\alpha_k - 2})\mathbf{q}, \end{aligned} \tag{5}$$

and to the integral of energy

$$\mathbf{p}^{\mathrm{T}}\mathbf{p} - 2\sum_{k=1}^{N} A_k \left|\mathbf{q}\right|^{-\alpha_k} = h. \tag{6}$$

Remark 2. The problem also admits the first integral of angular momentum (this is clear, since the force field is central), but this integral is useless for the purpose of the present paper.

3. REGULARIZED EQUATIONS OF MOTION

The potential (2), the motion equations (5), and the energy integral (6) present an isolated singularity at $\mathbf{q} = (0,0)$. Now we know that this singularity corresponds to the collision particle-centre (Mioc and Stavinschi 2000). To remove it and to obtain regular equations of motion, we resort to the powerful tool of McGehee-type transformations of the second kind (McGehee 1974). Three successive transformations are needed to this end, namely:

$$\begin{aligned} r &= \left|\mathbf{q}\right|, \\ \theta &= \arctan(q_2 / q_1), \\ \xi &= \dot{r} = (q_1 p_1 + q_2 p_2)/\left|\mathbf{q}\right|, \\ \eta &= r\dot{\theta} = (q_1 p_2 - q_2 p_1)/\left|\mathbf{q}\right|, \end{aligned} \tag{7}$$

which introduce the standard polar coordinates;

$$\begin{aligned} x &= r^{\alpha_N/2}\xi, \\ y &= r^{\alpha_N/2}\eta, \end{aligned} \tag{8}$$

which scale down the components of the velocity, and

$$\mathrm{d}s = r^{-\alpha_N/2-1}\mathrm{d}t, \tag{9}$$

which rescales the time.

Under these transformations, which all are real analytic diffeomorphisms, the equations of motion (5) become

$$\begin{aligned} r' &= rx, \\ \theta' &= y, \\ x' &= \frac{\alpha_N}{2}x^2 + y^2 - \sum_{k=1}^{N}\alpha_k A_k r^{\alpha_N - \alpha_k}, \\ y' &= \left(\frac{\alpha_N}{2} - 1\right)xy, \end{aligned} \tag{10}$$

where $' = \mathrm{d}/\mathrm{d}s$ and we kept by abuse the same notation for the new functions of the timelike variable s. As to the energy integral (6), it acquires the form

$$x^2 + y^2 = hr^{\alpha_N} + 2\sum_{k=1}^{N} A_k r^{\alpha_N - \alpha_k} . \tag{11}$$

Remark 3. It is clear that to obtain the energy integral (11) the steps (7) and (8) are sufficient.

4. A NECESSARY CONDITION FOR COLLISION

We are now in the position to state the main result of this paper:

Theorem 1. *A necessary condition for collisions to occur in the two-body problem associated to the quasihomogeneous potential (1) or (2) is* $A_N \geq 0$.

Proof. Under the McGehee-type transformations performed in Section 3, both the motion equations (10) and the energy integral (11) that result are well defined for the boundary $r = 0$. In other words, the phase space of the coordinates (r, θ, x, y) can be analytically extended to contain the boundary manifold

$$M_{r=0} := \{(r, \theta, x, y) \mid r = 0,\ \theta \in S^1,\ (x, y) \in \mathbf{R}^2\},$$

which is invariant under the flow because $r' = 0$ for $r = 0$.

Taking into account (11), let us define the *constant energy manifold*

$$M_h := \{(r, \theta, x, y) \in [0, +\infty) \times S^1 \times \mathbf{R}^2 \mid x^2 + y^2 = hr^{\alpha_N} + 2\sum_{k=1}^{N} A_k r^{\alpha_N - \alpha_k}\},$$

which corresponds to a fixed level of energy h.

Remark 4. Considering the energy constant h as a parameter, every phase trajectory lies on a manifold M_h.

The intersection of the above manifolds defines the *collision manifold*

$$M_0 := \{(r, \theta, x, y) \in [0, +\infty) \mid r = 0,\ \theta \in S^1,\ x^2 + y^2 = 2A_N\}. \tag{12}$$

We distinguish three possible situations:

(a) $A_N > 0$. Then M_0 is homeomorphic to a 2D cylinder in the 3D space of the coordinates (θ, x, y). Collisions are always possible.

Remark 5. Since $\theta \in S^1$ (the segment $[0, 2\pi]$ with the ends identified), the M_0 cylinder may also be considered to be homeomorphic to a 2D torus. Both the M_0 cylinder and the M_0 torus actually are imbedded in the 4D space of the coordinates (r, θ, x, y).

(b) $A_N < 0$. Then, since $(x, y) \in \mathbf{R}^2$, (12) shows that M_0 is the empty set. In other words, the particle does not encounter collisions.

(c) $A_N = 0$. In this situation, if $A_{N-1} \neq 0$, we denote A_{N-1} by A_N, and the above argument holds. If $A_{N-1} = 0$, we check whether A_{N-2} is zero or nonzero, and all is repeated. In the limit situation $A_k = 0$, $k = \overline{1, N}$, we are in the degenerate case of the force-free field, where collisions *are possible* for radial motion (zero angular momentum) with $h > 0$ (see Diacu et al. 2000).

Therefore collisions are possible only if $A_N \geq 0$. The theorem is proved.□

Remark 6. The condition $A_N \geq 0$ for collisions to occur is necessary, but not sufficient. A counterexample would be the case $N = 2$, $\alpha_1 = 1$, $\alpha_2 = 2$, $A_1 < 0$, $A_2 > 0$, $h > 0$, where there are initial conditions that lead to collisions, but there also are initial conditions thet lead to collisionless motion (see Diacu et al., 2000).

Remark 7. The collision manifold does not depend on the energy level h. This means that every phase trajectory shares this manifold (obviously, for $A_N \geq 0$).

REFERENCES

Delgado, J., Diacu, F. N., Lacomba, E. A., Mingarelli, A., Mioc, V., Perez, E., Stoica, C.: 1996, *J. Math. Phys.*, **37**, 2748.
Diacu, F., Mioc, V., Stoica, C.: 2000, *Nonlinear Analysis*, **41**, 1029.
McGehee, R.: 1974, *Invent. Math.*, **27**, 191.
Mioc, V., Stavinschi, M.: 1998, *Serb. Astron. J.*, **158**, 31.
Mioc, V., Stavinschi, M.: 2000, *Rom. Astron. J.*, **10**, 95 .
Saari, D. G.: 1974, *Celest. Mech.*, **9**, 55.
Stoica, C., Mioc, V.: 1997, *Astrophys. Space Sci.*, **249**, 161.

Received on 18 November 2000

ESCAPE DYNAMICS IN QUASIHOMOGENEOUS FIELDS

VASILE MIOC, MAGDA STAVINSCHI

Astronomical Institute of the Romanian Academy
Str. Cuțitul de Argint 5, RO-75212 Bucharest, Romania
E-mail: vmioc@roastro.astro.ro, magda@roastro.astro.ro

Abstract. The escape in the two-body problem associated to a quasihomogeneous potential (a sum of homogeneous potentials) is being tackled. The basic equations of the problem are put in a form for which the infinity is a singularity, then they are regularized via McGehee-type transformations. The singularity is replaced by a manifold pasted on the phase space, and the flow on this manifold is described; it is identical with the analogous flows corresponding to already studied concrete astronomical and physical situations.

Key words: celestial mechanics – quasihomogeneous fields – escape.

1. INTRODUCTION

A lot of concrete astronomical situations can be studied via the mathematical model of the n-body problem associated to quasihomogeneous potentials. This general notion (see, e.g., Mioc and Stavinschi 2000c,d) offers a unifying standpoint for many dynamical problems that imply fields of the most various nature. Among such fields we mention those of Schwarzschild, Fock, Manev, Hall-Newcomb, Reissner-Nordström (see, e.g., Brumberg 1972; Mioc and Blaga 1991; Diacu 1993, 1996; Mioc 1994; Stoica and Mioc 1997; Diacu et al. 2000; Mioc and Stavinschi 2000a; and the references therein). The gravitational or photogravitational field of a celestial body that presents geometric and dynamical symmetry with respect to an axis also joins this model (e.g., Belenkii 1981; Mioc and Stavinschi 1998a,b). Very well known situations, as for instance the Newtonian field, the purely radiative field, even the degenerate case of the force-free field, are included, too. Moreover, nonastronomical fields, as the Coulombian one, or that featured by Van der Vaals forces, also belong to this domain.

All such problems present singularities; in the two-body case they all are due to collisions (Mioc and Stavinschi 2000b). The local behaviour of the corresponding solutions was fully understood and described by Mioc and Stavinschi (2001), who used the powerful qualitative tool of the McGehee-type transformations (McGehee 1974).

Rom. Astron. J., Vol. 10, No. 2, p. 151–159, Bucharest, 2000

In this paper we tackle another limit situation that occurs in the two-body problem: the escape/capture, when one particle tends to/comes from infinity with respect to the other particle. Such an analysis contributes to the understanding of the particle dynamics at very great distance from the field-generating source.

2. BASIC EQUATIONS

Let us set up the mechanical framework of the problem. For the *two-body* model we state

Definition 1. We shall call *quasihomogeneous potential* a sum of potentials of the form

$$U = \sum_{k=1}^{N} A_k r^{-\alpha_k}, \tag{1}$$

where r is the distance between the two particles, A_k are real parameters, and $0 < \alpha_k < \alpha_{k+1}$, $k = \overline{1, N-1}$.

Remark 1. The expression (1) constitutes the reduction of the much more intricate formula of a quasihomogeneous potential for n bodies (see Mioc and Stavinschi 2000b,d) to the two-body case.

Since the force field featured by the potential (1) is central, the associated two-body problem may be reduced to a central force problem, by fixing one particle (hereafter *centre*) at the origin of the coordinate system, and studying the relative motion of the other particle. The problem is obviously 2-dimensional (motion confined to a plane $\mathbf{R}^2$), so let $\mathbf{q} = (q_1, q_2) \in \mathbf{R}^2$ be the position (configuration) vector of the particle, i.e., $|\mathbf{q}| = r$. Then (1) can be written as

$$U(\mathbf{q}) = \sum_{k=1}^{N} A_k |\mathbf{q}|^{-\alpha_k}, \tag{2}$$

with $U : (\mathbf{R}^2 \setminus \{(0,0)\}) \to \mathbf{R}$.

As shown by Mioc and Stavinschi (2000b,c, 2001), the motion may be described by the canonical equations

$$\begin{aligned} \dot{\mathbf{q}} &= \frac{\partial H(\mathbf{q}, \mathbf{p})}{\partial \mathbf{p}}, \\ \dot{\mathbf{p}} &= -\frac{\partial H(\mathbf{q}, \mathbf{p})}{\partial \mathbf{q}}, \end{aligned} \tag{3}$$

with the Hamiltonian function

$$H(\mathbf{q},\mathbf{p}) = \frac{|\mathbf{p}|^2}{2} - U(\mathbf{q}), \tag{4}$$

where $U(\mathbf{q})$ is provided by (2), and $\mathbf{p} = (p_1, p_2) \in \mathbf{R}^2$, $\mathbf{p} = \dot{\mathbf{q}}$, is the momentum vector.

Remark 2. The use of the Hamiltonian formalism points out the fact that the problem admits the first integral of energy $H(\mathbf{q},\mathbf{p}) = h$ (h = energy constant), which explicitly reads

$$T(\mathbf{p}) - U(\mathbf{q}) = h, \tag{5}$$

where $T : \mathbf{R}^2 \to \mathbf{R}_+$, $T(\mathbf{p}) = |\mathbf{p}|^2 / 2$, is the kinetic energy.

Remark 3. As expected, since the problem is a central force one, it also admits the first integral of angular momentum

$$L(\mathbf{q},\mathbf{p}) = q_1 p_2 - q_2 p_1 = C = \text{constant}. \tag{6}$$

To remove the isolated singularity at $\mathbf{q} = (0,0)$, Mioc and Stavinschi (2000c,d, 2001) resorted to the McGehee-type transformations of the second kind (McGehee 1974):

$$\begin{aligned} r &= |\mathbf{q}|, \\ \theta &= \arctan(q_2 / q_1), \\ \xi &= \dot{r} = (q_1 p_1 + q_2 p_2)/|\mathbf{q}|, \\ \eta &= r\dot{\theta} = (q_1 p_2 - q_2 p_1)/|\mathbf{q}|, \end{aligned} \tag{7}$$

$$\begin{aligned} x &= r^{\alpha_N/2}\xi, \\ y &= r^{\alpha_N/2}\eta, \end{aligned} \tag{8}$$

$$\mathrm{d}s = r^{-\alpha_N/2-1}\mathrm{d}t, \tag{9}$$

obtaining the regular equations of motion (with $' = \mathrm{d}/\mathrm{d}s$)

$$\begin{aligned} r' &= rx, \\ \theta' &= y, \\ x' &= \frac{\alpha_N}{2}x^2 + y^2 - \sum_{k=1}^{N}\alpha_k A_k r^{\alpha_N - \alpha_k}, \\ y' &= \left(\frac{\alpha_N}{2} - 1\right)xy, \end{aligned} \tag{10}$$

and the regular first integrals of energy and angular momentum, respectively:

$$x^2 + y^2 = hr^{\alpha_N} + 2\sum_{k=1}^{N} A_k r^{\alpha_N - \alpha_k} . \tag{11}$$

$$y = Cr^{\alpha_N/2-1} . \tag{12}$$

Equations (10)–(12) are the basic starting formulae for the investigation we shall perform about the escape/capture orbits.

3. NEW McGEHEE-TYPE TRANSFORMATIONS

We introduce the new variable ρ via the McGehee-type transformation of the first kind (McGehee 1973), which brings the infinity at the origin:

$$\rho = \frac{1}{r} . \tag{13}$$

The motion equations (10) turn to

$$\begin{aligned} \rho' &= -\rho x , \\ \theta' &= y , \\ x' &= \frac{\alpha_N}{2} x^2 + y^2 - \sum_{k=1}^{N} \alpha_k A_k \rho^{\alpha_k - \alpha_N} , \\ y' &= \left(\frac{\alpha_N}{2} - 1 \right) xy , \end{aligned} \tag{14}$$

while the integrals (11) and (12) become respectively

$$x^2 + y^2 = h\rho^{-\alpha_N} + 2\sum_{k=1}^{N} A_k \rho^{\alpha_k - \alpha_N} . \tag{15}$$

$$y = C\rho^{1-\alpha_N/2} . \tag{16}$$

These equations present singularities for $\rho = 0$, that is, physically speaking, when the particle escapes (in the future) or is captured (in the past); see (13).

Remark 4. Due to the symmetry (time-reversibility of motion equations), the escape and the capture are wholly similar (obviously, only from the mathematical standpoint). That is why we shall use, by abuse, the term *escape* for both situations.

To regularize the energy integral, we perform the second step, by resorting to the McGehee-type transformation of the second kind

$$u = \rho^{\alpha_N/2} x\,, \qquad v = \rho^{\alpha_N/2} y\,. \tag{17}$$

Now the equations of motion (14) become

$$\begin{aligned} \rho' &= -\rho^{1-\alpha_N/2} u\,, \\ \theta' &= \rho^{-\alpha_N/2} v\,, \\ u' &= \rho^{-\alpha_N/2}\left(v^2 - \sum_{k=1}^{N} \alpha_k A_k \rho^{\alpha_k} \right), \\ v' &= -\rho^{-\alpha_N/2}\, uv, \end{aligned} \tag{18}$$

whereas relations (15) and (16) respectively read

$$u^2 + v^2 = h + 2\sum_{k=1}^{N} A_k \rho^{\alpha_k}\,. \tag{19}$$

$$v = C\rho\,. \tag{20}$$

Observe that the first integrals are now regular, while the motion equations are still singular for $\rho = 0$. To remove this singularity, we rescale the timelike variable s by using the last McGehee-type transformation

$$d\tau = \rho^{-\alpha_N/2} ds\,. \tag{21}$$

In this way we obtain the final form of the motion equations

$$\begin{aligned} \frac{d\rho}{d\tau} &= -\rho u\,, \\ \frac{d\theta}{d\tau} &= v\,, \\ \frac{du}{d\tau} &= v^2 - \sum_{k=1}^{N} \alpha_k A_k \rho^{\alpha_k}\,, \\ \frac{dv}{d\tau} &= -uv, \end{aligned} \tag{22}$$

where we preserved, by abuse, the same notation for the new functions of τ.

Remark 5. All McGehee-type transformations used here, namely (13), (17), and (21), are real analytic diffeomorphisms.

4. INFINITY MANIFOLD

Both the equations of motion (22) and the first integrals (19)–(20) are well defined for $\rho = 0$. This means that the phase space can be analytically extended to contain the boundary manifold

$$M_{\rho=0} := \{(\rho, \theta, u, v) \mid \rho = 0,\ \theta \in S^1,\ (u, v) \in \mathbf{R}^2\}, \tag{23}$$

The integrals (19) and (20) also extend smoothly to this boundary.

As we have done in a previous paper (Mioc and Stavinschi 2000c), define the *constant energy manifold* in the space of the coordinates (ρ, θ, u, v) as

$$M_h := \{(\rho, \theta, u, v) \mid \rho \in [0, +\infty),\ \theta \in S^1,\ (19) \text{ holds}\}, \tag{24}$$

With this, we can define the *collision manifold* M_∞ as being the intersection

$$M_\infty := M_{\rho=0} \cap M_h = \{(\rho, \theta, u, v) \mid \rho = 0,\ \theta \in S^1,\ u^2 + v^2 = h\}. \tag{25}$$

In this way we have blown up the singularity at $\rho = 0$ and pasted the infinity manifold, instead of it, on the phase space.

Proposition 1. *The infinity manifold is invariant to the flow.*

Proof. By the first equation (22), $d\rho / d\tau = 0$ for $\rho = 0$. □

Proposition 2. *In the three-dimensional space of the coordinates* (θ, u, v), M_∞ *is homeomorphic to: a two-dimensional torus for* $h > 0$; *a circle for* $h = 0$; *the empty set for* $h < 0$.

Proof. Taking into account the energy integral for $\rho = 0$

$$u^2 + v^2 = h, \tag{26}$$

it is clear that $h < 0 \Rightarrow M_\infty = \emptyset$. Since $\theta \in [0, 2\pi]$, formula (25) points out the fact that M_∞ is homeomorphic to a cylinder of length 2π for $h > 0$, and to a segment of line of the same length for $h = 0$. But S^1 is the segment $[0, 2\pi]$ with the end points identified; the conclusion follows immediately. □

Corollary 1. *Escape is possible only for nonnegative energy levels. For* $h < 0$ *the orbits are always bounded.*

Remark 6. All manifolds mentioned in Proposition 2 are actually imbedded in the four-dimensional space of the coordinates (ρ, θ, u, v).

Let us now describe the flow on the M_∞ torus ($h > 0$). This flow is deprived of physical significance, but – due to the continuity of solutions with respect to the initial conditions – it provides valuable informations about the escape orbits.

Taking into account Proposition 1, equations (22) yield immediately the vector field on M_∞:

$$\begin{aligned} \frac{d\theta}{d\tau} &= v, \\ \frac{du}{d\tau} &= v^2, \\ \frac{dv}{d\tau} &= -uv, \end{aligned} \tag{27}$$

Proposition 3. *The flow on the M_∞ torus consists of two circles of degenerate equilibria: the upper circle*

$$\mathrm{UC} := \{(\theta, u, v) \mid \theta = \theta_0 \in S^1,\ u = \sqrt{h},\ v = 0\} \tag{28}$$

(with θ_0 = arbitrary constant), and the lower circle:

$$\mathrm{LC} := \{(\theta, u, v) \mid \theta = \theta_0 \in S^1,\ u = -\sqrt{h},\ v = 0\}, \tag{29}$$

connected by heteroclinic orbits that move from LC to UC.

Proof. It can be easily seen from the vector field (27) that the equilibrium points of the flow on M_∞ correspond to $v = 0$ and θ_0 = arbitrary constant. Taking into account (26), expressions (28) and (29) follow immediately. As regards the other orbits (with $v \neq 0$), the second equation (27), together with (28) and (29) shows that u is monotonically increasing from $-\sqrt{h}$ to $\sqrt{h}$. In other words, the phase curves on M_∞ with $v \neq 0$ eject from LC and tend to UC. The proposition is proved. □

The slope of the heteroclinic trajectories on M_∞ is given by

Proposition 4. *Every heteroclinic phase curve on M_∞ that starts from θ_0 on LC tends to $\theta_0 + \pi$ on UC.*

Proof. Let us put $u = \sqrt{h}\cos\alpha$, $v = \sqrt{h}\sin\alpha$. Taking into account equations (27), it follows easily that

$$d\alpha / d\theta = -1. \tag{30}$$

The flow on M_∞ plotted in the (θ, α) plane, with the slope given by (30), may be confined to the square $\{(\theta, \alpha) \in S^1 \times S^1\}$ of side length equal to 2π. Pasting together (therefore identifying) only the sides $\alpha = 0$ and $\alpha = 2\pi$, the square becomes the cylinder plotted in Fig. (equivalent to the M_∞ torus). This completes the proof. □

From Proposition 3 it follows immediately

Corollary 2. *The flow on the one-dimensional manifold M_∞ corresponding to the zero energy level ($h = 0$) consists only of degenerate equilibria (the two-dimensional torus M_∞ reduced to the two circles UC and LC identified).*

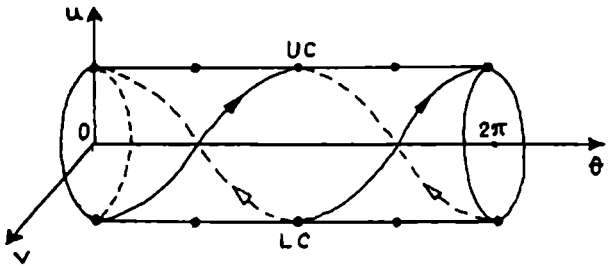

Fig. – The infinity manifold as a cylinder and the flow on it.

5. FINAL REMARKS

Remark 7. By virtue of (20), all orbits in the full phase space of the coordinates (ρ, θ, u, v) neighbour infinity in the zone of UC (the escape ones) or LC (the capture ones).

Remark 8. By (21), it is clear that the flows on the collision manifold M_0 (see Mioc and Stavinschi 2000c, 2001) and on the infinity manifold M_∞ have different time scales. Moreover, taking into account (9) and (21), we get $dt = r\,d\tau$, which means that the time scale on M_∞ also differs from the "physical time" used in classical celestial mechanics.

Remark 9. Examining (7), (8), and (17), one easily remarks that (u, v) are nothing but the polar components of the velocity $(\dot{r}, r\dot{\theta})$. With this, and with the relationship between τ and t (see Remark 8), equations (22) follow straightforwardly from the system (3) (explicited using (2), (4), and (7)). So, the start from equations (10) could be avoided. Nevertheless, we preferred this way for a unitary treatment of the limit manifolds M_0 and M_∞.

Remark 10. The same comments can be made as regards the first integrals (19) and (20), which could be directly obtained from (5) and (6), respectively (explicited via (2) and (7)).

Remark 11. To obtain the vector field (22), intended here to study the infinity manifold, we need neither start from already regularized equations as (10), nor use equation-regularizing transformations as McGehee's ones are. The reason is simple: for the initial equations of motion, infinity does not constitute a singularity.

The only argument for the technique used in Section 3 is that pointed out by Remark 9.

Remark 12. Perusing the results previously obtained for particular cases, as Fock's field (Mioc and Stavinschi 2000a), those of Manev-type (Stoica and Mioc 1997b) or Schwarzschild-type (Mioc and Stoica 1997), the zonal satellite problem (Mioc and Stavinschi 1998b), etc., one notices that the infinity manifold in the much more general case of quasihomogeneous potentials has exactly the same structure as regards the flow on it.

This provides a full understanding of the behaviour of orbits at escape in this very general case. This also offers a unifying point of view for escape situations in many concrete problems belonging to this class.

REFERENCES

Belenkii, I. M.: 1981, *Celest. Mech.*, **23**, 9.
Brumberg, V. A.: 1972, *Relativistic Celestial Mechanics*, Nauka, Moscow (in Russian).
Diacu, F. N.: 1993, *J. Math. Phys.*, **34**, 5671.
Diacu, F. N.: 1996, *J. Diff. Eq.*, **128**, 58.
Diacu, F. N., Mioc, V., Stoica, C.: 2000, *Nonlinear Analysis*, **41**, 1029.
McGehee, R.: 1973, *J. Diff. Eq.*, **14**, 70.
McGehee, R.: 1974, *Invent. Math.*, **27**, 191.
Mioc, V.: 1994, *Astron. Nachr.*, **315**, 175.
Mioc, V., Blaga, P.: 1991, *Rom. Astron. J.*, **1**, 103.
Mioc, V., Stavinschi, M.: 1998a, *Serb. Astron. J.*, **158**, 31.
Mioc, V., Stavinschi, M.: 1998b, *Serb. Astron. J.*, **158**, 37.
Mioc, V., Stavinschi, M.: 2000a, *Rom. Astron. J.*, **10**, 71.
Mioc, V., Stavinschi, M.: 2000b, *Rom. Astron. J.*, **10**, 95.
Mioc, V., Stavinschi, M.: 2000c, *Rom. Astron. J.*, **10**, 145.
Mioc, V., Stavinschi, M.: 2000d, *Phys. Scripta* (submitted).
Mioc, V., Stavinschi, M.: 2001, *Phys. Lett. A*, **279** (to appear).
Stoica, C., Mioc, V.: 1997a, *Astrophys. Space Sci.*, **249**, 161.
Stoica, C., Mioc, V.: 1997b, *Rom. Astron. J.*, 7, 183.

Received on 15 December 2000

THE THREE-AXIAL EARTH ROTATION: A NEW MATHEMATICAL APPROACH

VASILE MIOC, MAGDA STAVINSCHI

Astronomical Institute of the Romanian Academy
Str. Cuțitul de Argint 5, RO-75212 Bucharest, Romania
E-mail: vmioc@roastro.astro.ro, magda@roastro.astro.ro

Abstract. The three-axial Earth's rotation is generally treated by quantitative methods. The seldom used qualitative analysis, which depicts the general evolution all along the motion, can offer supplementary information. Tackling the problem from such a viewpoint, we exploit its Hamiltonian description using Andoyer-type variables, and consider it via KAM (Kolmogorov-Arnold-Moser) theory. The system of motion equations fulfils the condition of so-called "isoenergetic nondegeneracy". In astronomical translation, this means that the Earth's rotation is "sure" for almost all initial conditions: the chances for a drastic change are extremely improbable; this corroborates the data provided by observations and quantitative analysis. Another result offered by KAM theory is that the polhody will always be confined to a relatively negligible area. As a finel conclusion, the most various methods of mathematics, classical mechanics, celestial mechanics must be used to understand astronomical problems of essential importance, as the Earth's rotation is.

Key words: celestial mechanics – Earth's rotation – KAM theory.

1. INTRODUCTION

In the theory of Earth's rotation it is sufficient to consider in general the axes lying in the *Oxy*-plane as being equal. However, certain studies need to consider the problem in the three-axial case. This is the case analyzed by Kinoshita (1977), who used a Hamiltonian formalism. The nutation in this case was deeply investigated by Kinoshita and Souchay (1990), while Chandler's period in the same case was studied by Stavinschi and Souchay (1994).

By tradition, the Earth's rotation is studied by classical methods of astronomy, celestial mechanics, or geodynamics. Here we try to learn more about the terrestrial rotation via a less usual mathematical tool. Consequently we exploit the Hamiltonian description of the three-axial Earth rotation, applying some results of KAM (Kolmogorov-Arnold-Moser) theory to the associated dynamical system. This theory is one of the most powerful tools of the celestial mechanics. One of its basic results is the persistence of almost all invariant tori under a Hamiltonian

Rom. Astron. J., Vol. 10, No. 2, p. 161–165, Bucharest, 2000

perturbation (Moser 1962; Arnold 1963a). It has been proved for many situations belonging to modern celestial mechanics, as well as to classical astronomy (Arnold 1963b; Markeev 1978; Diacu and Holmes 1996).

We prove that the Hamiltonian does not fulfil the nondegeneracy condition, but satisfies the condition for isoenergetic nondegeneracy. These results point out two essential characteristics of the problem: (a) most invariant tori persist under the "perturbation" featured by the part of the Hamiltonian containing the angle variables, hence the Earth's rotation is "tame" for almost all initial data; (b) the action variables are confined all along the motion to a small neighbourhood of their initial values. In this way we add the modern qualitative methods of the theory of dynamical systems to the traditional methods used to study the Earth's rotation.

2. THE HAMILTONIAN

Kinoshita (1977) used the Hamiltonian formalism to set up the equations which describe the rotation of the Earth approximated by an ellipsoid with three unequal axes. He considered a geocentric inertial frame $OXYZ$ and a frame $Oxyz$ featuring the terrestrial rotation (see Stavinschi and Souchay 1994). The action variables (L, G, H) are as follows: G = total angular momentum of the Earth; L = projection of G onto the Oz-axis; H = projection of G onto the OZ-axis (which can correspond to the ecliptic axis for a reference epoch). The angle variables are: l = angle of the proper terrestrial rotation along the equator corresponding to the Oz-axis; g = rotation angle of the angular momentum axis around the Oz-axis (which draws on the Earth's surface a curve close to the polhody); h = luni-solar precession.

To first order in the products of inertia, the Hamiltonian is (Kinoshita 1977; see also Stavinschi and Souchay 1994):

$$\mathcal{H} = \frac{1}{2}\left(\frac{\sin^2 l}{A} + \frac{\cos^2 l}{B}\right)(G^2 - L^2) + \frac{L^2}{2C} - \frac{F}{2AB}(G^2 - L^2)\sin(2l) -$$

$$\frac{L}{C}\sqrt{(G^2 - L^2)}\left(\frac{E}{A}\cos L + \frac{D}{B}\right)\sin l + K, \qquad (1)$$

where (A, B, C) are the moments of inertia, (D, E, F) stand for the products of inertia, whereas K is the action variable conjugate to the time variable.

According to Munk and MacDonald (1960), the equatorial bulge of the Earth is featured by the supplementary moments of inertia

$$c_{11} = c_{22} = -\frac{ka_E^2\omega^2}{9G_N}, \quad c_{33} = -2c_{11}, \qquad (2)$$

in which a_E = mean equatorial terrestrial radius, G_N = Newtonian constant of gravitation, ω = amplitude of the terrestrial rotation vector, k = Love's number.

Denoting $\mu = -c_{11} / C$, considering the approximations

$$\begin{aligned} &\Delta A = \Delta B = -\mu C, \\ &\Delta C = 2\mu C, \\ &D \approx 3\mu C \sin J \cos l, \\ &E \approx 3\mu C \sin J \cos l \sin l, \\ &F \approx 0, \end{aligned} \tag{3}$$

and neglecting the quantities of second order in $\sin J$, the Hamiltonian acquires the form (Stavinschi and Souchay 1994):

$$\mathcal{H} = \frac{1}{2}\left(\frac{\sin^2 l}{A} + \frac{\cos^2 l}{B}\right)(G^2 - L^2) + \frac{L^2}{2C} -$$

$$3\mu\sqrt{G^2 - L^2}\left(\frac{\sin^2 L}{A} + \frac{\cos^2 L}{B}\right)\sin J + K, \tag{4}$$

Here J stands for the angle between the angular momentum vector and the Oz-axis, which means $L = G\cos J$. This angle being very small (of order 1"), the above neglection is allowed.

Observe that the variables H, g, and h do not appear in (4) (free rotation, as considered by Kinoshita 1977). This means that G is a constant of the motion (the first integral of the angular momentum). Therefore we shall consider $G = G_0$ (initial value) all along the motion.

3. KAM THEORY APPLIED TO THE PROBLEM

The dynamical system associated to the problem has clearly two degrees of freedom, because the behaviour of the variable g can be obtained with a sufficient accuracy via

$$g = g_0 + \int_0^t \frac{\partial \mathcal{H}(L(\tau), G_0, K(\tau), l(\tau), \tau)}{\partial G_0} \, d\tau, \tag{5}$$

after the approximate integration.

To apply KAM theory, let us write the Hamiltonian (4) in the form $\mathcal{H} = \mathcal{H}_0 + \varepsilon\mathcal{H}_1$, where $\mathcal{H}_0$ depends only on the action variables:

$$\mathcal{H}_0 = \frac{L^2}{2C} + K, \tag{6}$$

while ε is a small parameter which can be introduced artificially. It is obvious that the motion takes place on the manifold $\mathcal{H}(L, G_0, K, l, t) \equiv 0$.

The expression (6) yields immediately

$$\begin{vmatrix} \partial^2\mathcal{H}_0 / \partial L^2 & \partial^2\mathcal{H}_0 / \partial L \partial K \\ \partial^2\mathcal{H}_0 / \partial L \partial K & \partial^2\mathcal{H}_0 / \partial K^2 \end{vmatrix} = \begin{vmatrix} 1/C & 0 \\ 0 & 0 \end{vmatrix} = 0. \tag{7}$$

This means that the Hamiltonian does not satisfy the usual KAM condition for nondegeneracy (nonzero value of the determinant (7)). However it fulfils the condition

$$\begin{vmatrix} \partial^2\mathcal{H}_0 / \partial L^2 & \partial^2\mathcal{H}_0 / \partial L \partial K & \partial\mathcal{H}_0 / \partial L \\ \partial^2\mathcal{H}_0 / \partial L \partial K & \partial^2\mathcal{H}_0 / \partial K^2 & \partial\mathcal{H}_0 / \partial K \\ \partial\mathcal{H}_0 / \partial L & \partial\mathcal{H}_0 / \partial K & 0 \end{vmatrix} = \begin{vmatrix} 1/C & 0 & L/C \\ 0 & 0 & 1 \\ L/C & 1 & 0 \end{vmatrix} = -\frac{1}{C} \neq 0 \tag{8}$$

for isoenergetic nondegeneracy.

Taking into account (7) and (8), our problem satisfies the conditions of the following theorems (cf. Arnold et al. 1988):

Theorem 1 (Kolmogorov). *If the unperturbed system is nondegenerate or isoenergetically nondegenerate, then, for a sufficiently small Hamiltonian perturbation, the majority of the nonresonant invariant tori do not vanish. They are only slightly deformed, such that in the phase space of the perturbed system there exist invariant tori densely filled by conditionally periodic phase curves wrapping up around them. The number of frequencies on them is equal to the number of degrees of freedom. These invariant tori form the majority in the sense that the measure of the complement of their union is small when the perturbation is small. In the case of isoenergetic nondegeneracy, the invariant tori form the majority on every manifold of energy level.*

Theorem 2. *In an isoenergetically nondegenerate system with two degrees of freedom, for all initial conditions the values of the action variables remain close to their initial values all along the motion.*

A remark must be made here as regards Theorem 1. When we say that the set of destroyed tori has small measure when the perturbation is small, this means that the respective measure tends to zero as the perturbation does it.

4. CONCLUDING REMARKS

We have treated the problem considering it to be a perturbed problem ($\mathcal{H}_1$ being the perturbing Hamiltonian). The associated dynamical system proved to be degenerate, but nondegenerate isoenergetically. This has two main consequences:

(a) the majority (in Kolmogorov's sense) of the nonresonant invariant tori persist under the "perturbation". This means that almost all initial conditions (as far in the past as possible) lead to a "tame" rotation of the Earth. In astronomical translation, this means that the chances for a drastic change are extremely improbable; this corroborates the data provided by observations and quantitative analysis.

(b) all along the motion the values of the action variables L and K maintain themselves in the neighbourhood of their initial values (while the variable G is a constant of the motion). This confirms that the polhody will always be confined to a relatively negligible area.

As a final conclusion, the most various methods of mathematics, classical mechanics, celestial mechanics must be used to understand astronomical problems of essential importance, as the Earth's rotation is.

REFERENCES

Arnold, V. I., Kozlov, V. V., Neishtadt, A. I.: 1988, *Dynamical Systems III*, Springer-Verlag, New York.

Arnold, V. I.: 1963a, *Russ. Math. Surveys*, **9**, 9.

Arnold, V. I.: 1963b, *Russ. Math. Surveys*, **18**, 85.

Diacu, F., Holmes, P.: 1996, *Celestial Encounters. The Origins of Chaos and Stability*, Princeton University Press, Princeton.

Kinoshita, H.: 1977, *Celest. Mech.*, **15**, 277.

Kinoshita, H., Souchay, J.: 1990, *Celest. Mech.*, **48**, 187.

Kubo, Y.: 1991, *Celest. Mech. Dyn. Astron.*, **50**, 165.

Markeev, A. P.: 1978, *Libration Points in Celestial Mechanics and Cosmodynamics*, Nauka, Moscow (Russian).

Moser, J. K.: 1962, *Nachr. Akad. Wiss. Göttingen*, **2**, Math.-Phys. Kl., 1.

Munk, W. H., MacDonald, G. J. F.: 1960, *The Rotation of the Earth*, Cambridge University Press, London.

Stavinschi, M., Souchay, J.: 1994, in N. Capitaine (ed.), *Journées 1994 "Systèmes de référence spatio-temporels"*, Paris, 81.

Received on 30 August 2000

EXISTENCE OF QUASIPERIODIC ORBITS IN MANEV-TYPE PROBLEMS: A NEW PROOF

CRISTINA STOICA [1], VASILE MIOC [2]

[1] *University of Victoria, Department of Mathematics and Statistics*
Victoria, B. C., V8W 3P4, Canada
E-mail: cstoica@math.uvic.ca

[2] *Astronomical Institute of the Romanian Academy*
Str. Cuțitul de Argint 5, RO-75212 Bucharest, Romania
E-mail: vmioc@roastro.astro.ro

Abstract. A new proof of the existence of quasiperiodic motion in the Manev-type two-body problem is provided via classical mechanics methods. The set of such orbits is dense in the set of bounded noncollisional trajectories. This allows one to apply the classical results of KAM theory to this problem.

Key words: celestial mechanics – Manev-type fields – quasiperiodic orbits.

1. INTRODUCTION

The Manev-type two-body problem (associated to a potential of the form $A/r + B/r^3$, with r = distance between particles, and A, B = real parameters) constitutes a largely discussed subject during the last decade. Significant contributions to the full understanding of the problem have been brought by Lacomba et al. (1991), Casasayas et al. (1993), Diacu et al. (1995, 2000), Mioc and Stoica (1995a,b), Delgado et al. (1996), Stoica and Mioc (1996), Stoica (1997), Mioc (1998), Mioc and Stavinschi (1999a), Szenkovits (1999), Szenkovits et al. (1999), etc. Problems of more than two bodies in such a field were also tackled (see, e.g., Diacu 1993; Mioc and Blaga 1999; Mioc and Stavinschi 1999b). This topic deserves an extensive study, given the large class of concrete astronomical and physical situations that can be modelled in this way.

The phase space structure of the Manev-type two-body problem was fully described by Stoica (1997), Szenkovits et al. (1999), and Diacu et al. (2000) from analytic, geometric and physical viewpoints. A lot of types of motion – recoverable in classical models or not – was pointed out. Among them, of first importance for astronomy is the class of bounded noncollisional orbits (see Stoica 1995). They can

Rom. Astron. J., Vol. 10, No. 2, p. 167–175, Bucharest, 2000

obviously be periodic, as for instance in the particular case of the Newtonian model ($A > 0$, $B = 0$). But there also are quasiperiodic orbits, which fill densely an annulus and never close. Their existence, essential for applying the classical results of KAM theory (e.g., Lacomba et al. 1991), was proved by Diacu et al. (1995, 2000) and Delgado et al. (1996). In this paper we shall provide a quite different proof (based only on classical mechanics) of the existence of such orbits.

Section 2 recalls the basic equations of the problem in Hamiltonian formalism, along with the first integrals of angular momentum and energy. Section 3 surveys all possible orbits for the whole interplay between the field parameters (A, B) and the constants of angular momentum (C) and energy (h). We also provide the necessary and sufficient condition for the bounded noncollisional motion.

The motion of this type is tackled in Section 4. We offer a classical-type proof of the existence of quasiperiodic orbits, and we show that all initial conditions (but a zero Lebesgue measure set) that lead to bounded noncollisional motion provide quasiperiodic trajectories.

2. BASIC EQUATIONS

Let us recall that the potential function associated to Manev-type fields has the expression

$$U(\mathbf{q}) = \frac{A}{|\mathbf{q}|} + \frac{B}{|\mathbf{q}|^2}, \tag{1}$$

where $\mathbf{q} \in \mathbf{R}^3 \setminus \{(0,0,0)\}$ is the position (or configuration) vector of one body with respect to the other, while A and B are real parameters, $A \neq 0$. We see that the relative motion is treated within the framework of a central force problem for a particle of unit mass (see, e.g., Diacu et al. 2000).

Let us denote by $X = \{\mathbf{q} \in \mathbf{R}^3 \mid \mathbf{q} \neq (0,0,0)\}$ the configuration space, and let $\mathbf{p} \in \mathbf{R}^3$, $\mathbf{p} = \dot{\mathbf{q}}$, be the momentum vector. Finally, let us denote by $T^*X = \{(\mathbf{q}, \mathbf{p}) \mid \mathbf{q} \in \mathbf{R}^3 \setminus \{(0,0,0)\}, \mathbf{p} \in \mathbf{R}^3\}$ the cotangent bundle on which the associated Hamiltonian

$$H(\mathbf{q}, \mathbf{p}) = \frac{|\mathbf{p}|^2}{2} - \frac{A}{|\mathbf{q}|} - \frac{B}{|\mathbf{q}|^2} \tag{2}$$

is defined. By (2), the explicit form of the canonical equations of motion is

$$\begin{aligned} \dot{\mathbf{q}} &= \mathbf{p}, \\ \dot{\mathbf{p}} &= -\left(A + \frac{2B}{|\mathbf{q}|}\right)\frac{\mathbf{q}}{|\mathbf{q}|^3}. \end{aligned} \tag{3}$$

Two properties of the problem are obvious:

Theorem 2.1. *The motion equations admit the first integral of angular momentum*

$$\Omega(\mathbf{q},\mathbf{p}) := \mathbf{q}\times\mathbf{p}^{\mathrm{T}} = \text{constant} := \mathbf{C}. \tag{4}$$

Theorem 2.2. *The motion equations admit the first integral of energy*

$$H(\mathbf{q},\mathbf{p}) = \text{constant} := h. \tag{5}$$

The proofs are classical (e.g., Stoica 1997) and will not be resumed here.

Remark 2.3. The conservation of the angular momentum was clear since the force field is central. As to the conservation of energy, it was *a priori* stated, since we used the Hamiltonian formalism.

The two first integrals confine the motion to the manifold

$$S(\mathbf{C},h) = \{(\mathbf{q},\mathbf{p}) \in (\mathbf{R}^3 \setminus \{(0,0,0)\})\times\mathbf{R}^3 \mid \mathbf{q}\times\mathbf{p}^{\mathrm{T}} = \mathbf{C},\ H(\mathbf{q},\mathbf{p}) = h\}. \tag{6}$$

But, by Theorem 2.1, the motion is planar, hence the configuration space becomes $X = \{\mathbf{q} \in \mathbf{R}^2 \mid \mathbf{q} \neq \{(0,0)\}\}$. This means that the variables $(\mathbf{q},\mathbf{p})$ will belong to the cotangent bundle $T^*X = \{(\mathbf{q},\mathbf{p}) \mid \mathbf{q} \in \mathbf{R}^2 \setminus \{(0,0)\},\ \mathbf{p} \in \mathbf{R}^2\}$, whereas the integral set $S(\mathbf{C},h)$ turns to

$$S(\mathbf{C},h) = \{(\mathbf{q},\mathbf{p}) \in (\mathbf{R}^2 \setminus \{(0,0)\})\times\mathbf{R}^2 \mid q_1p_2 - q_2p_1 = C,\ H(\mathbf{q},\mathbf{p}) = h\}, \tag{7}$$

in which $\mathbf{q} = (q_1,q_2)$, $\mathbf{p} = (p_1,p_2)$, while C is the unique nonzero component of the vector $\mathbf{C}$ ($C = |\mathbf{C}|$).

Remark 2.4. For $C = 0$, the vectors $\mathbf{q}$ and $\mathbf{p}$ are parallel (radial motion).

3. CLASSIFICATION OF ORBITS

To exploit the symmetries of the problem, we shall pass to polar coordinates via the transformations

$$\begin{aligned} r &= |\mathbf{q}|,\\ \theta &= \arctan(q_2/q_1),\\ p &= \dot{r} = \frac{\mathbf{p}\cdot\mathbf{q}}{|\mathbf{q}|^2},\\ \Omega &= q_1p_2 - q_2p_1. \end{aligned} \tag{8}$$

With these new variables, the equations of motion read

$$\begin{aligned} \dot{r} &= p, \\ \dot{\theta} &= \frac{\Omega}{r^2}, \\ \dot{p} &= -\frac{A}{r^2} + \frac{\Omega^2 - 2B}{r^3}, \\ \dot{\Omega} &= 0. \end{aligned} \tag{9}$$

Observe that Theorem 2.1 reduces to the assertion $\Omega = C$. Also observe that the rotational symmetry as regards θ (that does not appear explicitly in either motion equations or first integrals) allows the factorization to S^1. In this way, $S(\mathbf{C}, h)$ may be reduced to the factor space $\widetilde{S}(\mathbf{C}, h)$ of codimension 1. Next, performing the reduction, and fixing $\Omega = C$, we obtain the reduced Hamiltonian

$$H(r, p) = \frac{p^2}{2} - \frac{A}{r} + \frac{C^2 - 2B}{2r^3}, \tag{10}$$

defined on $T^*(\mathbf{R}^+ \setminus \{(0,0)\}) \sim (\mathbf{R}^+ \setminus \{(0,0)\}) \times \mathbf{R}$, ($\sim$ denoting isomorphism). This is a one-degree-of-freedom problem, whose understanding reduces to the analysis of the phase portrait.

Such an analysis was performed by Stoica (1995, 1997). The allowed energy levels are given by

$$\frac{p^2}{2} = h - V(r) \geq 0, \tag{11}$$

formula in which, as it is easy to see, the amended potential $V(r)$ has the following expression:

$$V(r) := -\frac{1}{r}\left(A - \frac{C^2 - 2B}{2r}\right). \tag{12}$$

This defines the critical values

$$r_{cr} := \frac{C^2 - 2B}{A}, \tag{13}$$

as the distance corresponding to $\mathrm{d}V(r)/\mathrm{d}r = 0$, and

$$h_{cr} := V(r_{cr}) = -\frac{A^2}{2(C^2 - 2B)}. \tag{14}$$

Stoica's (1995, 1997) analysis pointed out the cases in which the real motion is possible, obtaining the following topologic classification of the reduced spaces $\widetilde{S}(\mathbf{C}, h)$ (hereafter $\widetilde{S}$ for sake of brevity):

(i) $A > 0$, $(C^2 - 2B) > 0$:

$$\begin{aligned} &h = h_{cr} \Rightarrow r = \text{constant} \Leftrightarrow \widetilde{S} \sim \text{a point}, \\ &h \in (h_{cr}, 0) \Rightarrow r \in [r_{\min}, r_{\max}] \Leftrightarrow \widetilde{S} \sim S^1, \\ &h \in [0, +\infty) \Rightarrow r \in [r_{\min}, +\infty] \Leftrightarrow \widetilde{S} \sim \mathbf{R}. \end{aligned} \tag{15}$$

The physical orbits are both bounded noncollisional and unbounded noncollisional (of the type capture-escape).

(ii) $A > 0$, $(C^2 - 2B) \leq 0$:

$$\begin{aligned} &h \in (-\infty, 0) \Rightarrow r \in (0, r_{\max}] \Leftrightarrow \widetilde{S} \sim \mathbf{R}, \\ &h \in [0, +\infty) \Rightarrow r \in (0, +\infty] \Leftrightarrow \widetilde{S} \sim \mathbf{R}. \end{aligned} \tag{16}$$

The physical orbits are only collisional, either bounded (of the type ejection-collision) or unbounded (of the type ejection-escape or capture-collision).

(iii) $A < 0$, $(C^2 - 2B) \geq 0$:

$$h \in (0, +\infty) \Rightarrow r \in [r_{\min}, +\infty] \Leftrightarrow \widetilde{S} \sim \mathbf{R}. \tag{17}$$

(iv) $A < 0$, $(C^2 - 2B) < 0$:

$$\begin{aligned} &h \in (-\infty, 0) \Rightarrow r \in (0, r_{\max}] \Leftrightarrow \widetilde{S} \sim \mathbf{R}, \\ &h \in (0, h_{cr}) \Rightarrow r \in \{(0, r_{\max}] \vee [r_{\min}, +\infty)\} \Leftrightarrow \widetilde{S} \sim \mathbf{R}, \\ &h = h_{cr} \Rightarrow r \in \{(0, r_{cr}) \vee \{r_{cr}\} \vee [r_{cr}, +\infty)\} \Leftrightarrow \{\widetilde{S} \sim \mathbf{R}\} \vee \{\widetilde{S} \sim \text{a point}\}, \\ &h \in (h_{cr}, +\infty) \Rightarrow r \in (0, +\infty) \Leftrightarrow \widetilde{S} \sim \mathbf{R}. \end{aligned} \tag{18}$$

This leads to a great variety of physical orbits: bounded and collisional (of the type ejection-collision, ejection – circular orbit, or circular orbit – collision), bounded and noncollisional (circular orbits), unbounded and collisional (of the type ejection-escape, or capture-collision), or unbounded and noncollisional (of the type circular orbit – escape, or capture – circular orbit).

Remark 3.1. For checking and comparison, see Mioc and Stoica (1997), Mioc (1998), or Szenkovits et al. (1999).

But, for the purposes of this paper, we are interested only in bounded noncollisional motion. The above results lead straightforwardly to (see Stoica 1997; Mioc and Stoica 1997)

Theorem 3.2. *The necessary and sufficient conditions for bounded and noncollisional motion in Manev-type fields are*

(a) $$\{A > 0,\ (C^2 - 2B) > 0,\ h_{cr} \le h < 0\}; \tag{19}$$

(b) $$\{A < 0,\ (C^2 - 2B) < 0,\ h = h_{cr},\ r_0 = r_{cr}\}, \tag{20}$$

where r_0 is the initial value.

Corollary 3.3. *The bounded noncollisional motion with $h = h_{cr}$ is circular.*

Remark 3.4. In the case $C = 0$, the amended potential reads

$$V(r) = -\frac{1}{r}\left(A + \frac{B}{r}\right). \tag{21}$$

The motion is rectilinear, the above mentioned types of behaviour remain qualitatively the same, but the physical trajectories are different. We have radial librations instead of periodic (noncircular) and quasiperiodic (see Section 4) orbits, rest instead of circular motion, etc.

Remark 3.5. In the full phase space, the nonfactorized sets $\widetilde{S}(\mathbf{C}, h)$ are isomorphic to $\mathbf{R} \times S^1$, $T^2 = S^1 \times S^1$, S^1, or $\emptyset$ (this last case corresponding to impossible real motion).

4. QUASIPERIODIC ORBITS

From the standpoint of astronomy, which provides the greatest number of concrete modellable situations, the most interesting case is that of bounded noncollisional motion. The existence of *periodic* such orbits (circular, elliptic, or rosette-shaped that close after a finite number of rotations) is clear. The existence of *quasiperiodic* orbits in Manev-type problems was also proved (Diacu et al. 1995, 2000; Delgado et al. 1996). In the sequel we provide a quite different proof of the existence of such orbits. We shall use a new parameterization of the independent variable in order to determine the motion frequencies on the set $\widetilde{S}(\mathbf{C}, h) \equiv T^2 = S^1 \times S^1$. In this way we point out the asymmetry of the Hamiltonian $H(r, p)$, which leads to phase curves that cover densely T^2.

The necessary conditions for such a motion are those stated by Theorem 3.2, formula (19). The equation of motion are

$$\begin{aligned} \dot{r} &= p, \\ \dot{p} &= -\frac{A}{r^2} + \frac{C^2 - 2B}{r^3}, \end{aligned} \tag{22}$$

As equations (22) cannot be solved in terms of elementary functions, we shall rescale the independent variable (time) via the transformation

$$dt = r\,d\tau . \tag{23}$$

Under this transformation, the system (22) becomes

$$\begin{aligned} r' &= pr , \\ p' &= -\frac{A}{r} + \frac{C^2 - 2B}{r^2} , \end{aligned} \tag{24}$$

where $' := d/d\tau$, and we kept by abuse the same notation for the new functions of the timelike variable τ. The system (24) leads to the second order equation

$$r'' = -A + \frac{C^2 - 2B}{r} + p^2 r , \tag{25}$$

or, using the explicited energy integral,

$$r'' = -A + 2hr . \tag{26}$$

This equation has the solution

$$r(\tau) = a\left[1 + e\cos\left(\frac{\tau - \tau_0}{\sqrt{a}}\right)\right], \tag{27}$$

where τ_0 is the initial moment and we have abridged

$$a = -\frac{A}{2h}, \tag{28}$$

$$e = \sqrt{1 + \frac{2h(C^2 - 2B)}{A^2}} . \tag{29}$$

By Theorem 3.2 and Corollary 3.3, the only case that interests us is that given by (19) with $h_{cr} < h < 0$. Taking into account (27), it results that the function $r(\tau)$ is periodic, of period $2\pi/\sqrt{a}$.

Let us consider the full set $\widetilde{S}(\mathbf{C}, h)$. The angular variables that define the torus given by the second formula (15) are, on the one hand, the corresponding variable in the plane (r, p) and, on the other hand, the angle θ discarded via factorization. To understand the dynamics on the torus, we shall calculate the variation

$$\Delta\theta = \int_0^T \dot{\theta}(t)\,dt = \int_0^{2\pi\sqrt{a}} \theta'(\tau)\,d\tau , \tag{30}$$

where T is the period. We shall use $\dot{\theta} = C/r^2(t)$ (see (9)) and $\theta' = C/r(\tau)$ (which follows immediately from (23)). Using (27), and abridging $\zeta = \tau/\sqrt{a}$, it results

$$\Delta\theta = (C / \sqrt{a}) \int_0^{2\pi} (1 + e \cos\zeta)^{-1} \, d\zeta = \frac{C}{\sqrt{a}} \frac{2\pi}{\sqrt{1 - e^2}}, \tag{31}$$

or, using (28) and (29),

$$\Delta\theta = 2\pi \sqrt{\frac{AC^2}{C^2 - 2B}}. \tag{32}$$

Hence we may say that, while $r(t)$ completes a period in the plane (r, p), the variable θ from the full phase space completes the arc $\Delta\theta$ given by (32). The frequency ratio will be

$$\frac{1}{2\pi \sqrt{\frac{AC^2}{C^2 - 2B}}} \Bigg/ \frac{1}{2\pi} = \sqrt{\frac{C^2 - 2B}{AC^2}}. \tag{33}$$

The expression of the ratio (33) allows us to state the main result of this paper under the form of

Theorem 4.1. *For* $\sqrt{(C^2 - 2B)/(AC^2)} \notin \mathbf{Q}$ *(set of rational numbers), the torus* T^2*, on which the bounded noncollisional motion takes place, is densely covered by quasiperiodic orbits. In the configuration space, the orbits fill densely an annulus. In the physical space, the trajectories are confined to an annulus of radii* $r_{\min}$ *and* $r_{\max}$*; the orbits are rosette-shaped and never close, filling densely the given surface.*

Corollary 4.2. *In the particular case* $\sqrt{(C^2 - 2B)/(AC^2)} \in \mathbf{Q}$*, the periodic orbits on the torus close after a finite number of cycles. Projecting this issue onto the configuration space, the result is wholly similar. As to the physical interpretation, the trajectory, confined to the same annulus of Theorem 4.1, is rosette-shaped and closes after a finite number of cycles.*

From Theorem 4.1 and Corollary 4.2 it follows immediately

Corollary 4.3. *In the set of initial conditions that lead to bounded noncollisional motion, those that provide quasiperiodic orbits have positive Lebesgue measure.*

In other words, for a fixed angular momentum C, all physical orbits for which conditions (19) hold are quasiperiodic, except a set of zero Lebesgue measure. This allows one to apply the classical results of KAM theory, as Lacomba et al. (1991) done.

In this way we provided a new proof of the existence of quasiperiodic orbits in the Manev-type two-body problem.

REFERENCES

Casasayas, J., Fontich, E., Nunes, A.: 1993, in E. Lacomba, J. Llibre (eds), *Hamiltonian Systems and Celestial Mechanics*, Advenced Series in Nonlinear Dynamics, Vol. 4, World Scientific, Singapore, 35.

Delgado, J., Diacu, F. N., Lacomba, E. A., Mingarelli, A., Mioc, V., Perez, E., Stoica, C.: 1996, *J. Math. Phys.*, **37**, 2748.

Diacu, F. N.: 1993, *J. Math. Phys.*, **34**, 5671.

Diacu, F., Mingarelli, A., Mioc, V., Stoica, C.: 1995, in R. J. Agarwal (ed.), *Dynamical Systems and Applications*, World Scientific Series in Applicable Analysis, Vol. 4, World Scientific, Singapore, 213.

Diacu, F., Mioc, V., Stoica, C.: 2000, *Nonlinear Analysis*, **41**, 1029.

Lacomba, E. A., Llibre, J., Nunes, A.: 1991, in T. Ratiu (ed.), *The Geometry of Hamiltonian Systems*, Proc. of a Workshop, 5-16 June 1989, Springer Verlag, New York, 373.

Mioc, V.: 1998, *Publ. Obs. Astron. Belgrade*, **60**, 126.

Mioc, V., Blaga, C.: 1999, *Hvar Obs. Bull.*, **23**, 41.

Mioc, V., Stavinschi, M.: 1999a, *Baltic Astron.*, **8**, 413.

Mioc, V., Stavinschi, M.: 1999b, *Phys. Scripta*, **60**, 483.

Mioc, V., Stoica, C.: 1995a, *C. R. Acad. Sci. Paris*, **320**, sér. I, 645.

Mioc, V., Stoica, C.: 1995b, *C. R. Acad. Sci. Paris*, **321**, sér. I, 961.

Mioc, V., Stoica, C.: 1997, *Baltic Astron.*, **6**, 637.

Stoica, C.: 1995, *Rom. Astron. J.*, **5**, 157.

Stoica, C.: 1997, Thesis, Astronomical Institute of the Romanian Academy, Bucharest.

Stoica, C., Mioc, V.: 1996, *Bull. Astron. Belgrade*, **154**, 1.

Szenkovits, F.: 1999, Thesis, Babeş-Bolyai University, Cluj-Napoca.

Szenkovits, F., Stoica, C., Mioc, V.: 1999, *Mathematica*, **41**, 105.

Received on 15 November 2000

THE BUCHAREST OBSERVATORY PHOTOGRAPHIC OBSERVATIONS IN THE WIDE-FIELD PLATE DATABASE

MILCHO TSVETKOV [1], MAGDA STAVINSCHI [2], KATYA TSVETKOVA [1], KONSTANTIN STAVREV [1], GHEORGHE BOCŞA [2], VASIL POPOV [1] CORNELIA CRISTESCU [2]

[1] *Institute of Astronomy, Bulgarian Academy of Sciences*
72 Tsarigradsko Shosse Blvd., BG-1784 Sofia, Bulgaria
E-mail: tsvetkov@skyarchive.org

[2] *Astronomical Institute of the Romanian Academy*
Str. Cuţitul de Argint 5, RO-75212 Bucharest, Romania
E-mail: magda@roastro.astro.ro

Abstract. The data in the Wide-Field Plate Database for the archived photographic observations obtained with the 0.38 m refractor and the 0.16 m camera of the Bucharest Observatory in the context of the their repeated use are being analyzed. A summary of the observational programs carried out with these two instruments since 1930 is presented. Results from the scanning of selected plates with the PDS 1010 of the Sofia Sky Archive Data Center are presented, too.

Key words: photographic observations – archiving – large databases.

1. INTRODUCTION

The photographic astronomical archives provide opportunities for new investigations, especially due to the unique factor of time. The importance of the repeated usage of archived observations is increased by the fact that the application of modern devices for plate digitization allows now to extract from the observations more information than it had been possible in the past, when they were made. The interest in using archived observations is expected to increase during the next years, in connection with the creation of the Uccle Direct Astronomical Plate Archive Centre (UDAPAC) in the Royal Observatory of Belgium, Brussels (see http://midasf.oma.be/~fido/ovid.html). The information concerning the usage of plate collections and the references to the papers, published already on the basis of plate collections, may be very useful for the potential user of the plates, since the papers may contain important information for the observations. The aim of this work is to present the Bucharest plate catalogues in the context of the repeated usage of the archived observations.

Rom. Astron. J., Vol. 10, No. 2, p. 177–186, Bucharest, 2000

2. THE BUCHAREST PLATE CATALOGUES

The Bucharest wide-field plate archives have been dated since 1930, when the two telescopes (a 0.38 m refractor and a 0.16 m camera) have been put in operation. Computer readable versions of the logbooks and a preliminary analysis of the plate data have been made by Vass et al. (1994) and Vass (1994). Since 1996, the Bucharest plate catalogues have been incorporated in the Wide-Field Plate Database (WFPDB; Tsvetkov 1992; Tsvetkov et al. 1998a), installed in CDS in Strasbourg with an on-line search possible through the VizieR system at http://vizier.u-strasbg.fr/cats/VI.htx. Analysis of the Bucharest plate catalogues, based on data retrieval from the WFPDB separately for the two telescopes, is presented in Tsvetkov et al. (2000).

The WFPDB contains 10 353 plates, obtained with the 0.38 m refractor (WFPDB instrument identifier BUC038) and 180 plates obtained with the 0.16 m camera (WFPDB instrument identifier BUC016). These are slightly reduced numbers in comparison with the numbers of plates in the original catalogues due to corrections in the original data during their preparation for inclusion in the WFPDB.

When the question concerns the repeated usage of archival plates, one has to take into consideration several things: coverage in time and space, magnitude limit of the plates, method of observation – single or multi-exposure, purpose of observations – monitoring or sky surveys, quality of the plates and the form of access to the needed plates in the plate vault. In some plate catalogues, explanations including some of the above mentioned things are given in the attached notes for each plate. The processing of the notes for the Bucharest plates from the two catalogues (84% of BUC038 plates and 25% of BUC016 plates have notes) shows that they contain mainly names of additional objects observed in the same field (with a minor planet numeration accepted since 1977) and duration of all exposures on the plate in case of a multi-exposure.

The graphic presentations of the coverage in time and space for the Bucharest plates can be found in Tsvetkov et al. (2000). In the distributions of the centers of the BUC038 plates and of the BUC016 plates on the celestial sphere in equatorial coordinates (J2000), there is a well expressed concentration of the observations in the zone of the ecliptic. This makes the plate collections extremely valuable, especially for near-Earth asteroid (NEA) investigations – detections, measurements, and making accurate predictions for future close encounters (as we done, e.g., for the potentially hazardous NEA 1997 XF11; Tsvetkov et al. 1998b).

Concerning the magnitude limit of the plates, several authors reported about reached maximum magnitude 12^m, for minor planets, and 9^m, for comets (Cristescu et al. 1969a; Cristescu 1974). Since 1972, using the Metcalf method and more sensitive plates, 15^m for minor planets has been reached.

The information about the used exposure duration is presented for both instruments in Table 1. For BUC038, mainly exposures up to 10 min (71%) were used. For BUC016, the exposures are longer, but usually less than 1 hour. As it can be seen from Table 2, where the distributions of the number of plates according to the multiplicity of the exposure are given for both telescopes, the observations have been performed mainly with double exposures for BUC038, and with single exposures for BUC016. The multiple exposures are 85% of all observations for BUC038, and 21% for BUC016.

Table 1

Number of plates according to the duration of exposure

Duration of exposure	BUC038		BUC016	
[min]	n	%	n	%
1 – 5	3810	37	23	13
6 – 10	3562	34	28	16
11 – 15	1582	15	13	7
16 – 20	442	4	26	14
21 – 25	96	1	8	4
26 – 30	162	2	28	16
31 – 35	45	< 1	6	3
36 – 40	52	< 1	10	6
41 – 45	31	< 1	4	2
46 – 50	25	< 1		
51 – 55	23	< 1	2	1
55 –60	407	4	15	8
> 60	27	< 1	16	9
Unknown	89	< 1	1	< 1

Table 2

Number of plates according to the multiplicity of exposure

Multiplicity of exposure	BUC038		BUC016	
[min]	N	%	n	%
1	1508	15	141	78
2	6415	62	35	19
3	2183	21	3	2
4	58	1		
5	13	< 1		
6	18	< 1		
7	4	< 1		
8	5	< 1		
9	32	< 1		
10	11	< 1		
> 10	22	< 1		
Unknown	84	< 1	1	< 1

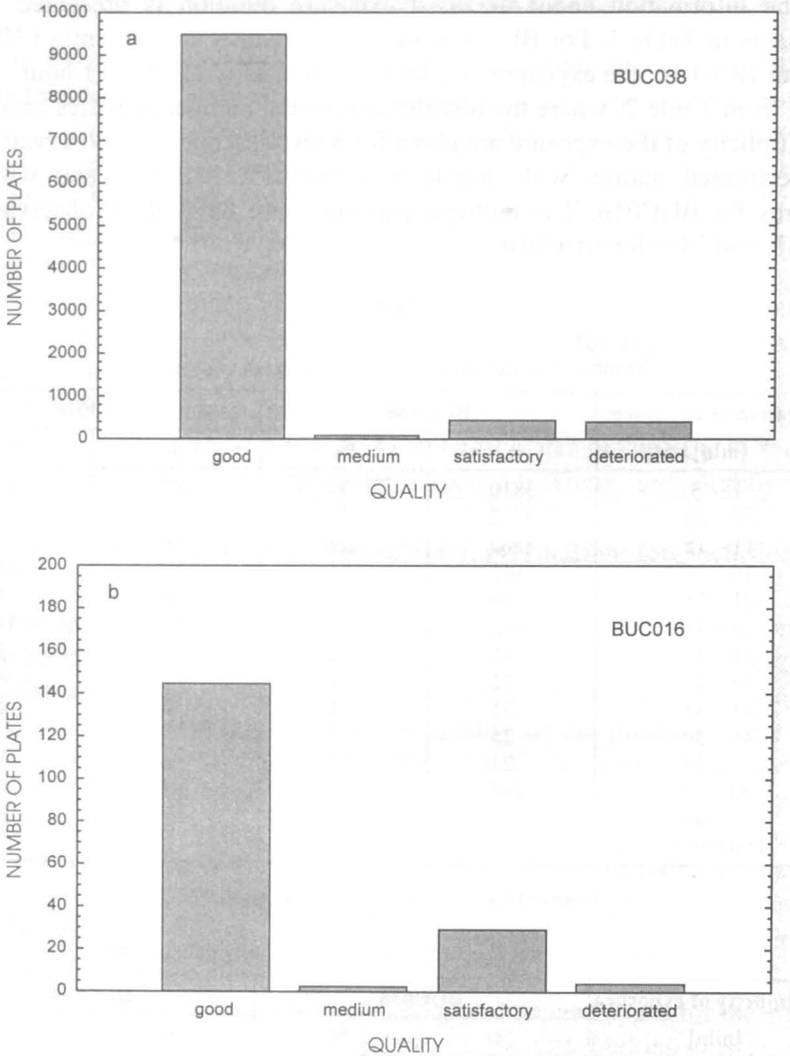

Fig. 1 – Number of plates versus plate quality for (a) BUC038, and (b) BUC016.

The Bucharest plate catalogues contain also information for the plate quality in sense of the physical state of the plates, the quality being estimated as good, medium, satisfactory, and deteriorated. In Fig. 1, the distributions of the number of plates versus plate quality are given for both instruments. As it can be seen, the majority of the plates are in good state.

Let us note that good permanent storage conditions are assured for the plates, having in mind such practical problems as humidity, dust, strong illumination, and optimum room temperature.

3. OBSERVATIONAL PROGRAMS

In Fig. 2, the distributions of the number of plates versus object type for BUC038 and BUC016 are given. One sees that the majority of plates in the Bucharest catalogues (78% of all plates) are devoted to asteroid observations. BUC038 was used actively also for observations of fundamental stars, while BUC016 was used almost exclusively for observations of comets and asteroids.

The wide-field plates of the Bucharest Observatory archives were accumulated mainly as a result of the conducting of the following observational programs:

3.1. PRECISE PHOTOGRAPHIC POSITIONS OF MINOR PLANETS AND COMETS

The program is running since 1930 (Cristescu et al. 1960b,d, 1961, 1966, 1968, 1969b, 1970a,b; Cristescu and Gheţu 1967a,b; Ionescu Vlăsceanu and Novacevski-Rusu 1960; Ionescu Vlăsceanu 1965a,b; Ionescu Vlăsceanu and Cristescu 1967; Bocşa 1970; Bocşa et al. 1973a,b). Choosing appropriate coordinates, the images of at least two minor planets have been obtained on each plate in some cases. Among the comet observations, there are those of 1943c, discovered by the Romanian astronomer Daimaca, and of Van Gent-Peltier-Daimaca (1943f-1943g). The orbit of the minor planet 584 Semiramis, in Ephemerides of Minor Planets for 1978, was improved by Bocşa. Some of the observations are done in the framework of a collaboration with Nice Observatory, France. The results are sent to the Minor Planet Center, Cambridge (USA).

3.2. CERES PROGRAM

Since 1954 the Bucharest Observatory has participated in the program initiated by the Institute of Theoretical Astronomy in Leningrad (today Institute of Applied Astronomy, St. Petersburg, Russia), for observations of 10 designated asteroids (1 Ceres, 2 Pallas, 3 Juno, 4 Vesta, 6 Hebe, 7 Iris, 11 Parthenope, 18 Melpomene, 39 Laetitia, and 40 Harmonia; Cristescu et al. 1959, 1960a,c, 1972), and later of 5 more (25 Phocaea, 148 Gallia, 389 Industria, 532 Herculina, and 704 Interamnia; Cristescu et al. 1973, 1974), for the determination of an inertial system of stellar reference. With this program can be explained the great amount of plates with images of the above asteroids.

3.3. STELLAR PROPER MOTIONS

The first stage (1957–1965) of this joint program with the Pulkovo Observatory used distant galaxies as fixed reference points for the determination of stellar proper motions. The second stage (1980–1990) used faint distant stars.

3.4. KIEV PROGRAM CONFOR

This program has been aimed to make connection between radio (VLBI observations) and optical (FK5) reference frames since 1992. More than 180 new plates have been obtained with BUC038 since 1993 according to this program and will be soon included in the WFPDB.

3.5. THE GALILEAN SATELLITES OF JUPITER

Photographic determinations of the orbits of the Galilean satellites of Jupiter were performed by Petrescu (1935, 1938, 1939), Bocşa (1994), Stavinschi and Bocşa (1996).

3.6. STELLAR CLUSTERS

Within the framework of this program, determinations of the brightness of M13 and Hyades by Demetrescu and Cristescu (1967) were made. The existence of plates in the Pleiades region for the period 1955–1958 gives the possibility to use them in the project on investigation of long-term variability of the Pleiades red dwarf stars, together with the Byurakan, Konkoly, Rozhen, Potsdam and Sonneberg observatories.

3.7. CLOSE BINARIES AND MIRA CETI-TYPE VARIABLE STARS

Photometric studies were conducted for such types of variable stars. There are more than 80 plates, which might be objects of future usage of the archived observations having in view the long period of time coverage.

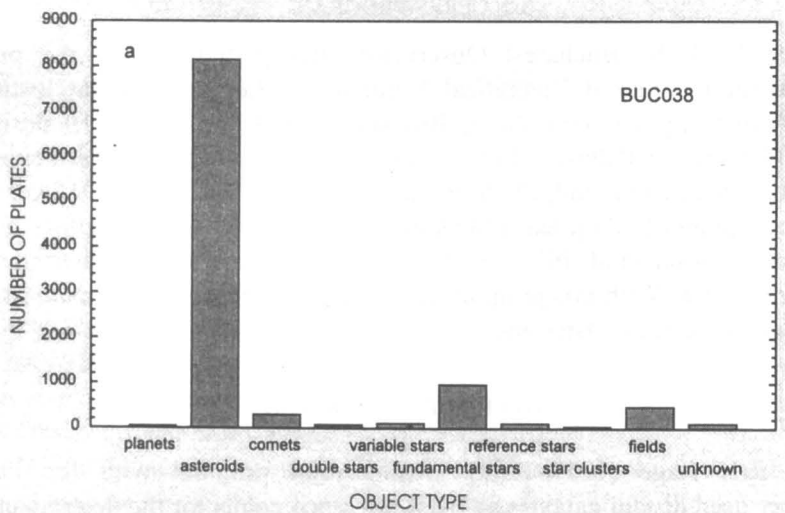

Fig. 2 – Number of plates versus object type for (a) BUC038.

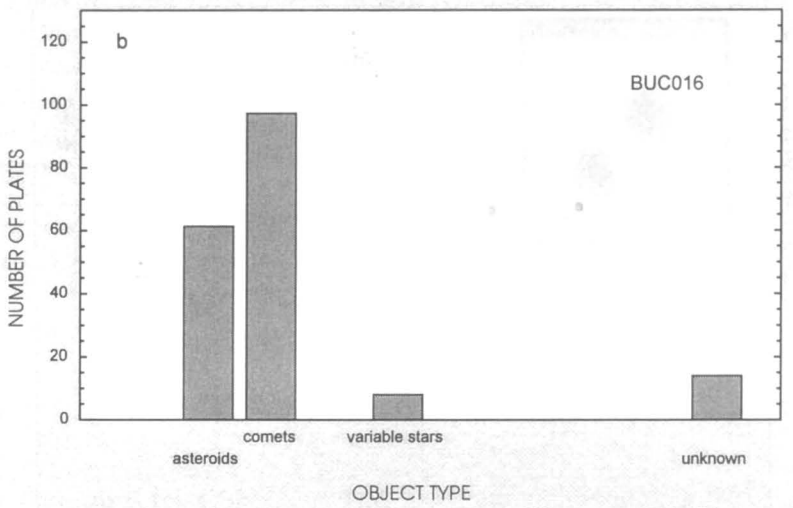

Fig. 2 – Number of plates versus object type for (b) BUC016.

3.8. OTHER PROGRAMS

Here are related such programs as Moon eclipses, Stellar occultations, Venus Mercury passages in 1970 and 1973, observed and published together with the U.S. Naval Observatory, Positional measurements of the planets Pluto and Jupiter (Cristescu et al. 1973; Stavinschi and Bocşa 1994).

The results from the above programs are published mainly in the Romanian periodic journals *Studii şi Cercetări de Astronomie şi Seismologie*, (1956–1962), *Studii şi Cercetări de Astronomie* (1963–1974) and *Contributions to Astronomy* (1975), as well as in *Astronomische Nachrichten*, *Journal des Observateurs*, and the IAU Circular Letters.

4. PLATE DIGITIZATION

Plate digitization and image processing of the Bucharest Observatory plates are possible with the help of the PDS1010 microdensitometer and the software of the Sofia Sky Archive Data Center. In the frames of a joint project, in May 2000, we began the scanning of selected interesting plates, each one containing images of more than 4 minor planets. Two such plates are BUC038 208151 and BUC016 101605, taken on 2 May 1973 and 5 October 1938, respectively.

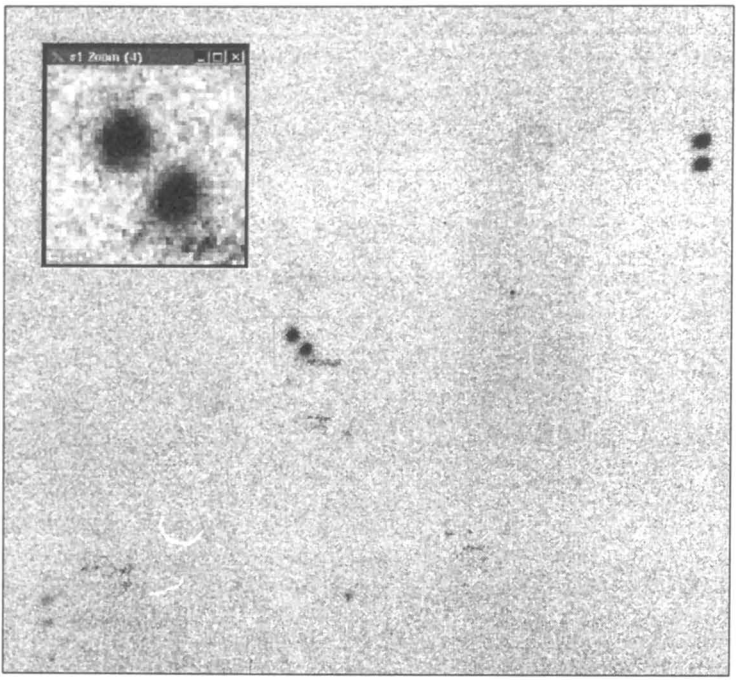

Fig. 3 – Digitized images of the minor planet 230 Athamantis taken with the 0.38 m refractor.

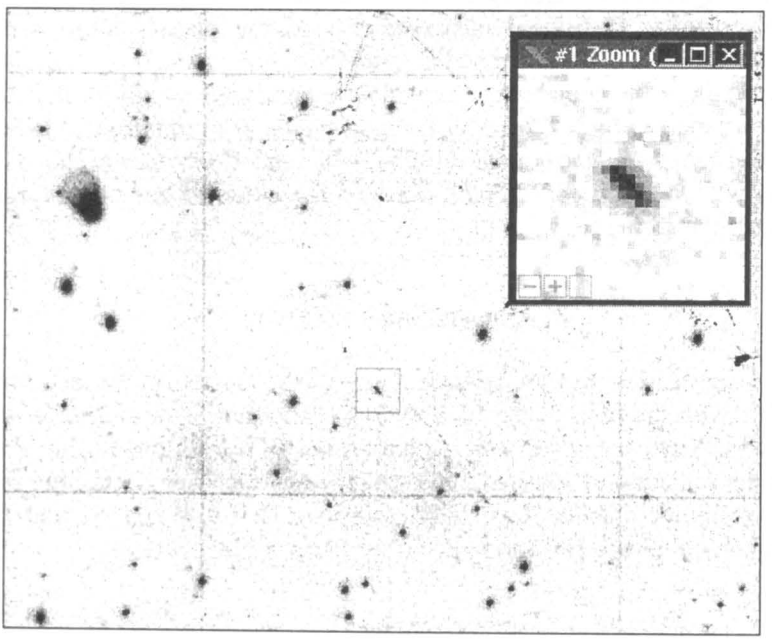

Fig. 4 – Digitized image of a minor planet taken with the 0.16 m camera.

Regions (2000× 1500 pixels) of the above mentioned plates, containing the images of the minor planets 108 Hecuba, 230 Athamantis, 322 Billjackson, and 932 Hooveria (BUC038), and 64 Angelina, 73 Klytia, 208 Lacrimosa, and 258 Tyche (BUC016), have been scanned with a 20 μm square diaphragm and step size of 20 μm. In Fig. 3 a part of the scanned region with the image of the minor planet 230 Athamantis is shown. Fig. 4 shows part of the scanned region of plate BUC016 101605.

Acknowledgement. The authors are grateful to Dr. Gheorghe Vass for useful discussions.

BIBLIOGRAPHY

Bocşa, G.: 1970, *St. Cerc. Astron.*, **15**, 225.
Bocşa, G.: 1994, *Rom. Astron. J.*, **4**, 175.
Bocşa, G., Cristescu, C., Gheţu, I., Milet, B.: 1973a, *St. Cerc. Astron.*, **18**, 105.
Bocşa, G., Cristescu, C., Gheţu, I., Ionescu Vlăsceanu, V., Milet, B.: 1973b, *St. Cerc. Astron.*, **18**, 115.
Cristescu, C.: 1974, in: C. Cristescu, W. J. Klepczynski, B.Milet (eds), *Asteroids, Comets, Meteoric Matter*, 22nd IAU Coll., Ed. Acad. R.S.R., Bucharest.
Cristescu, C., Gheţu, I.: 1967a, *St. Cerc. Astron.*, **12**, 75.
Cristescu, C., Gheţu, I.: 1967b, *St. Cerc. Astron.*, **12**, 205.
Cristescu, C., Milet, B.: 1973, *St. Cerc. Astron.*, **18**, 103.
Cristescu, C., Ionescu Vlăsceanu, V., Vlaicu, S., Novacevski-Rusu, L., Popovici, G.: 1959, *St. Cerc. Astron. Seism.*, **4**, 331.
Cristescu, C., Ionescu Vlăsceanu, V., Vlaicu, S.: 1960a, *St. Cerc. Astron. Seism.*, **5**, 181.
Cristescu, C., Ionescu Vlăsceanu, V., Vlaicu, S.: 1960b, *St. Cerc. Astron. Seism*, **5**, 193.
Cristescu, C., Ionescu Vlăsceanu, V., Vlaicu, S.: 1960c, *St. Cerc. Astron. Seism*, **5**, 301.
Cristescu, C., Ionescu Vlăsceanu, V., Vlaicu, S.: 1960d, *St. Cerc. Astron. Seism*, **5**, 319.
Cristescu, C., Ionescu Vlăsceanu, V., Vlaicu, S.: 1961, *St. Cerc. Astron. Seism*, **6**, 71.
Cristescu, C., Gheţu, I., Vlaicu, S.: 1966, *St. Cerc. Astron*, **11**, 127.
Cristescu, C., Gheţu, I., Ionescu Vlăsceanu, V.: 1968, *St. Cerc. Astron.*, **13**, 201.
Cristescu, C., Ionescu Vlăsceanu, V., Gheţu, I., Bocşa, G.: 1969a, *St. Cerc. Astron.*, **14**, 123.
Cristescu, C., Bocşa, Gh., Ionescu Vlăsceanu, V.: 1969b, *St. Cerc. Astron.*, **14**, 173.
Cristescu, C., Ionescu Vlăsceanu, V., Bocşa, G.: 1970a, *St. Cerc. Astron.*, **15**, 237.
Cristescu, C., Ionescu Vlăsceanu, V., Bocşa, G.: 1970b, *St. Cerc. Astron.*, **15**, 261.
Cristescu, C., Ionescu Vlăsceanu, V., Gheţu, I., Bocşa, G.: 1972, *St. Cerc. Astron.*, **17**, 85.
Cristescu, C., Ionescu Vlăsceanu, V., Milet, B.: 1974, *St. Cerc. Astron.*, **19**, 109.
Demetrescu, G., Cristescu, C.: 1967, *Elements of Stellar Dynamics*, Ed. Acad. R.S.R., Bucharest (Romanian).
Ionescu Vlăsceanu, V.: 1965a, *St. Cerc. Astron.*, **10**, 93.
Ionescu Vlăsceanu, V.: 1965b, *St. Cerc. Astron.*, **10**, 99.
Ionescu Vlăsceanu, V., Cristescu C.: 1967, *St. Cerc. Astron.*, **12**, 185.
Ionescu Vlăsceanu, V., Novacevski-Rusu, L.: 1960, *St. Cerc. Astron. Seism.*, **5**, 201.
Petrescu, G.: 1935, *J. Obs.*, **18**, 179.
Petrescu, G.: 1938, *J. Obs.*, **21**, 13.
Petrescu, G.: 1939, *J. Obs.*, **22**, 8.
Stavinschi, M., Bocşa G.: 1996, *Ann. Physique*, **21**, 169.
Tsvetkov, M.: 1992, *IAU WGWFI Newsletter*, **2**, 51.

Tsvetkov, M. K., Stavrev, K. Y., Tsvetkova, K. P., Semkov, E. H., Mutafov, A. S., Michailov, M.-E.: 1998a, in B. McLean et al. (eds), *New Horizons from Multi-Wavelength Sky Surveys*, Kluwer Acad. Publ., Dordrecht, 462.

Tsvetkov, M. K., Stavrev, K.Y., Tsvetkova, K.P., Semkov, E.H., Mutafov, A.S., and Borisova, A.P.: 1998b, *IAU WGSS Newsletter*, **10**, 10.

Tsvetkov, M. K., Stavinschi, M., Tsvetkova, K. P., Stavrev, K. Y., Bocşa, G., Popov, V. N., Cristescu, C.: 2000, *Baltic Astron.* (in press).

Vass, G.: 1994, *Rom. Astron. J.*, **4**, 183.

Vass, G., Bocşa, G., Ionescu Vlăsceanu, V., Alexiu, A., Bîrlan, M.: 1994, *Rom. Astron. J.*, **4**, 179.

Received on 18 December 2000

THE ARCHIVE OF ASTROMETRIC PLATES OBTAINED AT THE ASTRONOMICAL OBSERVATORY OF CLUJ

GHEORGHE DORIN CHIŞ, CRISTINA BLAGA, LIVIU MIRCEA

Astronomical Institute of the Romanian Academy
Astronomical Observatory Cluj-Napoca
Str. Cireşilor 19, RO-3400 Cluj-Napoca, Romania
E-mail: dorin@roastro.astro.ro, cpblaga@math.ubbcluj.ro, liviu@email.ro

Abstract. Within the framework of the Wide-Field Plate Database Project we have begun to archive the photographic plates kept in the library of the Cluj Observatory. The aim of this note is to present the wide-field plates obtained at Cluj between 1952 and 1957. These plates contain 142 positions of 15 small planets and 4 comets.

Key words: astrometry – wide field plates archive.

1. INTRODUCTION

In the library of the Astronomical Observatory of Cluj-Napoca there are stored the photographic plates obtained between 1943 and 1974 by the astronomers of this observatory. We are going to archive these plates in the frames of the Wide-Field Plates Database Project. The aim of this project initiated by the Working Group on Wide-Field Imaging at the 21st General Assembly of the IAU is to inventory all the wide-field photographic plates obtained, along the time, over the world, in professional observatories, and to organize an on-line access to the data. A description of the project was given by Tsvetkov et al. (1994).

In this note we are interesed in the plates made for astrometric purposes, i.e., with the aim to determine positions of small planets and comets visible from Cluj between 1952 and 1957. In that period the main observational activity in our observatory was concentrated in the area of variable stars. This is the reason why only about 1.6% from the plates contain positions of asteroids and comets.

The astrometric plates were obtained by several astronomers. Almost all photographic plates in question now were made by Gheorghe Chiş (1913-1981), who was involved also in other topics related to comets: observations of faint comets with filar micrometer (Chiş, 1949) and cometary ephemerides computations (Chiş, 1950). Occasionally he had the support of Ştefan Radu and Ioan Todoran, who worked at that time at the observatory. The measurements of the coordinates

Rom. Astron. J., Vol. 10, No. 2, p. 187–193, Bucharest, 2000

and the position determinations were made by Ioan Todoran, in the case of the small planets, and by Elvira Botez for comets. The results of the measurements and the methods used to reach them were described by Chiş et al. (1960).

2. LOCATION OF THE OBSERVATORY AND INSTRUMENTS

The old Astronomical Observatory of the Cluj University, whose construction was started in 1927, was located near the southern border of the city, at the latitude $\varphi = 46°45'33.8''\,\mathrm{N}$ and longitude $L = 1^h34^m23.46^s\,\mathrm{E}$, not very far from the center of the city, because, belonging to the university, its main goal was to give to the students the opportunity to watch the sky through a telescope. In 1931, the equatorial building was ended and two years later the Prin equatorial was installed there. This instrument was used to obtain the photographic plates. It has two parts: a Newton telescope and a refractor (Fig. 1). The Newton telescope has a parabolic mirror with diameter $D = 50$ cm and focal length $F = 250$ cm. The telescope's mirror was cut in Couder's optical manufacture from Observatoire de Paris. The objective of the refractor came from Germany (Zeiss); it has a diameter $D = 20$ cm and a focal length $F = 300$ cm.

The limit photographic magnitude for an exposure of 10 minutes was approximately 14.5 for the Newton telescope and 12.5 for the refractor. The plate scale was 68.8 arcsec/mm, respectively 82.5 arcsec/mm.

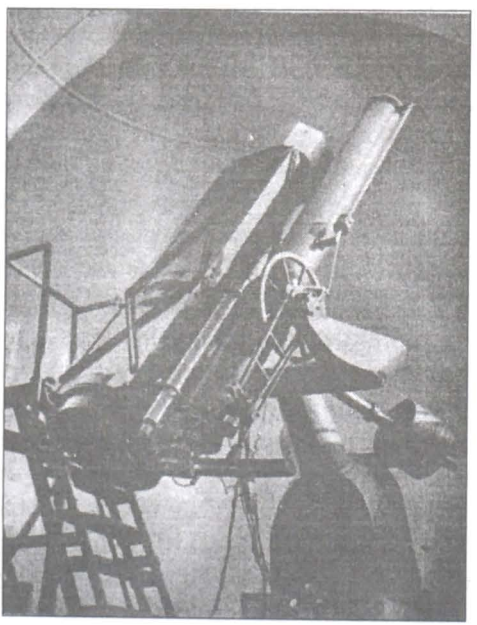

Fig. 1 – The Prin equatorial (Newton telescope – left, Zeiss refractor – right).

3. THE PLATES ARCHIVE

Table 1 contains the list of the astrometric plates that exist in our observatory. The size of the plates was usually 6 × 9 cm for the Newton telescope and 9 × 12 cm for the refractor. The field angular size is then 2°.30, respectively 2°.06.

In the first column we mention the number of the plate written on the envelope in which it is kept: *E* means that the plate was obtained with the equatorial and *O* – that it was made with the aid of the Newton telescope. *V* comes from visual; this means that to obtain the plate there has been used a filter (GG11 for photovisual). The Roman figures in brackets emphasize the fact that the plate was exposed more than one time. These ones give the number of exposures considered to determine the position of the object. The lowercase letter *b* means that the plate is broken, but not in the part where the small body or the comet is placed. The letter *m* means that during the exposure the instrument was moved following the comet. On these plates the trails of the stars are visible.

In the second column there is mentioned the date at which the observation was made using the day, the month, and the year (DD.MM.YYYY). The third and fourth columns contain right ascension (in hours, minutes seconds and fractions of second) and the declinations (degrees, arcminutes arcseconds) of the observed body at the epoch 1950.0. In the next two columns there are listed the moment of the beginning of the observation in UT (hh mm ss) and the duration of the exposure in seconds.

In the seventh column we have written the abbreviated name of the observed body. The full name of the objects are the following: for the small planets 1 Ceres, 349 Dembowska, 8 Flora, 11 Parthenope, 51 Nemausa, 6 Hebe, 241 Germania, 109 Felicitas, 490 Veritas, 509 Yolanda, 196 Filomela, 19 Fortuna, 22 Kalliope, 7 Iris, 364 Isara, and for the comets 1954 X Abell (1953 g), 1955 III Mrkos (1955 e), 1957 III Arend-Roland (1956 h), 1957 V Mrkos (1957 d).

There were used different types of emulsion, listed in the last column of the table. We have used the following abbreviations for them: Guill. for Guilleminot Superfulgur plates, Afga Iso for Agfa Isochrom Orthochromatic, Afga Ips for Agfa Isopan rendered (sensibilised) with a solution of distilled water, alcohol, ammonia and silver tungstate, Agfa Pan for Agfa Isopan and Agfa Ast for Afga Astro-Plates Panchromatic, IsoSPan for Agfa Isopan ISS Super Panchromatic and Isopan F for Agfa Isopan F plates fine-grain structure, also Super Ortho-Panchromatic.

These 142 positions of small planets and comets recorded on photographic plates at the Observatory of Cluj, between 11 December 1952 and 1 October 1957, are incorporated into the Wide-Field Plate Database (http://www.skyarchive.org) (Tsvetkov et al., 2000).

Table 1

Main characteristics of the plates obtained at Cluj between 11 December 1952 – 24 September 1957

No. plate	Date	$\alpha_{1950.0}$	$\delta_{1950.0}$	Time	Duration	Object	Emulsion
1	2	3	4	5	6	7	8
E52(I)	11.12.1952	04 27 59.2	+19 22 40	18 52 30	600s	Ceres	Guill.
E52(II)	11.12.1952	04 27 57.5	+19 22 46	19 37 30	600s	Ceres	Guill.
E53(I)	11.12.1952	04 34 37.2	+30 36 46	20 15 30	600s	Dembr.	Guill.
E53(II)	11.12.1952	04 34 34.5	+30 36 46	21 14 30	600s	Dembr.	Guill.
E67(I)	02.03.1953	10 27 14.6	+17 28 05	18 41 09	600s	Flora	Guill.
E67(II)	02.03.1953	10 27 11.8	+17 22 22	19 35 24	600s	Flora	Guill.
E68(I)	05.03.1953	10 16 57.2	+14 38 58	18 42 50	600s	Parthen.	Guill.
E68(II)	05.03.1953	10 16 54.3	+14 39 20	20 06 50	600s	Parthen.	Guill.
O6(I)	17.05.1953	15 50 09.4	- 04 13 02	22 11 15	630s	Nemausa	Guill.
O6(II)	17.05.1953	15 50 07.0	- 04 12 42	23 08 00	600s	Nemausa	Guill.
E86(I)	17.07.1953	19 28 45.6	- 10 11 53	21 22 30	240s	Hebe	Guill.
E86(II)	17.07.1953	19 28 34.4	- 10 12 04	21 51 30	240s	Hebe	Guill.
O28(I)	01.09.1953	22 14 03.3	- 02 32 57	22 49 32	1140s	Germania	Agfa Iso
O28(II)	01.09.1953	22 14 01.3	- 02 33 13	23 47 32	600s	Germania	Agfa Iso
O33(I)	10.09.1953	23 17 07.3	- 09 05 13	19 54 51	1320s	Felicitas	Agfa Iso
O33(II)	10.09.1953	23 17 04.7	- 09 05 19	20 56 21	600s	Felicitas	Agfa Iso
O34(II)	15.09.1953	23 23 59.0	- 01 56 01	21 45 11	1200s	Veritas	Agfa Ips
O34(III)	15.09.1953	23 23 57.8	- 01 56 14	22 36 11	600s	Veritas	Agfa Ips
O43(I)	30.09.1953	00 21 43.1	+15 00 56	18 58 50	1200s	Yolanda	Agfa Ips
O43(II)	30.09.1953	00 21 40.3	+15 00 26	20 17 50	1260s	Yolanda	Agfa Ips
O45(I)	30.10.1953	02 22 57.4	+07 25 45	01 43 18	1200s	Filomela	Agfa Pan
O45(II)	30.10.1953	02 22 56.3	+07 25 39	02 36 18	1200s	Filomela	Agfa Pan
O55(I)	05.05.1954	14 12 38.1	- 13 02 23	21 22 12	600s	Fortuna	Agfa Pan
O55(II)	05.05.1954	14 12 36.9	- 13 02 16	21 54 12	600s	Fortuna	Agfa Pan
O57(I)	08.05.1954	15 20 42.2	- 12 34 14	23 17 07	600s	Kalliope	Agfa Ast
O57(II)	10.05.1954	15 18 56.7	- 12 25 29	22 45 05	600s	Kalliope	Agfa Ast
O149(I)	06.08.1954	21 23 46.9	- 06 16 36	23 29 50	600s	Iris	Agfa Ips
O149(II)	07.08.1954	21 23 44.9	- 06 16 42	00 13 50	600s	Iris	Agfa Ips
O201(I)	26.09.1954	00 06 55.8	- 11 44 08	00 37 00	660s	Isara	IsoSPan
O201(II)	26.09.1954	00 06 54.5	- 11 44 24	01 16 00	600s	Isara	IsoSPan
O205(I)	01.10.1954	00 17 10.2	- 00 58 42	00 54 00	600s	Nemausa	IsoSPan
O205(II)	01.10.1954	00 17 08.3	- 00 59 00	01 34 00	600s	Nemausa	IsoSPan
O60(b)	12.05.1954	07 04 50.1	+53 21 59	19 45 02	600s	1954 X	Guill.
O61	12.05.1954	07 04 55.5	+53 21 16	20 11 03	600s	1954 X	Guill.
O62	15.05.1954	07 16 36.3	+51 28 58	19 57 00	600s	1954 X	Guill.
O63	15.05.1954	07 16 39.3	+51 28 24	20 17 00	600s	1954 X	Guill.
O64	25.05.1954	07 52 32.6	+44 28 43	20 01 48	600s	1954 X	Guill.
O65	25.05.1954	07 52 34.9	+44 28 15	20 17 48	600s	1954 X	Guill.
O69	27.05.1954	07 59 11.8	+42 56 21	20 17 46	600s	1954 X	Guill.
O70	27.05.1954	07 59 13.6	+42 55 57	20 33 46	240s	1954 X	Guill.
O77	03.06.1954	08 20 58.0	+37 16 27	20 08 40	240s	1954 X	Guill.
O78	03.06.1954	08 20 59.5	+37 15 59	20 20 40	240s	1954 X	Guill.
O79	03.06.1954	08 21 00.6	+37 15 37	20 32 40	300s	1954 X	Agfa Ast
O82	09.06.1954	08 38 07.8	+32 03 16	20 15 30	240s	1954 X	Agfa Ast
O83	09.06.1954	08 38 09.5	+32 02 41	20 32 00	150s	1954 X	Agfa Ast
O86(b)	10.06.1954	08 40 51.6	+31 09 18	20 19 28	240s	1954 X	Agfa Ast

1	2	3	4	5	6	7	8
O87	10.06.1954	08 40 52.6	+31 08 58	20 28 28.	240s	1954 X	Agfa Ast
O90	14.06.1954	08 51 24.5	+27 30 04	20 11 49	180s	1954 X	Agfa Ast
O91	14.06.1954	08 51 26.8	+27 29 41	20 20 19	240s	1954 X	Agfa Ast
O360	16.07.1955	11 20 42.8	+51 05 25	20 01 41	180s	1955 III	Agfa Ast
O361	16.07.1955	11 20 45.7	+51 04 59	20 10 11	180s	1955 III	Agfa Ast
O362(m)	16.07.1955	11 20 49.6	+51 04 34	20 22 41	540s	1955 III	Agfa Ast
O363	16.07.1955	11 20 54.7	+51 03 58	20 37 10	180s	1955 III	Agfa Ast
O365	18.07.1955	11 35 27.2	+49 02 31	19 51 34	183s	1955 III	Agfa Ast
O366	18.07.1955	11 35 30.0	+49 02 05	20 02 04	180s	1955 III	Agfa Ast
O367	18.07.1955	11 35 33.1	+49 01 36	20 12 38	180s	1955 III	Agfa Ast
O368	18.07.1955	11 35 37.3	+49 01 00	20 26 34	180s	1955 III	Agfa Ast
O371	19.07.1955	11 42 11.6	+48 00 15	19 51 00	180s	1955 III	Agfa Ast
O372	19.07.1955	11 42 14.4	+47 59 54	20 00 00	180s	1955 III	Agfa Ast
O373	19.07.1955	11 42 16.4	+47 59 30	20 08 30	180s	1955 III	Agfa Ast
O374	19.07.1955	11 42 20.9	+47 58 47	20 25 00	180s	1955 III	Agfa Ast
O375	19.07.1955	11 42 22.8	+47 58 26	20 33 30	120s	1955 III	Agfa Ast
O385	22.07.1955	12 00 11.4	+44 54 17	19 49 50	180s	1955 III	Agfa Ast
O386	22.07.1955	12 00 13.7	+44 53 57	19 58 20	180s	1955 III	Agfa Ast
O387	22.07.1955	12 00 14.8	+44 53 35	20 06 20	180s	1955 III	Agfa Ast
O388	22.07.1955	12 00 17.4	+44 53 13	20 14 50	180s	1955 III	Agfa Ast
O389	27.07.1955	12 24 36.1	+39 53 21	20 20 04	620s	1955 III	Agfa Ast
O390	27.07.1955	12 24 28.7	+39 52 44	20 37 04	360s	1955 III	Agfa Ast
O509	30.12.1956	00 26 34.5	+08 31 20	17 30 56	601s	1957 III	Agfa Ast
O510	30.12.1956	00 26 33.7	+08 31 06	17 53 00	600s	1957 III	Agfa Ast
O511(I)	30.12.1956	00 26 32.7	+08 30 54	17 15 57	600s	1957 III	Agfa Ast
O513	01.01.1957	00 25 02.0	+07 50 34	18 24 04	602s	1957 III	Agfa Ast
O514(I)	01.01.1957	00 25 01.5	+07 50 20	18 43 14	600s	1957 III	Agfa Ast
O514(II)	01.01.1957	00 25 00.9	+07 50 02	18 57 49	600s	1957 III	Agfa Ast
O515	01.01.1957	00 25 00.9	+07 49 48	19 15 44	600s	1957 III	Agfa Ast
O516	03.01.1957	00 23 37.7	+07 11 12	18 37 47	600s	1957 III	Agfa Ast
O517(I)	03.01.1957	00 23 36.8	+07 11 02	18 55 47	600s	1957 III	Agfa Ast
O518	03.01.1957	00 23 36.1	+07 10 38	19 25 47	610s	1957 III	Agfa Ast
E376	27.04.1957	03 10 41.7	+50 58 26	19 00 26	1200s	1957 III	Isopan F
E376a	27.04.1957	03 11 16.1	+51 04 19	20 08 26	600s	1957 III	Isopan F
O519 m	27.04.1957	03 11 56.4	+51 1 10	21 22 26	600s	1957 III	IsoSPan
O520I m	28.04.1957	03 24 53.6	+53 11 49	21 02 22	60s	1957 III	IsoSPan
O520II m	28.04.1957	03 24 56.5	+53 12 11	21 05 22	120s	1957 III	IsoSPan
O521(I)	28.04.1957	03 25 01.4	+53 13 00	21 15 24	180s	1957 III	IsoSPan
O522(I)	28.04.1957	03 25 07.4	+53 13 59	21 26 22	120s	1957 III	IsoSPan
O523(I)	28.04.1957	03 25 20.5	+53 15 42	21 48 22	300s	1957 III	IsoSPan
O524(I)	29.04.1957	03 38 29.2	+55 01 05	21 31 18	120s	1957 III	IsoSPan
O526(III)	29.04.1957	03 38 43.0	+55 03 04	21 57 48	90s	1957 III	IsoSPan
O527(I)	05.05.1957	04 55 20.9	+61 23 11	20 18 59	11s	1957 III	IsoSPan
O527(II)	05.05.1957	04 55 22.2	+61 23 16	20 22 00	31s	1957 III	IsoSPan
O527(III)	05.05.1957	04 55 24.0	+61 23 24	20 24 30	90s	1957 III	IsoSPan
O528(I)	05.05.1957	04 55 30.4	+61 23 36	20 37 50	10s	1957 III	IsoSPan
O528(III)	05.05.1957	04 55 32.1	+61 23 46	20 41 00	120s	1957 III	IsoSPan
O528(IV)	05.05.1957	04 55 33.4	+61 23 52	20 44 00	30s	1957 III	IsoSPan
O529(I)	05.05.1957	04 55 37.3	+61 23 58	20 50 00	10s	1957 III	IsoSPan
O529(II)	05.05.1957	04 55 37.9	+61 24 02	20 52 00	30s	1957 III	IsoSPan

1	2	3	4	5	6	7	8
O529(III)	05.05.1957	04 55 38.9	+61 24 10	20 54 00	90s	1957 III	IsoSPan
O530	05.05.1957	04 55 52.1	+61 24 44	21 04 00	1800s	1957 III	IsoSPan
E381(I)	05.05.1957	04 56 07.1	+61 25 32	21 53 00	300s	1957 III	IsoSPan
E381(II)	05.05.1957	04 56 09.4	+61 26 05	22 00 00	120s	1957 III	IsoSPan
O531(I)	05.05.1957	04 56 36.6	+61 26 50	22 48 00	180s	1957 III	Agfa Ast
O532(I)	11.05.1957	05 59 32.3	+63 25 43	21 06 38	180s	1957 III	IsoSPan
O533(I)	11.05.1957	05 59 34.1	+63 25 44	21 14 38	180s	1957 III	IsoSPan
O534(I)	11.05.1957	05 59 38.3	+63 25 44	21 24 38	12s	1957 III	IsoSPan
O534(II)	11.05.1957	05 59 39.2	+63 25 46	21 26 38	30s	1957 III	IsoSPan
O535(II)	11.05.1957	05 59 41.7	+63 25 49	21 35 38	30s	1957 III	IsoSPan
O535(III)	11.05.1957	05 59 42.8	+63 25 50	21 37 08	90s	1957 III	IsoSPan
O536(I)	11.05.1957	05 59 44.0	+63 25 54	21 44 08	10s	1957 III	IsoSPan
O536(II)	11.05.1957	05 59 45.4	+63 25 55	21 45 08	30s	1957 III	IsoSPan
O536(III)	11.05.1957	05 59 46.2	+63 26 01	21 46 38	90s	1957 III	IsoSPan
O537	11.05.1957	06 00 07.2	+63 26 19	22 13 37	3600s	1957 III	Isopan F
E382	11.05.1957	06 00 22.7	+63 26 22	23 22 38	300s	1957 III	IsoSPan
O540(II)	12.05.1957	06 08 20.1	+63 32 34	20 49 34	30s	1957 III	IsoSPan
O540(III)	12.05.1957	06 08 22.6	+63 32 35	20 51 34	90s	1957 III	IsoSPan
O541(III)	12.05.1957	06 08 27.1	+63 32 39	21 06 04	90s	1957 III	IsoSPan
O542(II)	12.05.1957	06 08 31.3	+63 32 41	21 15 34	45s	1957 III	IsoSPan
O542(III)	12.05.1957	06 08 32.1	+63 32 43	21 17 34	90s	1957 III	IsoSPan
OV127	14.05.1957	06 24 36.2	+63 39 44	19 33 57	180s	1957 III	Isopan F
OV128	14.05.1957	06 24 38.6	+63 39 44	19 41 27	180s	1957 III	Isopan F
O543(III)	14.05.1957	06 24 43.6	+63 39 53	19 57 57	90s	1957 III	Agfa Ast
O544(III)	14.05.1957	06 25 29.6	+63 39 57	20 23 27	90s	1957 III	Agfa Ast
OV129(I)	15.05.1957	06 32 34.2	+63 40 43	20 21 24	180s	1957 III	Isopan F
O545(II)	15.05.1957	06 32 43.6	+63 40 40	20 56 24	30s	1957 III	Agfa Ast
O545(III)	15.05.1957	06 32 44.2	+63 40 40	20 57 24	90s	1957 III	Agfa Ast
O546(III)	15.05.1957	06 32 46.5	+63 40 40	21 07 24	90s	1957 III	Agfa Ast
O547(III)	15.05.1957	06 32 50.0	+63 40 38	21 17 24	90s	1957 III	Agfa Ast
OV131	30.05.1957	07 53 48.3	+62 21 09	22 44 43	300s	1957 III	Isopan F
OV132	30.05.1957	07 53 50.0	+62 21 07	22 59 43	300s	1957 III	Isopan F
O548(III)	30.05.1957	07 53 52.9	+62 21 06	23 21 43	90s	1957 III	Agfa Ast
O549(II)	30.05.1957	07 53 54.2	+62 20 58	23 36 43	60s	1957 III	Agfa Ast
O549(III)	30.05.1957	07 53 54.7	+62 20 58	23 39 43	180s	1957 III	Agfa Ast
OV133	02.06.1957	08 04 36.4	+61 59 49	20 46 25	540s	1957 III	Isopan F
O550(III)	02.06.1957	08 04 39.8	+61 59 37	21 15 55	270s	1957 III	Agfa Ast
O553(I)	08.06.1957	08 24 18.7	+61 15 19	21 50 00	300s	1957 III	Agfa Ast
O553(II)	08.06.1957	08 24 20.7	+61 15 17	22 05 00	600s	1957 III	Agfa Ast
O554(I)	08.06.1957	08 24 23.6	+61 15 15	22 25 00	300s	1957 III	Agfa Ast
O554(II)	08.06.1957	08 24 35.4	+61 15 04	22 40 00	600s	1957 III	Agfa Ast
O565(III)	15.08.1957	11 08 45.7	+35 45 47	19 31 18	90s	1957 V	IsoSPan
O566	15.08.1957	11 08 54.9	+35 45 20	19 48 18	205s	1957 V	Isopan F
OV156 Ib	24.09.1957	14 45 44.0	- 00 08 59	17 38 42	270s	1957 V	Isopan F
OV157 Ib	24.09.1957	14 45 45.2	- 00 10 34	17 57 42	270s	1957 V	Agfa Pan
O572	24.09.1957	14 45 46.9	- 00 11 13	18 10 12	600s	1957 V	IsoSPan

Acknowledgements. We would like to thank Dr. Katya Tsvetkova, from the Institute of Astronomy, Bulgarian Academy of Sciences, for the support she gave us during the period in which we have prepared the material in the present archive. Last, but not least, we want to thank Dr. Elvira Botez, who helped us to find answers to questions that appeared during the elaboration of this note.

REFERENCES

Chiş, G.: 1949, *J. Obs.*, **32**, No. 3, 39.

Chiş, G.: 1950, *St. Cerc. Şt.*, **1**, 56.

Chiş, G., Todoran, I., Botez, E.: 1960, *St. Cerc. Astron. Seism.*, **5**, 333.

Tsvetkov, M. K., Stavrev, K. Y., Tsvetkova, K. P., Ivanov, P. V., Iliev, M. S.: 1994, in H.T. MacGillivray, E.B.Thomson, B.M. Lasker, I.N. Reid, D.F. Malin, R.M. West, H. Lorenz (eds), *The WG WFI Plate Database (WFPDB): Present Status*, Proc. IAU Symp. No. 161, 359.

Tsvetkov, M. K., Tsvetkova, K., Stavrev, K., Popov, V., Lukarski, H., Borisova, A., Michailov, M.-E. S., Borisov, G., Christov, S.: 2000, in IAU 24th General Assembly, *Abstract Book*, 223.

Received on 29 November 2000

LIGHT CURVE AND TIMES OF MINIMA FOR HU TAU FROM VISUAL OBSERVATIONS

VALERIU TUDOSE, ADRIAN SONKA

Faculty of Physics, University of Bucharest
Str. Atomiştilor 1, P.O. Box MG-6, RO-76900 Bucharest – Măgurele, Romania
E-mail: tudosev@yahoo.com, senko@personal.ro

Abstract. In this paper we determine three times of minima and we represent the light curve of HU Tau. The visual observations were performed during December 1998, in Bucharest, with a 50 mm refractor, $F/D = 8$.

Key words: visual photometry – eclipsing binaries – HU Tau.

1. INTRODUCTION

The variable star HU Tau (HD 29365, SAO 76680, HIP 21604) was recognized as an eclipsing binary by Strohmeier and Knigge (1960). Spectroscopic observations have been published by Mammano et al. (1967) who found the system to be a single-lined spectroscopic binary. Photoelectric photometry of this system was performed by Tumer and Kurutac (1979), Dumitrescu and Dinescu (1980), Parthasarathy and Sarma (1980), Melendo (1985), Ito (1988). The parameters of this system are listed in Table 1 (Maxted et al. 1995; Batten et al. 1989).

Table 1

Star	P [days]	E	i [°]	m_1 [$m_\odot$]	m_2 [$m_\odot$]	R_1 [$R_\odot$]	R_2 [$R_\odot$]
HU Tau	2.0563	0.0	78.4 ±0.1	4.43 ±0.09	1.14 ±0.03	2.57 ±0.03	4.21 ±0.03

2. OBSERVATIONS

The visual observations were made in December 1998, from Bucharest, by one of the authors (A. S.), with a 50 mm refractor, $F/D = 8$. The comparison stars were: HD 29104 (SAO 94022, HIP 21408, Vmag = 6.4), HD 28483 (SAO 93973,

HIP 21008, Vmag = 7.1) and HD 28226 (SAO 76618, HIP 20842, Vmag = 5.7). Out of 85 magnitude estimations, 9 were rejected (poor atmospheric conditions, large differences from the light curve trend. For the calculations we used the ephemeris (Ito 1988):

$$\text{Min I} = \text{HJD } 2446485.9967 + 2^{\text{d}}.0563056\,E\,.$$

Table 2

HJD	Mag	Phase	HJD	Mag	Phase
2451157.3786	5.9	0.735	2451174.2906	6.3	0.960
2451157.4090	5.9	0.750	2451174.3019	6.4	0.965
2451157.4536	5.9	0.772	2451174.3169	6.5	0.973
2451162.4106	5.9	0.182	2451174.3314	6.6	0.980
2451162.4460	5.9	0.200	2451174.3448	6.7	0.986
2451167.2138	6.0	0.518	2451174.3564	6.7	0.992
2451167.2734	6.0	0.547	2451174.3689	6.7	0.998
2451167.3526	5.9	0.586	2451174.3831	6.6	0.005
2451167.3909	5.9	0.604	2451174.3960	6.4	0.011
2451167.4709	5.9	0.643	2451174.4148	6.4	0.020
2451167.5022	5.9	0.658	2451174.4373	6.1	0.031
2451168.2179	6.7	0.007	2451174.4481	6.0	0.036
2451168.2525	6.6	0.023	2451175.1960	5.9	0.400
2451168.2887	6.3	0.041	2451175.2273	5.9	0.415
2451168.3250	6.2	0.059	2451175.2581	5.9	0.430
2451171.3470	6.0	0.528	2451175.3919	6.0	0.495
2451172.1815	5.9	0.934	2451176.1876	5.9	0.882
2451172.2032	5.9	0.945	2451176.2251	5.9	0.900
2451172.2415	6.2	0.963	2451176.2622	5.9	0.919
2451172.2595	6.3	0.972	2451176.2905	5.9	0.932
2451172.2753	6.5	0.980	2451176.3126	6.0	0.943
2451172.2907	6.6	0.987	2451176.3293	6.1	0.951
2451172.3040	6.7	0.994	2451176.3480	6.2	0.960
2451172.3165	6.7	1.000	2451176.3572	6.3	0.965
2451172.3336	6.7	0.008	2451176.3676	6.4	0.970
2451172.3503	6.4	0.016	2451176.3738	6.4	0.973
2451172.3670	6.2	0.024	2451176.3793	6.5	0.975
2451172.3990	6.0	0.040	2451176.3938	6.6	0.983
2451172.4186	5.9	0.049	2451176.3997	6.7	0.985
2451173.2674	5.9	0.462	2451176.4084	6.7	0.990
2451173.2936	6.0	0.475	2451176.4168	6.7	0.994
2451173.3145	6.0	0.485	2451176.4313	6.7	0.001
2451173.3386	6.0	0.497	2451176.4351	6.6	0.003
2451173.3678	6.0	0.511	2451176.4593	6.5	0.014
2451174.1877	5.9	0.910	2451176.4747	6.3	0.022
2451174.2448	6.0	0.937	2451176.4926	6.2	0.031
2451174.2606	6.0	0.945	2451176.5105	6.1	0.039
2451174.2789	6.1	0.954	2451176.5397	5.9	0.053

Table 2 lists the observation times, the magnitude estimations and the phases. Fig. 1 shows the light curve built with the data provided by Table 2.

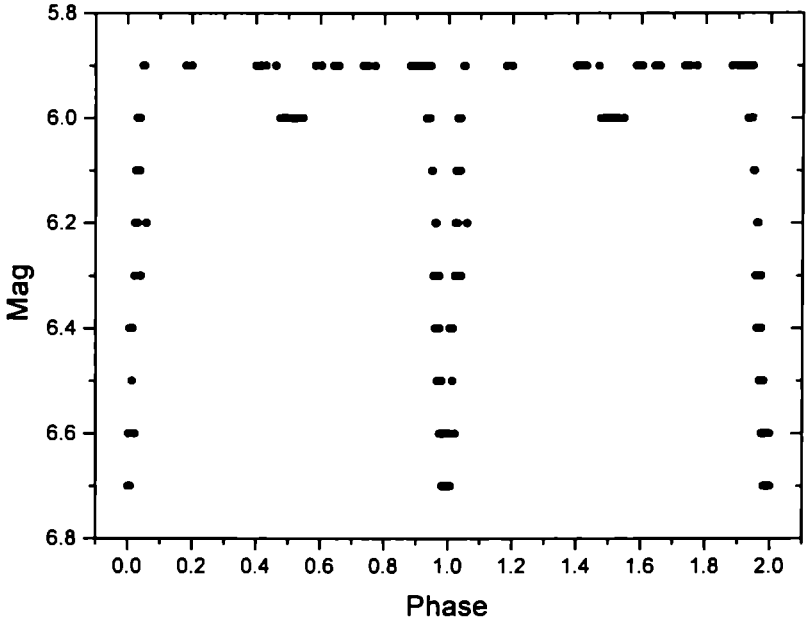

Fig. 1 – Light curve of HU Tau.

3. TIMES OF MINIMA

From the observations, we were able to determine three successive minima (Table 3). For each minimum, both the descending and ascending branch of the light curve were observed. The time of minimum was measured by the tracing paper method.

Table 3

HJD	O-C [days]
2451172.3152 ± 0.004	-0.0020
2451174.3569 ± 0.004	-0.0166
2451176.4200 ± 0.004	-0.0152

4. CONCLUSIONS

Even if the visual observation method is not so precise as the photoelectric or CCD photometry techniques, in some particular cases, especially if the amplitude of the light variation is large, it is possible to determine the trend of the light curve and the times of minima, with a satisfactory accuracy. One of the major problems in visual observations is the subjectivity in estimating the magnitudes and this

shortcoming can be diminished mainly by the observer's experience. Another important source of errors is the poor resolution in magnitude. This is a consequence of the fact that the human eye cannot distinguish a variation of light smaller than one tenth of a magnitude. In conclusion, it is preferable to use the visual observations as additional data (with adequate weights) to more precise determinations.

REFERENCES

Batten, A. H., Fletcher, J. M., MacCarthy, D. G.: 1989, *Publ. Dominion Astrophys. Obs.*, **17**, 1.
Dumitrescu, A., Dinescu, R.: 1980, *Inf. Bull. Variable Stars*, No. 1740.
Ito, Y.: 1988, *Inf. Bull. Variable Stars*, No. 3212.
Mammano, A., Mannino, G., Margoni, R: 1967, *Mem. Soc. Astron. Ital.*, **38**, 459.
Maxted, P. F. L., Hill, G., Hilditch, R. W.: 1995, *Astron. Astrophys.*, **301**, 141.
Melendo, E. G.: 1985, *I.A.P.P.P. Comm.*, **20**, 27.
Parthasarathy, M., Sarma, M. B. K.: 1980, *Astrophys. Space Sci.*, **72**, 477.
Strohmeier, W., Knigge, R.: 1960, *Veroff. Bamberg*, No. 5.
Tumer, O., Kurutac, M.: 1979, *Inf. Bull. Variable Stars*, No. 1547.

Received on 16 December 2000

KENNETH R. MEYER, *Periodic solutions of the N-body problem*, Lecture Notes in Mathematics, No. 1719, Springer-Verlag, Berlin, 1999, 144 pp., ISBN 3-540-66630-3.

This book grew out of a series of lectures given by the author at the Universidade Federal de Pernambuco, Recife, Brazil, on periodic orbits in the N-body problem; many interesting results of his own are included. The reader is led from general results on Hamiltonian systems to some basic applications to the central problems of celestial mechanics.

Chapter 1 contains a motivation for choosing periodic orbits as subject: since Newton's solution of the two-body problem, they imposed themselves in celestial mechanics, and their importance was recognized by Poincaré as a way to understand the N-body problem.

The N-body problem and some of its well-known special cases described also by Hamiltonian systems (Kepler problem, circular and elliptic restricted three-body problem, Hill's lunar equations) are mentioned in Chapter 2.

The basic concepts of Hamiltonian formalism and symplectic geometry are reviewed in Chapter 3, with emphasis on systems of coordinates related with the N-body problem.

Chapter 4 is dedicated to central configurations, which give rise to simple periodic solutions (Lagrangian solutions for the planar three-body problem or Euler-Moulton ones in the case of the collinear N-body problem).

The systems that admit continuous symmetries, implying the existence of integrals, are studied in Chapter 5. For such systems, the Jacobian of Poincaré's continuation method is singular; but the integrals may be used to reduce (by the Meyer-Marsden-Weinstein method) the problem to a lower-dimensional one, which is still Hamiltonian. The theory is applied to the N-body problem, using its invariance under the group of Euclidean motions.

Chapter 6 contains results on the existence, continuation, and stability of periodic solutions in general, but also for Hamiltonian systems with symmetries.

The basic results from the first six chapters are applied in the next six to provide classes of periodic orbits for various problems of celestial mechanics:

- two particles with small mass move on approximately circular orbits around a particle of large mass (satellite orbits);
- the $(N+1)$-body problem with one small mass;
- the $(N+1)$-body problem with $N-1$ particles and the center of mass of the remaining pair moving approximately on a relative equilibrium solution, while the two bodies move approximately on a small circular orbit about their center of mass (lunar orbit);
- the $(N+1)$-body problem with N primaries moving approximately on a relative equilibrium solution, while one particle moves at a great distance approximately on a circular Kepler problem about the center of mass (cometary orbits);
- lunar theory, using Delaunay's model and the better one proposed by Hill as limiting cases of the three-body problem;
- the planar N-body problem related to the periodic system of the elliptic restricted problem.

The book contains 57 problems, an index, and a list of 92 references. Many results have been obtained recently, hence they can be used as a basis for further research. This book represents a valuable introduction to some of the well-known old and new problems of celestial mechanics, using the modern tools of the Hamiltonian theory.

Mira-Cristiana Anisiu

ADVANCES IN SOLAR RESEARCH AT ECLIPSES, FROM GROUND AND FROM SPACE, Proceedings of the NATO Advanced Study Institute, 9–20 August 1999, Bucharest, Romania, Edited by Jean-Paul Zahn and Magda Stavinschi, NATO Science Series, Series C: Mathematical and Physical Sciences – Vol. 558, Kluwer Academic Publishers, Dordrecht-Boston-London, 2000, 310 p., ISBN 0-7923-6623-9 HB, ISBN 0-7923-6624-7 PB.

The aim of this Advanced Study Institute was to give an account on the most recent results obtained in solar research. Bucharest was chosen to host it because the capital city of Romania was located right in the middle of the totality path of the last eclipse of the millenium. Furthermore, the eclipse was close to reach here its longest duration.

The lectures highlight the fast progress in the last few years mainly due to the observations carried out from space. The results spread through journals and specialized meetings were presented here in a more pedagogical way for the benefit of the younger scientists. Emphasis was put on the physical interpretation of the phenomena rather than on their detailed description.

The topics covered subjects from astrometry to astrophysics and from outer solar corona to deep solar interior. In the beginning an overview of the Moon's motion and of the Earth's rotation tried to explain the discrepancies in the computed duration of the totality phase.

Thereafter the series of lectures uncovered the theory and observation of solar atmosphere with emphasis on phenomena relevant to solar eclipse observations. A set of lectures, addressed mainly to observers, focused on solar corona, various coronal phenomena and large scale characteristics. Solar activity and solar active regions were also presented.

Another set of lectures focused on the theoretical subjects such as modeling of the electron density distribution or the evolution of the magnetic fields. Models of the solar atmosphere, non-LTE radiation processes and fine structure of line profiles were discussed within the framework of solar eclipse observations.

Finally subjects such as the theory of the solar interior and its sounding and the theory of solar luminosity variations were addressed.

This ASI was attended by 76 participants from 18 different countries: 61 students and 15 lecturers. The posters presented by the students were published in the *Supplement* of the *Romanian Astronomical Journal*, Vol. 9, 1999.

Adrian Oncica

CORRELATED PHENOMENA AT THE SUN, IN THE HELIOSPHERE AND IN SPACE. The Proceedings of the 31st ESLAB Symposium held in Noordwijk, The Netherlands, between September 22–25, 1997, Editor: A. Wilson, ESTEC, Noordwijk, The Netherlands, 546 p., ISBN 92-9092-660-0.

The symposium was dedicated to 'space-physics', namely solar-terrestrial relations, in a global and thus more fundamental context. Starting at the Sun and its atmosphere – as the source of energy and perturbations – the topics of the conference proceed not only through the quasi two-dimensional interplanetary space, but also looked at the heliosphere in three dimensions. The fundamental question was: what does all this mean for the Earth and its environment, and thus ultimately for us? This question not only deepens a traditional intellectual pursuit, but it also has a direct bearing on our existence and, in its final consequences, on our survival. A most remarkable set of scientific satellites was at that time strategically placed in the heliosphere and near the Earth: SOHO, Yohkoh, Ulysses, WIND, ACE, UARS, Sampex, Polar, Geotail and Interball. Even if some of these missions became operational only a relatively short time before the symposium, and others, like Cluster, were still missing, the results of the measurements made by those satellites provided data of unsurpassed quality, affording a comprehensive view of the heliosphere and the solar-terrestrial system.

The topic of that conference was a multi-disciplinary approach to modern science, and brought an opportunity for a better understanding of the complex physical structures and processes that occur in and near the Sun, in the heliosphere and in geospace.

The programme of the conference consisted of four topics.

The first session was devoted to '*Solar Corona and Solar Wind: the Quasi-Steady State*'. It included subjects as: observations and models of the fast and slow solar wind, studies of the composition of the solar wind, analysis of the results given by SOHO and Ulysses, numerical simulations of MHD turbulence.

The second chapter, '*Transient Phenomena: Clouds & CME from the Sun to the Earth*' covered the results given from Ulysses, SOHO, Interball, but reported also the analysis of certain specific active regions, such as the NOAA active region No. 8038 during 10–13 May 1997. Some studies of the CMEs developments and their association with interplanetary events were also done.

The third session, '*Solar Variability and Climate*', had a subject that became very fashionable and important in the following years. There were reported studies of total solar irradiance variations and local climatic effects of energetic particles impinging on the atmosphere.

The last session reviewed the planned projects: '*Goals for Future Correlated Studies towards Solar Maximum*'. It was the place for announcing future projects, as International Solar Cycle Studies – ISCS (1998–2002), a project planned for the rising phase of the 23rd solar cycle and designed to improve the understanding of how the Sun dramatically evolves from a quiet Sun to an extremely active one over a period of five years. The research program was divided in three working groups, each of them aiming to study the phenomena from different layers of the Sun to the heliosphere. Then we are informed that there are programs designed for the solar-terrestrial research and space weather, invaluable for obtaining new understanding of the Earth's space environment as the peak years of solar activity in Cycle 32 was approaching. Another paper speculates about how to take advantage of the future data from spacecraft, including TRACE, HESSI and SOLAR-B, emphasizing the use of heliospheric observations to help probe the connectivity of the corona/solar wind interface region.

The last article concerns with ESA's current and future programmes related to climate studies. ESA's Earth observation space missions give data which are required not only for process studies and the improvement/validation of numerical models used to predict climate change, but also to help monitoring some of the key climate variables. The discussion was set in the overall context of the international initiatives as the World Climate Research Programme (WCRP) and the International Geosphere-Biosphere Programme (IGBP). The Committee on Earth Observation Satellites (CEOS) was planning to combine all sources of data such to ensure the optimal use of resources.

The first three sessions benefitted of a rich list of poster papers (more than 40), which fulfilled the subjects discussed in the oral presentations.

Concluding, this book offers a valuable source of documentation through its topics of a huge interest for the present and future of our planet.

Georgeta Mariş

THE SOLAR CYCLE AND TERRESTRIAL CLIMATE. The Proceedings of The First Solar and Space Weather Euroconference held in Santa Cruz de Tenerife, Tenerife, Spain, between September 25-29, 2000, Editor: A. Wilson, ESA Publications Division, ESTEC, Noordwijk, The Netherlands, 680 p., ISBN 92-9092-693-7.

This was the first of the two meetings within the framework of *Solar and Space Weather Euroconferences (SOLSPA)* organised by IAC (Instituto de Astrofisica de Canarias) in connection with the Annual Meeting of JOSO (*Joint Organisation for Solar Observations).*

The conference brought together solar physicists and atmospheric scientists to review contemporary knowledge on global warming and its causes. A clear warning that something might go wrong is the increase of the mean temperature of the Earth over the last 150 years. Apart from an intrinsic variability, three external agents could be responsible for this: the increasing emission of greenhouse gases (such as carbon dioxide, produced by the burning of fossil fuels), the emission of different types of aerosols of natural and anthropogenic origins, and the increase in the mean level of the magnetic activity on the Sun. This last contribution was emphasized during the conference which consisted of two parts: the first one was devoted to the study of solar variability and how could it influence the terrestrial climate, whereas the second one was dedicated to the estimate of the different contributions of greenhouse gases, aerosols and solar activity to climate change, together with the presentation of some important projects.

The first part of the proceedings was dedicated to the subjects of the oral presentations, which were:

Solar Variability: the origin of the solar cycle, magnetic sources of solar variability, studies of the total solar irradiance variations, solar variability in ionizing radiation (UV, X-rays), the dynamo theory of the Maunder minimum, and drift-time measurements of the solar diameter.

Mechanisms of Solar-Terrestrial Relations: ocean temperature response to changing solar irradiance, solar forcing of El Nino and La Nina, atmospheric effects of the irradiance, and corpuscular radiation.

The Long-Term Terrestrial Record of Climate Change: CO_2 and astronomical forcing of the late quaternary, some relations between sedimentation and climatic shifts.

The Solar Contribution to Climate Change: the connection between solar cycle lengths and terrestrial temperatures, natural variability of global mean temperature.

Non-Solar Sources of Global Warming: climate change investigations, the climatic impacts of increased CO_2, the Intergovernmental Panel on Climate Change (IPCC) report for 2001.

SOLSPA Summary, presented by Dr. E. N. Parker.

Then we find an impressive number of poster papers covering a large area of interest as: *The Solar Cycle*, *The Terrestrial Record of Solar Variability* and *Non-Solar Sources of Climate Change*.

The final part of the book is dedicated to the development of Solar Physics in Europe and the annual meeting of JOSO, which had the following subjects, related to its working groups: *Data Handling in Solar and Geophysical Research*, *Meeting on the 1999 Solar Eclipse*, *Meeting on Observing Techniques and Recent Instrumental Development*.

Concluding, this book is a very good source of information on a subject of a wide and extremely fashionable interest, gathering together a large number of articles of both solar physics and atmospheric science, which are pursuing the problem of terrestrial climate and global warming. From the material included here, it appears that the understanding of the peculiar variability of the Sun and the complex physics of the terrestrial response has improved but there is still more work to be done for creating a predictive climate model.

Miruna Daniela Popescu

MAGNETIC FIELDS AND SOLAR PROCESSES. 9th European Meeting on Solar Physics, 12–18 September 1999, Florence, Italy, edited by A. Wilson and ESA Publications Division, ISBN 92-9092-792-5.

Each year the Solar Physics Section of the Joint Astrophysics Division of the EAS and EPS held meetings on key problems on which recent progress has been striking lately. The theme chosen for this Euroconference was a physical principle, the magnetic field. The work discussed addresses

the Sun outside its immediate core (> 0.2 solar radii) but well within the heliosphere (<< 100 solar radii). Eleven key problems were selected:

Helioseismology – Interior – Dynamo. Detailed observation of pressure modes and the determination of the internal rotation rate, tomographic imaging of emerging magnetic fields, GONG observations and results were among the topics.

Waves – Atmospheric dynamics. Important progress was presented on the development of shock waves and nonlinear coupling of various waves in flux tubes. The MHD spectroscopy in a fashion similar to helioseismology was hoped.

Solar prominences. As the most beautiful structures in the solar corona they form a stepping stone in the understanding of the dynamics of the solar atmosphere. Fibrils or thread structures, sizes and filling factor as well as observed wave modes were presented.

Emerging flux – Coronal heating. The explosive events are a natural result of the reshuffling of the solar magnetic fields arising from the connective flows. The newly discovered microscale heating was discussed. The contribution of this process to the heating of the solar corona was the main question.

Solar flares. Impressive results were presented both on 3D numerical modelling of magnetic explosions and on new analytical developments regarding quasi-separatrix layers. On the observational/modelling front the relation between the location of X-ray sources in and above flare loops and the site of reconnection was clarified.

Coronal mass ejection – Space weather. Since the advent of SOHO this field developed into a mature subject. Dynamic 3D MHD modelling of CMEs allowed for the reproduction of white light structures and dimmings in X-rays. It was reached a better understanding of the solar wind influence on Earth's magnetosphere oscillations and of the Interplanetary Magnetic Field effects on terrestrial magnetic field reconnections.

Particle acceleration in the Solar System. The key question addressed here was how a large fraction of the available energy in a solar flare is fed into the particle acceleration. Subsecond timing studies and time-of-flight delay measurements in radio and hard X-ray emission shed new insights on particle acceleration in flares. Detailed numerical simulation work on direct electric acceleration allowed a direct comparison between the observed energy spectrum of the particles and the synthesized one.

Solar wind – Heliosphere. It appears now that the fast/dilute solar wind is the result of heating in open field regions, coronal holes, often in form of explosive events. On the other hand, slow/dense solar wind is driven by heating in closed magnetic structures at a relatively large gas pressure. Ulysses observations of large amplitude magnetic field fluctuations near poles are discussed.

Radio coronal magnetic field measurements – Radio instrumentation. There was a special session of the Committee of European Radio Astronomers (CESRA). Main subjects were polarization measurements and radio magnetography, millisecond radio spikes, and thermal radio radiation from hot coronal loops.

Data storage management in solar databases. A joint discussion on databases, present status and new perspectives was also held. Flexible data storage and retrieval, newly expected large data bases and their storage media, peculiarities and drawbacks were among the subjects.

Early results from TECONET. In 1998 the "Eclipse 99" Working Group of Joint Organization for Solar Observations (JOSO) introduced the project of coordinated coronal observations across Europe at the occasion of the August 11, 1999 total solar eclipse. This network called TECONET (Trans-European Coronal Observing Network) involved 28 amateur and professional teams. The science returns from the JOSO Working Group 7 project was presented.

Adrian Oncica

THE NOT IN THE 2000'S. Proceedings of the Workshop held on La Palma, April 12-15, 2000, Eds: N. Bergvall, L.O. Takalo, V. Piirola, University of Turku, 2000, 208 p., ISBN 951-29-1827-7.

NOT telescope (the La Palma 2.3 m telescope of the Nordic Astronomical Community) offers extraordinary capabilities, in particular its high image quality. The telescope has a significant effect in the development of the fields of Cosmology, Stellar Astrophysics and Celestial Mechanics for all the nordic countries.

In order to fit with the new giant telescopes, the Workshop tried to develop the strategy of the observations for increasing the efficiency and for the optimization of data aquisition.

The Workshop main goals were: (1) to give opportunities to the users of NOT to present and to discuss their viewpoints about the needs and solutions to keep NOT competitive; (2) to review the instrumentation available at the NOT and to trace the future instrumentation program.

The program of the Workshop included six sections with about 30 papers. The sections concern: General implication of the NOT to Nordic Astronomy; Science with NOT; Technical developments and operational strategies of NOT; NOT from the European perspective; Funding resources for NOT; and a Panel Discussion.

NOT is engaged in the following scientific programs: High resolution imaging of gravitationally lensed quasars; Study of gravitational arcs and of the bias effect in clusters of galaxies; Identification and photometric monitoring of gamma-ray bursts; Imaging of damped Lyman-alpha absorbers; Photopolarimetry of AGNs and magnetic white darfs; Participation to Supernova Cosmology Project; Stellar polarimetry and Stromgren photometry of globular clusters; High resolution spectroscopy of pre-MS stars and cataclysmic variables; Infrared studies of the IMF and brown dwarfs.

Technical developments and operational strategies discussions of the Workshop dealt with: Direct imaging with the highest possible spatial resolution; Wide field imaging without distorsions; Low-resolution spectroscopy with MOS option; Wavelengh coverage from UV to near-infrared (in difference to 8 m class telescopes); Operational versability, flexibility and economy; Maximum standardization and commonality of hardware and software components and user interfaces; Cost of the new investment and operation.

From the European perspective, NOT is engaged in a series of cooperations as: Gravitational lenses – time delay project; Dust at high redshifts, Stellar activity and magnetic cycles; Supernova Cosmology Project; Star formation projects; Interacting binary stars project.

The Panel Discussion dealt with the needed technical future developments of the NOT telescope: Rapid response imaging facilities; Rapid response spectroscopic facility; The Cassegrain instrument position available for the future projects. The discussions showed that the telescope aperture is not the only determining factor for the quality of the research, but also,the "human factor" must be taken into account. Keeping the flexibility of the operation to optimize the return, and specializing in the strong fields in instrument development and research applications, NOT will remain competitive almost for the next decade.

All these scientific programs are supported, at a necessary level, by the Academies of the Nordic Countries.

Marian Doru Şuran

NOTICE TO AUTHORS

ROMANIAN ASTRONOMICAL JOURNAL appears twice a year and is open to original contributions in Astronomy and related disciplines. The contributions – in English or French – can be accepted only if they were neither published before nor destined to another publication.

Manuscripts should, preferably, be submitted as e-mail attachments to roaj@roastro.astro.ro. They must be written in a well-known editor, preferably a recent version of Word. Authors who cannot submit an electronic version of their manuscript should sent it to the Editorial Board. In this case two copies of the manuscript (along with the text of the article on floppy disk) are required. The first page should contain: article's title (brief and informative), author's name and affiliation, followed by an *Abstract* in English and *Key words*. The text should be clear and concise (it is recommended not to exceed 10 pages). The *Abstract* will present clearly the principal conclusions on the work, in no more than 10–15 lines.

Chapters and Paragraphs. Papers, except short notes, should be divided into chapters, numbered by Arabic numerals. Chapters may be divided into paragraphs denoted by the number of the chapter and the number of the paragraph; each chapter and each paragraph should have a short descriptive title (e.g. "3.2. Results").

Formulae have to be centered and numbered consecutively in Arabic numerals, too, but included in brackets on the right-hand side of the manuscript.

Tables should be numbered consecutively in Arabic numerals; they should be introduced in the text at their appropriate place.

Figures and Illustrations should be submitted separately, in such a form as to permit reproduction without retouching. Any lettering should be large enough to be legible after the figure has been reduced in size for printing. Captions should be introduced in the text at their appropriate place. All figures should be numbered consecutively in Arabic numerals and referred to in the text, e.g. Fig. 2 or Figs. 2–5. Photographs should be given only if essential and should be enlarged enough to permit clear reproduction.

References are indicated in the text by the author's name and year of publication. They should be listed in alphabetic and chronologic order at the end of the paper, as follows: name and initials of the author(s), year of publication, suitable abbreviation of the journal (or title of the book and editing house), its volume and page.

The *fonts* to be used are: 11 for the text proper, 13 for the paper title, 9 for author's name and affiliation, abstract, key words, titles of chapters and paragraphs, figure captions, tables, running titles, and references.

Detailed instructions for the preparation of manuscripts can be found at http://roastro.astro.ro/~roaj.

Please pay attention to these recommendations; the manuscripts that do not observe them will be returned to the authors.

ROMANIAN
ASTRONOMICAL
JOURNAL

Vol. 10, No. 2, 2000

CONTENTS

ISSN 1210-5168

Rom. Astron. J., Vol. 10, No. 2, p. 109–204, Bucharest, 2000